

Real-time allosteric modulation at human and rat adenosine A1 receptor

Dissertation

zur Erlangung des akademischen Grades
doctor rerum naturalium (Dr. rer. nat.)

vorgelegt dem Rat der Medizinischen Fakultät
der Friedrich-Schiller-Universität Jena

von M. Sc. Nelly Dorothea Rüttiger
geboren am 03.07.1989 in Baden-Baden

Gutachter:

1. Prof. Dr. Carsten Hoffmann, Universitätsklinikum Jena
2. Prof. Dr. Klaus Benndorf, Universitätsklinikum Jena
3. Prof. Dr. Stephen J Hill, University of Nottingham

Tag der öffentlichen Verteidigung: 23.03.2021

Table of Contents

Table of Contents	I
Abbreviations	IV
Zusammenfassung	VII
Summary	IX
1 Introduction	1
1.1 G protein-coupled receptors	1
1.1.1 Classification of GPCRs	2
1.1.2 Heterotrimeric G protein	3
1.1.3 Receptor affinity and kinetics	4
1.2 Adenosine receptors	6
1.2.1 Adenosine A1 receptor	7
1.2.2 Adenosine receptor ligands	7
1.2.3 Diseases and therapeutic targeting	9
1.3 Allostery	11
1.3.1 Allosteric interactions at GPCRs	13
1.3.2 State of the art	15
1.3.3 Allosteric modulator PD 81,723	16
1.4 Fluorescence microscopy	19
1.4.1 Fluorescence resonance energy transfer	19
1.4.2 GPCR FRET sensors in intact living cells	22
2 Aims of the study	23
3 Material and Methods	24
3.1 Material	24
3.1.1 Chemicals and reagents	24
3.1.2 DNA	26
3.1.3 Cell lines	26
3.1.4 Kits	27
3.1.5 Medium and buffers	27
3.1.6 Ligand preparation	28
3.1.7 Equipment	28

3.2	Methods.....	29
3.2.1	Molecular biology	29
3.2.1.1	Polymerase chain reaction	29
3.2.1.2	Electrophoretic separation of DNA.....	29
3.2.1.3	Transformation of nucleotides in bacteria	29
3.2.1.4	Isolation of nucleotides from bacteria	30
3.2.1.5	Concentration and purity of nucleotides.....	31
3.2.1.6	Molecular cloning	31
3.2.2	Cell culture	32
3.2.3	Transient and stable transfection of HEK293 cells.....	32
3.2.4	FIAsH-labeling.....	33
3.2.5	FRET measurements	34
3.2.6	Confocal analysis	34
3.2.7	Data analysis.....	34
4	Results	36
4.1	Investigation of rat and human adenosine A1 receptor.....	36
4.1.1	Orthosteric characterization of rat A1 FIAsH3 CFP sensor	37
4.1.2	Orthosteric kinetics of rat and human A1 FIAsH3 CFP receptor	39
4.1.3	Measuring procedure of allosteric modulation at adenosine A1 receptors	41
4.1.4	Determination of PD 81,723 affinity for adenosine-occupied receptor.....	43
4.1.5	Influence of allosteric modulator on orthosteric affinity	45
4.1.6	Probe dependency of allosteric modulator PD 81,723	46
4.1.7	Visualization of allosteric modulation on G protein level	47
4.1.8	Determination of allosteric kinetics	49
4.2	Investigation of mutations in the putative allosteric binding site.....	54
4.2.1	Orthosteric characterization of mutants in the second extracellular loop.....	54
4.2.1.1	Adenosine affinity of mutants in the second extracellular loop	55
4.2.1.2	Orthosteric kinetics of mutants in the second extracellular loop.....	56
4.2.2	Allosteric characterization of mutants in the second extracellular loop.....	57
4.2.2.1	PD 81,723 affinity of mutants in the second extracellular loop	57
4.2.2.2	Influence of PD 81,723 on orthosteric affinity of mutants in the second extracellular loop.....	59
4.2.2.3	Allosteric kinetics of mutants in the second extracellular loop	61

5	Discussion.....	66
5.1	Orthosteric and allosteric characterization of human and rat adenosine A1 receptor 67	
5.1.1	Orthosteric characterization.....	67
5.1.2	Allosteric characterization.....	70
5.1.3	Kinetic aspects of allosteric modulation.....	73
5.2	Investigation of putative allosteric binding site.....	76
5.2.1	Orthosteric characterization of mutants in the second extracellular loop.....	76
5.2.2	Allosteric characterization of mutants in the second extracellular loop.....	78
6	Conclusions and outlook.....	81
7	Appendix.....	83
8	References.....	90
9	Acknowledgement.....	XI
10	List of figures.....	XII
11	List of tables.....	XIV
12	Publications and conferences.....	XV
12.1	Publications.....	XV
12.2	Attended conferences.....	XV
13	Curriculum vitae.....	XVII
14	Ehrenwörtliche Erklärung.....	XVIII

Abbreviations

a.u.	Arbitrary units
A1AR	Adenosine A1 receptor
AC	Adenylyl cyclase
ADA	Adenosine deaminase
Ado	Adenosine
AMP	Adenosine monophosphate
ANOVA	Analysis of variance
AP2	Adaptor protein-2
AR	Adenosine receptor
ATL525	2-amino-4,5,6,7-tetrahydro-benzo[b]thiophen-3-yl)biphenyl-4-yl-methanone
ATP	Adenosine triphosphate
bp	Base pair
BRET	Bioluminescence resonance energy transfer
cAMP	Cyclic adenosine monophosphate
CHA	N ⁶ -Cyclohexyladenosine
cGMP	Cyclic guanosine monophosphate
CNS	Central nervous system
CPA	N ⁶ -Cyclopentyladenosine
DCLP	Dichroic longpass
DMEM	Dulbecco's Modified Eagle Medium
DMSO	Dimethyl sulfoxide
DNA	Deoxyribonucleic acid
dNTPs	Deoxyribonucleotide triphosphates
DPCPX	8-cyclopentyl-1-3-dipropylxanthine
EC ₃₀	Effective concentration at 30 % of response
EC ₅₀	Effective concentration at 50 % of response
ECL	Extra cellular loop
ecto5'NT	Ecto-5'-nucleotidase
EDT	1,2-Ethanedithiole
EF	Endonuclease free
ENTs	Equilibrative nucleoside transporters
EtOH	Ethanol
FBS	Fetal bovine serum
FDA	Food and drug administration (USA)
FIAsH	Fluorescein arsenical helix binder

FRET	Förster/fluorescence resonance energy transfer
g	Gram
GAP	GTPase-activating protein
GDP	Guanine diphosphate
GEF	Guanine nucleotide-exchange factor
GPCR	G protein-coupled receptor
GRK	G protein-coupled receptor kinase
GTP	Guanine triphosphate
h	Hour
HEK293	Human embryonic kidney cell line
Hz	1 Hertz = 1/s
ICL	Intra cellular loop
K_D	Dissociation constant
K_i	Dissociation constant of inhibitor
k_{obs}	Observed rate of complex formation
k_{off}	Rate of complex dissociation
k_{on}	Rate of complex formation
l	Liter
m	Milli
M	Molar
min	Minute
MD	Molecular dynamics simulations
n	Nano
NAM	Negative allosteric modulator
Nluc	Nano-luciferase
NECA	5'-N-Ethylcarboxamidoadenosine
nm	Nanometer
NTPDases	Nucleotide triphosphate diphosphohydrolases
OAR*	Active orthoster-alloster-receptor-complex
o/n	Over night
OR*	Active orthosteric-receptor complex
PAM	Positive allosteric modulator
PBS	Phosphate buffered saline
PCR	Polymerase chain reaction
PD	PD 81,723
PD 81,723	(2-Amino-4,5-dimethyl-3-thienyl)-[3-(trifluoromethyl)phenyl]methanone
PDE	Phosphodiesterase

Abbreviations

P _i	Inorganic phosphate
PLC	Phospholipase C
R	Inactive unoccupied receptor
rpm	Rounds per minute
RT	Residence time
s	Second
SAM	Silent allosteric modulator
TM	Transmembrane
w/v	Weight per volume
wt	Wild type
x g	Times gravity as a unit of centrifugal force
μ	Micro
95 %CI	Confidence intervals 95 %

Zusammenfassung

Die Adenosin-Rezeptoren (A1, A2A, A2B und A3) werden im menschlichen Körper in nahezu allen Geweben exprimiert und sind an vielen physiologischen als auch pathophysiologischen Prozessen beteiligt. Um Adenosin-Rezeptoren (ARs) pharmakologisch zu regulieren wurden Agonisten mit unterschiedlichen Affinitäten zu den AR-Subtypen entwickelt. Doch nur wenige Substanzen wurden bisher als Medikament oder diagnostisches Werkzeug für den Einsatz an Patienten zugelassen. Gründe hierfür sind neben zu geringer Effektivität hauptsächlich schwere Nebenwirkungen, die auch infolge von Co-Aktivierung anderer Adenosinrezeptor-Subtypen neben dem Zielrezeptor bedingt sind. Eine Strategie um Nebenwirkungen zu reduzieren ist das Prinzip der allosterischen Modulation, wobei eine Substanz (allosterischer Modulator) die Effekte eines Agonisten am Rezeptor moduliert. Allosterische Modulatoren binden per Definition an andere Stellen des Rezeptors (allosterische Bindestelle) als an die Bindestelle des endogenen Agonisten (orthosterische Bindestelle). Die orthosterische Bindestelle ist unter den Adenosin-Rezeptor-Subtypen hochkonserviert, wohingegen die allosterische Bindestelle durch ihre höhere strukturelle Variabilität Subtypselektivität aufweist. PD 81,723 ist ein positiver allosterischer Modulator, welcher die Reaktion des A1-Rezeptors auf Agonisten oder den endogenen Liganden Adenosin (Ado) verstärkt. Allosterische Modulation am A1AR wurde hauptsächlich mittels Radioliganden-Bindungsstudien untersucht. Für diese Studien werden Zell-Lysate hergestellt, wodurch eine große Menge an Adenosin freigesetzt wird. Daher ist dieses Verfahren zur Untersuchung von allosterischer Modulation in Kombination mit Adenosin nicht geeignet.

In dieser Arbeit wurde zum ersten Mal allosterische Modulation am A1AR von Ratte und Mensch in Gegenwart von Adenosin in lebenden HEK293-Zellen untersucht. Ein Mess-Schema zur Aufzeichnung von positiven allosterischen Effekten wurde etabliert, welches durch Fluoreszenz-Resonanz-Energie-Transfer Sensoren die Beobachtung der Rezeptor-Konformationsänderung in Echtzeit ermöglicht. Hiermit wurde erstmalig die Affinität von PD 81,723 zum Adenosin-besetzten Rezeptor von Mensch und Ratte bestimmt. Im Vergleich zum Ado-besetzten humanen A1AR zeigte PD 81,723 eine 5-fach geringere Affinität zum NECA-besetzten Rezeptor. Dieses Phänomen wird als probe dependency bezeichnet. Des Weiteren konnte erfolgreich der Einfluss von PD 81,723 auf die Konzentrations-Wirkungskurve von Adenosin gemessen werden. Die entwickelte Vorgehensweise eignete sich hervorragend, um

eine weitere Eigenschaft von positiven allosterischen Modulatoren zu analysieren und zwar die Verlangsamung der Dissoziation des Liganden-Rezeptor-Komplexes (Ado-PD 81,723-A1AR). Die Dissoziation von Adenosin wurde in der Anwesenheit oder Abwesenheit von PD 81,723 von der aktiven Konformation des Liganden-Rezeptor-Komplexes aufgezeichnet. Die erhobenen Daten weisen darauf hin, dass PD 81,723 die Verlangsamung der Dissoziation des Liganden-Rezeptor-Komplexes durch einen anderen Mechanismus verursacht, als durch sterische Blockierung von Adenosin in der orthosterischen Bindetasche. Darüber hinaus konnte mit der entwickelten Verfahrensweise die Dissoziations-Kinetik von PD 81,723 vom Ado-besetzten Rezeptor gemessen werden. Durch diese drei detaillierten kinetischen Messungen wurde deutlich, dass die wesentlich längere Dissoziationsdauer von PD 81,723 vom aktiven Adenosin-Rezeptor-Komplex der zeitlimitierende Faktor sein muss. Daraus konnte gefolgert werden, dass der Adenosin-besetzte Rezeptor ein hochaffines Ziel für den allosterischen Modulator PD 81,723 darstellt.

Zur Untersuchung der potentiellen allosterischen Bindestelle, welche in der zweiten extrazellulären Schlaufe des A1-Rezeptors vermutet wird, wurden drei Aminosäuren durch Alanin-Austauschmutation verändert, S161A, E172A und I175A. Der Einfluss dieser drei Mutationen wurde auf die Affinität und das kinetische Verhalten von PD 81,723 in Gegenwart von Adenosin für Mensch und Ratte untersucht. Am A1AR des Menschen zeigte S161A eine signifikant höhere Affinität von PD 81,723 gegenüber der Affinität von PD 81,723 zum Wildtyp. Für die homologe Mutante im A1 Rezeptor der Ratte wurde hingegen keine Änderung in der Affinität festgestellt. Ein möglicher Grund für diese Diskrepanz liegt in den abweichenden Aminosäuren zwischen den Spezies (Mensch M162, Ratte V162). Die zu S161A benachbarte Aminosäure 162 wurde gegen das jeweilige Pendant in Mensch und Ratte ausgetauscht und es konnte gezeigt werden, dass der humane S161A-Phänotyp durch die Mutation von S161A M162V im kinetischen Verhalten gerettet wurde.

Alleinstellungsmerkmale dieser Arbeit sind, dass allosterische Modulation im Hinblick auf Kinetik am aktiven Liganden-Rezeptor-Komplex detailliert aufgeklärt werden konnte und dass die Messungen mit dem endogenen Liganden Adenosin ohne jegliche Modifizierung durchgeführt wurden. Letzteres ist für die Planung klinischer Studien hierzu wichtig, da variierende Adenosinspiegel in Probanden bisher kaum berücksichtigt wurden. Im Ganzen zeigt diese Arbeit neue und einmalige Einblicke in die Interaktionen von Adenosin, PD 81,723 und A1AR für Mensch und Ratte.

Summary

Adenosine receptors (A1, A2A, A2B and A3) are widely distributed throughout the human body. They are involved in a plethora of physiological and pathophysiological processes. Several agonists have been identified with varying affinity to pharmacologically target specific adenosine receptor (AR) subtypes. Yet, very few compounds have been approved as drugs or diagnostic tools for the use in patients because of insufficient efficacy. Moreover, the high amount of side effects, also mediated by co-activation of AR subtypes limits their use as drugs. One strategy to circumvent the issue of adverse effects is the principle of allosteric modulation, in which a substance (allosteric modulator) is modulating the effects of an agonist. Per definition allosteric modulators bind to distinct sites of the receptor (allosteric binding sites), which are different from the binding site of the endogenous agonist (orthosteric binding site). The orthosteric binding site is highly conserved among adenosine receptor subtypes. Allosteric binding sites display higher sequence variability and show therefore subtype-selectivity. PD 81,723 is a positive allosteric modulator which specifically enhances the response of the adenosine A1 receptor subtype induced by an agonist or the endogenous ligand adenosine (Ado). Allosteric modulation at the A1AR has been investigated mainly by radioligand binding studies using membrane lysates. Stressed or injured cells release high amounts of adenosine and precursors thereof which makes these experimental settings not suitable to monitor allosteric effects in combination with the endogenous ligand adenosine.

This work provides unique insights on allosteric modulation of human and rat A1 adenosine A1 receptors with adenosine as the orthosteric ligand in living HEK293 cells. In order to measure positive allosteric effects an experimental procedure was established using fluorescence resonance energy transfer-based A1AR sensors to observe conformational change of the receptor in real time. This work is the first report on the affinity of PD 81,723 for human and rat adenosine A1 receptor occupied by adenosine in living cells. The affinity of PD 81,723 towards the Ado-occupied human A1AR was increased 5-fold when compared to the NECA-occupied receptor. This change in PD 81,723 affinity is a property of allosteric modulation and is called probe dependency. Furthermore, this work also reports the influence of PD 81,723 on the adenosine concentration-response curves for human and rat adenosine A1 receptor. The protocol developed in this work helps to elucidate a further property of allosteric modulation: the decrease in the dissociation time of the ligand-receptor

complex (Ado-PD 81,723-A1AR). Adenosine dissociation from the ligand-receptor complex was recorded in the absence and presence of PD 81,723. The data indicates that PD 81,723 does not slow the dissociation of adenosine from the orthosteric binding pocket by steric hindrance. The dissociation kinetics of PD 81,723 from the active ligand-receptor complex could be measured for the first time. The comparison of these three kinetic measurements identified the time limiting step of ternary complex dissociation: the significantly slower dissociation of PD 81,723 from active adenosine receptor complex. Thus, A1AR occupied by adenosine is a high-affinity target for PD 81,723.

The putative allosteric binding site, presumably located in the second extracellular loop, was investigated by three single alanine-exchange mutants, S161A, E172A, and I175A. The influence of these three mutations was investigated on the affinity and kinetic behaviour of PD 81,723 in the presence of adenosine. PD 81,723 showed a significant increased affinity for human S161A than for human wt, whereas no change in affinity was observed for the homolog mutant rat S161A compared to rat wt. This difference may originate from differing amino acids; human M162 and rat V162. To elucidate this difference, the adjacent amino acid of human S161A was exchanged for the respective amino acid of rat. As expected, the kinetic phenotype of human S161A was rescued by the mutation of S161A M162V.

In summary, measurements of positive allosteric modulation in combination with endogenous ligand adenosine and detailed kinetics of allosteric modulation at human and rat A1AR were reported for the first time in this work. Data of allosteric modulation in the presence of adenosine are important for the design of clinical trials, since varying adenosine levels in patients have not been considered to date. Altogether this study shows new and unique insights in the interactions of adenosine and PD 81,723 at human and rat adenosine A1 receptor.

1 Introduction

1.1 G protein-coupled receptors

G protein-coupled receptors (GPCRs) are cell-surface receptors which transmit an external stimulus into the cell. The transduction occurs via the activation of heterotrimeric guanine nucleotide-binding proteins (G proteins), which themselves activate cellular signaling cascades. Ligand-induced GPCR and G protein activation consists of several steps (Figure 1). First, a ligand docks on a specific binding site and activates the receptor by inducing a conformational change. Subsequently this leads to the activation of the G protein (further described in 1.1.2), which is interacting with the intracellular domains of the receptor (Oldham and Hamm 2008). The activated G protein regulates effector proteins, which transmit the signal further into the cell.

The receptor signaling is terminated by desensitization and internalization of the receptor. In detail, after the G protein dissociates from the receptor docking site, the G protein-coupled receptor kinases (GRKs) start to phosphorylate amino acids like serine and threonine at the C-terminus of the receptor. β -arrestin is recruited to the phosphorylated amino acids of the receptor. In the classical view, the binding of β -arrestin prevents G proteins from rebinding to the activated receptor conformation and thereby terminating the signaling pathway (Pavlos and Friedman 2017). Receptor-coupled β -arrestins represent a starting signal for the clathrin pathway. Receptor-mediated endocytosis occurs by recruiting proteins like AP2, clathrin and dynamin which internalize the receptor into the cytosol by forming vesicles. The receptors take different pathways, recycling from the endosomal vesicles to the membrane, degradation in lysosomes or long-term down regulation (Rajagopal and Shenoy 2018).

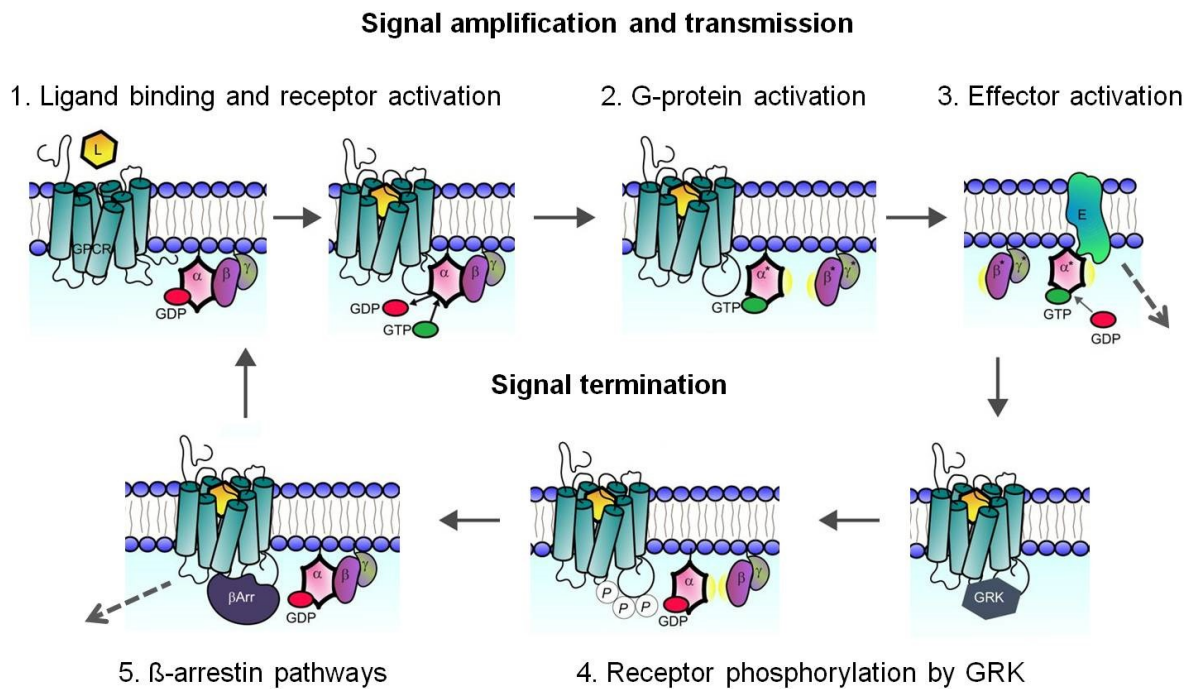


Figure 1: GPCR signaling cycle. Signal transmission consists of three steps. 1) Specific ligand binding to the target receptor and subsequent change of receptor conformation, 2) G protein activation by subunit rearrangement or dissociation, 3) G protein subunits bind to effector proteins and the signaling is further transmitted by distinct pathways [dashed arrow]. The G protein signaling is terminated by 4) recruitment of GRKs (G protein-coupled receptor kinases), which phosphorylate the receptor C-terminus, and 5) subsequent recruitment of β -arrestins. β -arrestins initiate endocytosis of the receptor [dashed arrow] followed by distinct pathways for degradation, down regulation or recycling to the cell surface. Pictures were taken and modified from (Hanlon and Andrew 2015).

GPCRs are involved in the most important processes of an organism to sense its environment by detecting light, mechanic pressure and odorants. Furthermore, they are essential for internal physiological communication of organs and tissues via activation by hormones, ions and nucleotides. The structure of the receptor embedded in the membrane is an hourglass-shaped cylinder formed by seven transmembrane helices (TM domains) resulting in an extracellular N-terminus, three extracellular loops (ECL), three intracellular loops (ICL), and an intracellular C-terminus.

1.1.1 Classification of GPCRs

There are 1265 genes in the human genome and 2334 genes in the rat genome coding for GPCRs (Ono et al. 2005), (<http://sevens.cbrc.jp>, accessed 2019). Next to pseudo genes, expressed receptors were identified via *in vivo* experiments but a notable amount of these receptors are orphans. Orphan receptors are GPCRs without known ligand or stimulus. To keep an overview of this enormous number of receptors two classification systems were developed, the first one is categorizing via

structure similarity and function, A-F System (Kolakowski 1994) whereas the GRAFS system was built up on phylogenetic considerations (Schiøth and Fredriksson 2005). The A-F system contains class A, which harbors “rhodopsin-like” receptors; class B (Secretin/Adhesion) receptors which have large N-terminal domains; class C (Glutamate) and class F (Frizzled) receptors which have their binding pocket within the N-terminus, but there are also GPCRs only found in non-vertebrates, classes D and E. The GRAFS system subdivides GPCRs in five classes; Glutamate, Rhodopsin, Adhesion, Frizzled/Taste2, and Secretin. The largest class in the GRAFS system is the Rhodopsin family, which is further sub-grouped by the chemical nature of the corresponding ligands (Schiøth and Fredriksson 2005).

1.1.2 Heterotrimeric G protein

Guanine nucleotide-binding proteins transmit signals from activated G protein coupled receptors to downstream effector proteins, e.g. membrane-bound enzymes or ion-channels. The heterotrimeric G protein belongs to the GTPase super family, which hydrolyses guanine triphosphate (GTP) to guanine diphosphate (GDP) and pyrophosphate (P_i). The GTP-bound protein is the active mode, whereas the GDP-bound form is the inactive mode of the G protein. The GDP-bound protein requires another protein which catalyzes the release of the GDP from the guanine nucleotide-binding site to return to its active mode. This protein is called guanine nucleotide-exchange factor, shortly as GEF. The opponent of the GEF is the GTPase-activating protein (GAP) which accelerates the GTP hydrolysis and thereby switching the G protein back in the inactive mode. The trimeric G protein consists of three subunits, G_α, G_β and G_γ. The G_α-subunit and the G_γ-subunit contain membrane anchor domains (Wedegaertner et al. 1995). Several isoforms of G_α-, G_β- and G_γ-subunits exist, forming multiple heterotrimeric G protein combinations, which can activate or inhibit different effector proteins. The most prominent α-subunit isoforms are the stimulatory G_{α_s} subunits, which activate the adenylyl cyclase (AC) and its counterpart are the G_{α_i} subunits, which inhibit the AC activity. The adenylyl cyclase regulates the level of the second messenger cyclic adenosine monophosphate (cAMP). Other effector proteins are for instance the phospholipase C, which gets activated by the G_{α_q} subunit (Mukhopadhyay and Ross 1999) and the cGMP phosphodiesterase (PDE), which gets activated by the G_{α_t} subunit (Fung et al. 1981). PDE is important in the signaling pathway of light detection in rod cells.

The trimeric G protein is associated with the GPCR in the inactive GDP-bound state. Upon ligand binding the receptor undergoes a conformational change which leads to a release of GDP and subsequent uptake of cytosolic GTP by the G α -subunit. During this exchange the G protein rearranges its subunits and the α -subunit detaches from the binding site of the receptor. The G β - and G γ -subunits stay in complex with each other while the GTP-bound G α -subunit docks to a nearby effector protein. The G α -subunit activates the effector protein by hydrolyzing GTP and returning to the GDP-bound state. The G α subunit reassembles with the G $\beta\gamma$ -complex and recycles back to the activated receptor. The G protein activation cycle continues until the receptor is desensitized (1.1). The G $\beta\gamma$ -complex can also activate its own set of effector proteins, like the K⁺ channel (Logothetis et al. 1987).

1.1.3 Receptor affinity and kinetics

GPCRs are specifically bound by their endogenous ligands. The specific binding of a ligand and a receptor is described by a high affinity towards each other. Affinity is a measure of the strength of interaction between ligand and receptor. Typically, the binding affinity is reported as the dissociation constant K_D measured at equilibrium conditions. The equilibrium dissociation constant indicates the concentration required to occupy 50 % of the available receptors. At chemical equilibrium, the concentration of the free ligand and free receptor equals the concentration of the ligand-receptor complex, which means that the complex formation and complex dissociation are in balance.



The rate of complex formation k_{on} given in units of $M^{-1}s^{-1}$ and the rate of complex dissociation k_{off} is given in units of s^{-1} . On-rates are concentration dependent whereas off-rates are concentration independent. This is due to the different nature of the chemical reaction. A binding event is a bimolecular reaction of one ligand molecule and one receptor molecule forming a complex. In an unbinding event the reaction starts with one complex and divides into two molecules, which is called a unimolecular reaction. The concentration of the free molecules is obsolete for the velocity of the unimolecular reaction. Experimentally, on-rates are obtained by fitting an association curve with a mono-exponential equation (see methods section 3.2.7)

resulting in the time constant tau. The reciprocal of tau is termed as the observed on-rate k_{obs} (s^{-1}). As explained above k_{on} is dependent on the ligand concentration used for the association experiment. Therefore it is necessary to convert the observed on-rate k_{obs} to k_{on} ($M^{-1}s^{-1}$) with the following equation:

$$k_{on} = \frac{(k_{obs} - k_{off})}{[ligand\ concentration]}$$

For the calculation of k_{on} the determination of the off-rate, k_{off} , is required. The off-rate is obtained by mono-exponential fitting the dissociation curve. The equilibrium dissociation constant K_D can be obtained by the ratio of k_{off} and the calculated k_{on} .

$$K_D = \frac{k_{off}}{k_{on}}$$

This equation describes the link between affinity and kinetics under equilibrium conditions. However, the equilibrium state as stabilized in closed *in vitro* systems, is not occurring under physiological conditions (Copeland 2016). *In vivo* the concentration of ligands varies over time (due to metabolism) as well as the amount of available receptors in the membrane is not constant (because of desensitization, internalization or recycling to the cell surface). Experimental simulation of an open system is achieved by intact living cells expressing the receptor of interest in physiologic buffer together with a ligand perfusion system.

By comparing *in vitro* performance with *in vivo* efficacy of approved drugs it became apparent that, in addition to promising K_D values, further parameters had to be described for the evaluation of drug candidates (Copeland et al. 2006). For instance, tiotropium, an muscarinic-antagonist, compared to a similar compound, showed a superior *in vivo* effect correlating with the slower dissociation kinetics of tiotropium (Disse et al. 1999, Dowling and Charlton 2006). This compound is selective for the muscarinic receptor subtype M3, which was not predicted from the originally calculated K_D values for M1, M2 and M3, but was explained by the separately determined dissociation kinetics (Disse et al. 1993).

A compound can elicit its effects only when bound to its target. This dwell-time (or lifetime of compound-target complex) can be estimated from association rate and dissociation rate of the compound and is referred to as residence time. Per definition

the residence time (RT) is the reciprocal of the dissociation rate, k_{off} (Copeland et al. 2006). RT was defined solely by $1/k_{\text{off}}$, because the inspected compounds showed little variance in association rates compared to the variation in dissociation rates (some even by orders of magnitude). This assumption might be valid for various ligands, but there is increasing awareness of the impact of different association-rates on the ligand-receptor complex stability (Louvel et al. 2014, de Witte et al. 2016). Therefore, it is important to gain knowledge of all relevant parameters of drug candidates such as their affinity, RT, dissociation and association kinetics.

1.2 Adenosine receptors

Adenosine receptors belong to the class A or rhodopsin-like receptors and are part of the purinergic receptor family: the P-family. The P-family includes adenosine responding receptors as well as receptors which respond to ATP and related nucleotides. The latter are further divided in GPCRs, called P2Y and non-GPCRs, called P2X receptors (Abbracchio and Burnstock 1994). The P2X receptors are ligand gated ion-channels, which regulate the passage of intra- and extracellular cations upon binding of ATP. The four adenosine receptor subtypes A1, A2A, A2B and A3 are ubiquitously distributed throughout the body (Fredholm et al. 2001). Adenosine receptors can form homodimers, e.g. A1-A1 (Ciruela et al. 1995) and dimers with other subtypes e.g. A1-A2A (Ciruela et al. 2006). In addition, adenosine receptors form heterodimers with other GPCRs, like dopaminergic receptors e.g. A1-D1 (Gines et al. 2000) detected by immune-precipitation and later on confirmed by fluorescence-based techniques (Briddon et al. 2008). The adenosine receptors A1 and A3 are coupled to G_i which inhibits the adenylyl cyclase activity whereas A2A and A2B are coupled to G_s which stimulates the adenylyl cyclase (Fredholm et al. 2001). Besides cAMP levels, other second messenger pathways are regulated by adenosine receptors, like inositol triphosphate and diacylglycerol levels. Depending on the tissue, adenosine receptor subtypes signal via $G_{q/11}$, $G_{15/16}$ and G_{olf} (Linden et al. 1999, Offermanns and Simon 1995, Kull et al. 2000).

The first adenosine receptor with a resolved crystal structure was the A2A receptor (Jaakola et al. 2008). Most recently crystal structures for the human A1AR were published; two showing inactive receptor conformations with bound antagonists; PSB36 (Cheng et al. 2017), DU172 (Glukhova et al. 2017) and one showing the

active receptor in complex with endogenous ligand adenosine and G protein (Draper-Joyce et al. 2018). The extracellular loops were resolved in detail and revealed new sub-structures: namely the alpha-helix in the second extracellular loop which showed a broader extracellular cavity compared to the A2A adenosine receptor. Such spatial information is important for the determination of binding sites of agonistic drug candidates and allosteric modulators (1.3.3). Although static crystal structures provide detailed molecular insights, ligand binding and unbinding dynamics are not fully understood. Therefore it is required to gain more knowledge on ligand-residue interactions by mutational studies.

1.2.1 Adenosine A1 receptor

The adenosine A1 receptor is widely distributed in the brain tissue, especially in the cortex, cerebellum and hippocampus as well as in the spinal cord. High levels of A1AR expression are also found in heart tissue, aorta, and vas deference. A1AR is also expressed in retina, kidney, adrenal gland, spleen, placenta, testis as well as in adipose tissue (Fredholm et al. 2000, Fagerberg et al. 2014). Various functions of adenosine receptors were dedicated to the AR subtypes by the generation and investigation of single subtype knock-out mice (Wei et al. 2011). Via the A1AR adenosine mediates tubuloglomerular feedback in the loop of Henle and renin release (Brown et al. 2001), lowers anxiety, is involved in neuroprotection (Johansson et al. 2001), and promotes habituation to an new environment (Gimenez-Llort et al. 2005). Furthermore A1AR is involved in vasodilatation (Sato et al. 2005), in regulation of heart rate (Koeppen et al. 2009) and in sleep (Bjorness et al. 2009). Upon agonist stimulation of A1AR, adenylyl cyclase activity is inhibited by G α_i -subunits which leads to lower cAMP levels (Fredholm et al. 2000). A1AR mediated G $\beta\gamma$ signaling regulates phospholipase C (PLC) activity and increases intracellular Ca²⁺ levels (Nalli et al. 2014). Furthermore A1AR activation induces the opening of K⁺ channels and the closing of Ca²⁺ channels (Kirsch et al. 1990, Schulte and Fredholm 2000).

1.2.2 Adenosine receptor ligands

The endogenous ligand adenosine is involved in many biochemical processes. Extracellular adenosine originates from cells releasing ATP. ATP is released upon shear stress or osmotic-dependent volume changes in the cell (Grierson and Meldolesi 1995, Ferguson et al. 1997). Extracellular levels of ATP are controlled by

enzymes, mainly ectonucleotidases as well as phosphatases. ATP is hydrolyzed to AMP by NTPDases (also named CD39) or by pyrophosphatase. AMP is further processed by ecto-5'-nucleotidase, ecto5'NT (or CD73) to adenosine. Additional extracellular adenosine is derived from AMP breakdown to adenosine in the cytosol and transported via equilibrative nucleoside transporters, ENTs (Anderson et al. 1999). The effects of pathophysiological or physiologic adenosine levels on adenosine receptors are blocked or reversed by antagonists. The most famous antagonist of adenosine receptors is caffeine (1,3,7-trimethylxanthine). Caffeine and theophylline (1,3-dimethylxanthine), which is another natural occurring xanthine, are not subtype-selective for adenosine receptors, but antagonist DPCPX (8-cyclopentyl-1-3-dipropylxanthine) shows high affinity for the A1AR subtype. The radio labeled version of DPCPX became the standard antagonist in radioligand competition assays (Lohse et al. 1987).

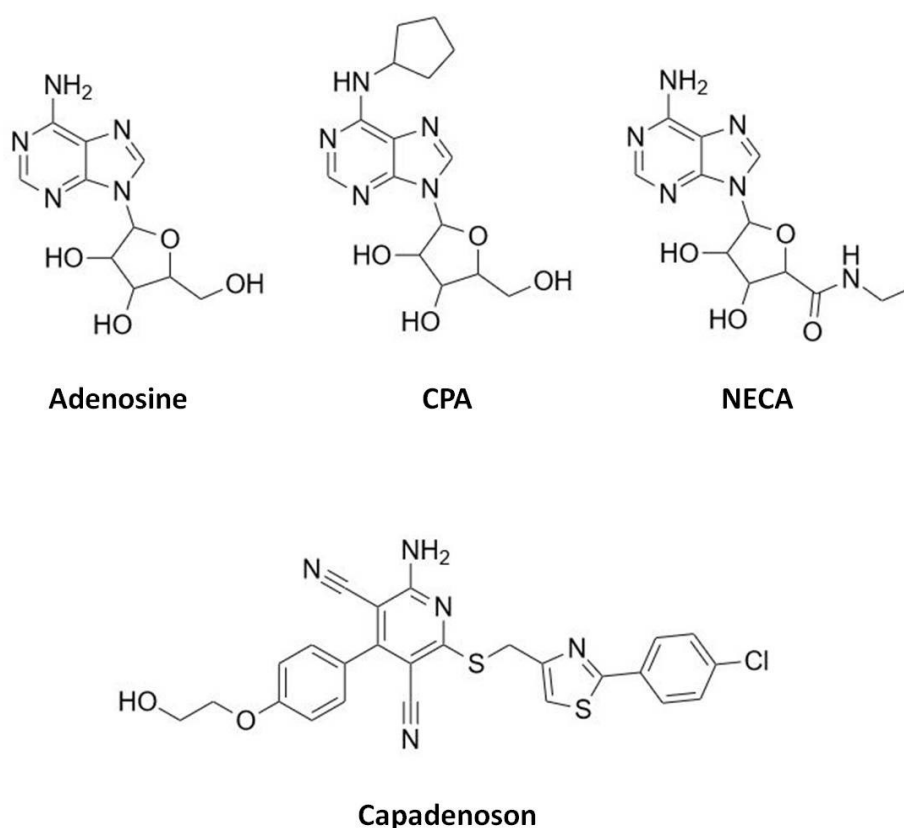


Figure 2: Structures of A1AR agonists. Endogenous agonist adenosine, CPA (N6-Cyclopentyladenosine) and NECA (5'-N-ethylcarboxamidoadenosine) as well as the atypical, non-nucleoside, agonist capadenoson (BAY68-4986). Chemical structures were drawn with the online tool ChemDraw JS (<https://chemdrawdirect.perkinelmer.cloud/js/sample/index.html>).

Numerous A1AR agonists, developed in the last decades, are mainly based on the structure of adenosine (Figure 2). Modification at position N⁶ with a cyclopentylgroup resulted in a higher affinity for A1AR, this agonist is called N⁶-cyclopentyladenosin (CPA) and shows a higher selectivity for A1AR compared to the other AR subtypes. NECA (5'-N-ethylcarboxamidoadenosine) is a modification of adenosine at the ribose moiety leading to an increased affinity for all subtypes (Table 1). Capadenoson, also known as BAY 68-4986, is not based on the structure of adenosine (non-nucleoside agonist). Capadenoson was categorized as partial agonist; inducing low response although full receptor occupancy.

Table 1: Binding affinities of adenosine receptor agonists. Data is represented in nM. K_i-values are represented for A1, A2A and A3. ^a EC₅₀ values for adenosine were determined from adenylyl cyclase assay as well as for A2B due to the lack of radio labeled ligands for A2B receptor subtype (Klotz et al. 1998). Data compiled from (Yan et al. 2003).

		A1	A2A	A2B	A3
Ado	human	100 ^a	310 ^a	15,000 ^a	290 ^a
	rat	73 ^a	150 ^a	5100 ^a	6500 ^a
NECA	human	14	20	330	25
	rat	5.1	9.7	-	113
CPA	human	2.3	794	18,600 ^a	42
	rat	5	3370	-	26

1.2.3 Diseases and therapeutic targeting

Adenosine receptors are promising targets in treating a plethora of disorders, mainly concerning the central nervous system and the cardiovascular system. Istradefylline, an A2A adenosine receptor antagonist, was approved by the FDA for therapeutic use in Parkinson's disease (Hauser et al. 2003). Increased expression of A1 adenosine receptors were identified in cases with disorders of the respiratory system (McNamara et al. 2004, Brown et al. 2008). In these cases, AR antagonists proved to be helpful in the treatment of asthma and chronic obstructive pulmonary disease. Furthermore, it was shown that A1AR antagonism is a promising strategy in sepsis treatment (Wilson et al. 2014). The role of A1AR in cancer is inconsistent and highly dependent on the cancer type (Kazemi et al. 2018).

A1AR agonists are considered for treatment of diseases including type II diabetes, angina, epilepsy, neuropathic pain and arrhythmias. Treatment of the A1AR-mediated supraventricular tachycardia was achieved by application of adenocard,

commercial name of adenosine. This was unfortunately accompanied by undesirable adverse effects, like atrial fibrillation due to lack of AR subtype-selectivity (Mason and DiMarco 2009). A1AR agonists (Tecadenoson, DTI-0009, and GW-493838) with optimized subtype-selectivity completed phase II in clinical studies for treatment of arrhythmias, heart failure or neuropathic pain. Unfortunately, no results were posted on ClinicalTrials.gov (accessed 2020).

The partial A1AR agonist, capadenoson (Figure 2) has been investigated in clinical trials for the treatment of atrial fibrillation (ClinicalTrials.gov, Identifier: NCT00568945, no results; accessed 2020) and angina pectoris (Tendera et al. 2012). The latter study revealed that in Caucasian men with stable angina capadenoson lowered exercise heart rate. However, the international randomized study was withdrawn (ClinicalTrials.gov, Identifier: NCT00518921; accessed 2020). Neladenoson bialanate, a derivative of capadenoson, was investigated for improvements of exercise capacity among patients with heart failure. No significant dose-response relationship for neladenoson bialanate was identified in the clinical study over 20 weeks (Shah et al. 2019). A1 adenosine receptors have a diverse role in regulating the kidney function. Ischemia and reperfusion of the renal tissue occurs during transplant surgery of the organ and results in ischemic-reperfusion injury. In rats, a pretreatment with A1AR specific agonist CCPA (2-chlorocyclopentyladenosine) showed improved renal function 24 h after ischemia (Lee et al. 2004). In mice and rabbits, CCPA causes a decrease in heart rate and systolic blood pressure (Dana et al. 1998, Park et al. 2012). Although preclinical data proved evidence for the therapeutic potential of A1AR agonists, successful drug development is hampered due to adverse side effects (Borea et al. 2018). Since side effects can occur from co-activation of adenosine receptors (Yan et al. 2003), new strategies for specific targeting of receptor subtypes are required.

1.3 Allostery

The phenomenon of allosterism was first observed for inhibitors of enzymes (Monod and Jacob 1961). Other proteins, like membrane receptors were also described to be allosterically regulated (Barker et al. 1986, Bruns and Fergus 1990). An allosteric modulator is an exogenous receptor ligand, which binds to a site distinct from the endogenous ligand binding site. Allosteric binding sites are less conserved than binding sites of endogenous ligands among receptor families, potentially allowing for selective targeting of subtypes (May et al. 2007).

In the field of allosteric studies, the endogenous ligands, agonists or antagonists of a receptor are called orthosteric ligands. Allosteric modulators can change the response of the receptor induced by an orthosteric ligand in a positive (PAM) or negative manner (NAM), or do not change the response, also called silent allosteric modulators (SAM). Classical allosteric modulators are not able to activate the receptor in the absence of a bound orthosteric ligand (Christopoulos 2002). Allosteric modulators alter the dissociation kinetics of orthosteric ligands. This property is used to identify new allosteric molecules by radio labeling techniques (1.3.2).

Allosteric molecules which nonspecifically target GPCRs have been identified, like brilliant black at adenosine receptors (May et al. 2010) and amiloride analogs (Massink et al. 2020). A broad definition of the term allosteric modulator includes the G protein itself. Consequently this would characterize all proteins and molecules binding apart from the orthosteric site as allosteric ligands, like fatty acids of the surrounding membrane or even sodium ions of the interstitium (van der Westhuizen et al. 2015). Studies investigating endogenous allosteric modulators, like extracellular cations allosterically modifying A2A receptor (Ye et al. 2018), provide useful information for MD simulations but are of minor benefit for the drug discovery-discussion, aiming for specific modulation without changing the overall physiology.

The actions of allosteric modulators, in the definition of synthetic extracellular approaching molecules, are dependent on the orthosteric ligand bound to the receptor. This phenomenon is called probe dependency (Kenakin 2005, Kollias-Baker et al. 1994). The term probe refers to the orthosteric ligand. An allosteric modulator may enhance a response of one probe, while it decreases the response of another probe or exhibit no effect. For instance, the bound probe could cause a

conformational change of the receptor and thereby creating or improving the binding site for the allosteric molecule, which results in an increased allosteric binding affinity.

Another important property of allosteric modulators is quantified by the cooperativity factor (Ehlert 1988, May et al. 2007). This factor describes the direction (PAM or NAM) and the strength of the allosteric influence on the orthosteric binding affinity or orthosteric efficacy. Cooperativity defines the degree of communication between the allosteric binding site and the orthosteric ligand binding site and vice versa. In the presence of a negative allosteric modulator the concentration of the agonist to reach the half maximal effect is increased (right-shift of concentration-response curve) and in the presence of positive allosteric modulator the EC_{50} is decreased (left-shift of concentration-response curve). As shown in Figure 3, the extent of the shift is limited, based on the theory that all available allosteric binding sites are occupied at high concentrations of modulator. The ceiling effect of allosteric effect bears a therapeutic advantage over agonist or antagonist treatment; the danger of overdosing is avoided.

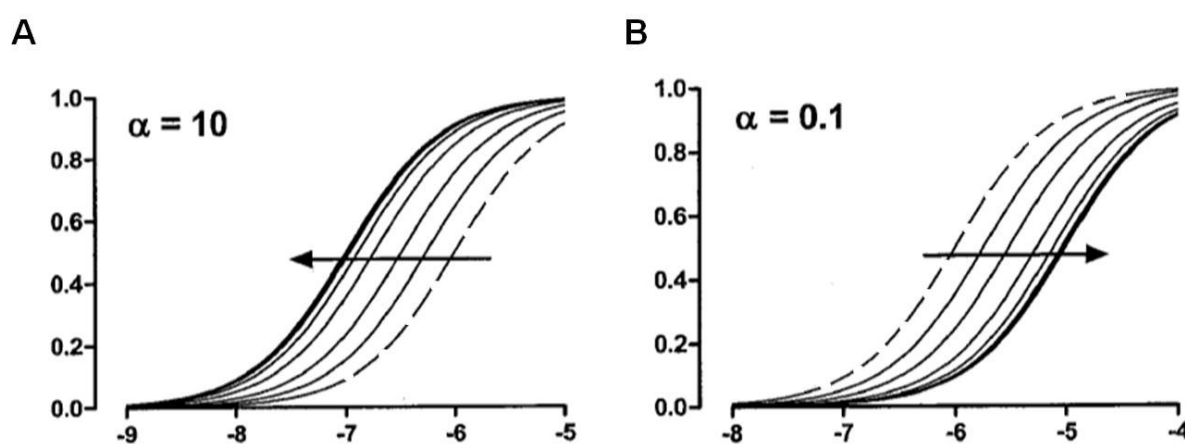


Figure 3: Cooperativity of orthosteric ligand and allosteric modulator. **A**, positive cooperativity of allosteric modulators is characterized by shifting concentration-binding curve of the orthosteric ligand [dashed line] to the left. With increasing concentrations of allosteric modulator the curve is shifted further until a limit is reached (bold solid line). The extent of the shift defines the cooperativity factor $\alpha > 1$. **B**, negative cooperativity ($\alpha < 1$) results in the right-shift of the concentration-binding curve. Picture was taken and modified from (Christopoulos and Kenakin 2002).

1.3.1 Allosteric interactions at GPCRs

Allosteric ligands can regulate affinity and efficacy of the orthosteric ligand. Two molecules bound to distinct sites at a GPCR interact via conformational changes and might influence the binding properties and the effect-transmission of each other. Several models exist to map the complex interplay of orthosteric ligand, allosteric modulator and the receptor. The allosteric ternary complex model, ATCM (Christopoulos 2002) focuses on the ability of allosteric modulator to change the affinity of the orthosteric ligand and vice versa. In literature, the ligands in allosteric models are denoted by A for agonist and B for second agonist or allosteric modulator (Christopoulos and Kenakin 2002). In this present work, the terms used in the field of allosteric modulation were instead used. The ATCM for GPCRs requires the binding of two ligands, the orthosteric ligand (O) and the allosteric ligand (A), to the receptor (R) forming a tri-molecular complex (OAR), see Figure 4 B. The orthosteric ligand binds to the receptor with an affinity constant K_{Ortho} forming a bimolecular complex OR. The allosteric ligand can bind to the receptor, with an affinity constant K_{Allo} , forming the bimolecular complex AR. The single ligand can bind to the binary complex (either O to AR, or A to OR) with different binding affinities governed by the cooperativity of the binding sites (αK_{Ortho} or αK_{Allo}) and subsequent formation of triple-complex OAR.

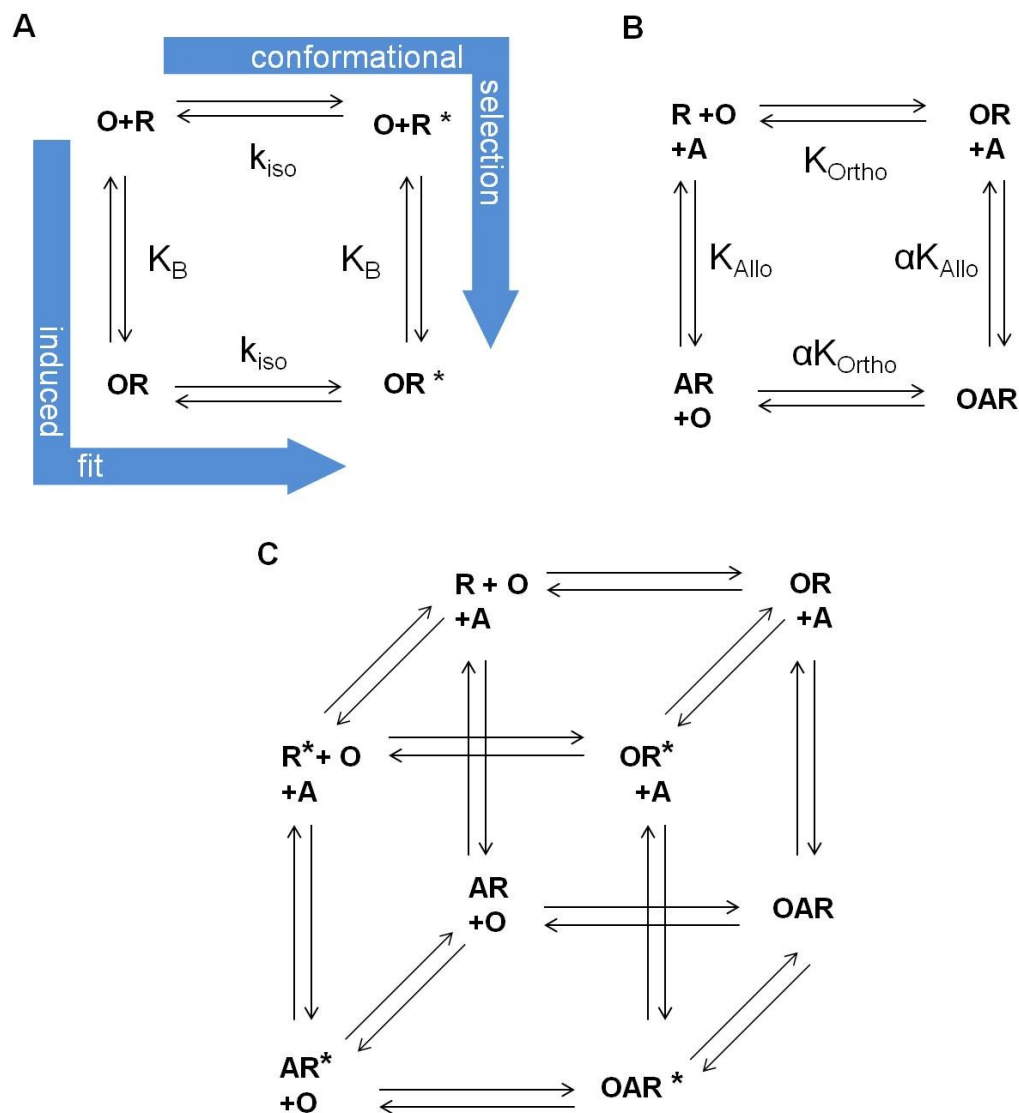


Figure 4: Receptor binding models. **A**, two state model of orthosteric ligand binding. Binding of orthosteric ligand (O) to the inactive receptor (R) can either occur via an induced fit mechanism with the intermediate state of inactive orthosteric-receptor complex (OR) or via a conformational selection mechanism with the intermediate state of spontaneous active receptor R^* . Both theoretical pathways result in the active receptor ligand complex (OR^*). K_B , binding constant under equilibrium conditions; k_{iso} , rate constant of isomerization of receptor states R and R^* . **B**, allosteric ternary complex model, ATCM. Receptor is either bound by orthosteric ligand resulting in OR, or receptor is bound by allosteric modulator (A) resulting in allostere-receptor complex (AR). O can bind to AR and A can bind to OR with binding constant altered by factor α . K_{Ortho} , binding constant of orthosteric ligand; K_{Allo} , binding constant of allosteric modulator; α , cooperativity factor. **C**, allosteric two-state model shows interactions of orthosteric ligand and/or allosteric modulator with the receptor in inactive or active state (isomerization and binding rate constants are not indicated due to clarity reasons).

The classical ATCM is based on equilibrium constants neglecting the ability of the allosteric modulator to change the efficacy of the orthosteric ligand in addition to changing its affinity. Furthermore the simple ATCM does not take into account that the receptor may exhibit different binding affinities either in its inactive conformation

or active conformation. The two-state model of receptor activation considers the occurrence of inactive (R) and active (R*) receptor states (Leff 1995). This model includes two kinetic pathways of receptor activation by an orthosteric ligand; induced fit mechanism or conformational selection, as explained in Figure 4 A. By combining the simple ATCM with the two-state model, the allosteric two-state model was developed (Hall 2000), Figure 4 C). Another layer of complexity was added by incorporation of the interactions between G protein and receptor, resulting in the quaternary allosteric complex model (Christopoulos and Kenakin 2002). The focus of this work is on the allosteric two-state model, see Figure 4 C. For the first time the states of OR* and OAR* will be experimentally resolved by recording receptor conformational changes using FRET. Biosensors based on the FRET technique are explained in chapter 1.4.2.

1.3.2 State of the art

Currently, the methods to determine allosteric modulation of G protein-coupled receptors are based on dissociation experiments of radio labeled ligands at isolated membranes. In order to determine orthosteric ligand binding properties, the receptors are incubated with the radio labeled orthosteric ligand until ligand-receptor-equilibrium is reached. In a second step a saturating concentration of unlabelled orthosteric ligand is applied. The unlabelled orthosteric ligand competes with the radio labeled orthosteric ligand, and the dissociation rate of the radioligand is consequently determined (Figure 5 A). In different research groups, infinite dilutions are used to initiate dissociation of radioligand instead of using unlabeled ligand. To quantify the influence of the allosteric ligand on the orthosteric ligand, the kinetic dissociation assay is conducted in the presence of unlabeled allosteric ligand (Figure 5 B). In principle the receptors are incubated with radio labeled orthosteric ligand until equilibrium is reached. In a second step unlabeled allosteric ligand along with unlabeled orthosteric ligand is applied. In the third step a saturating concentration of unlabelled orthosteric ligand is applied to replace the radio labeled orthosteric ligand from the receptor. Moreover, different protocols are used for the dissociation assay in the presence of allosteric modulator (e.g. in the second step: the unlabeled allosteric ligand is applied before the unlabeled orthosteric ligand is applied). These varying experimental conditions have to be considered in comparing binding data of orthosteric ligands and allosteric modulators.

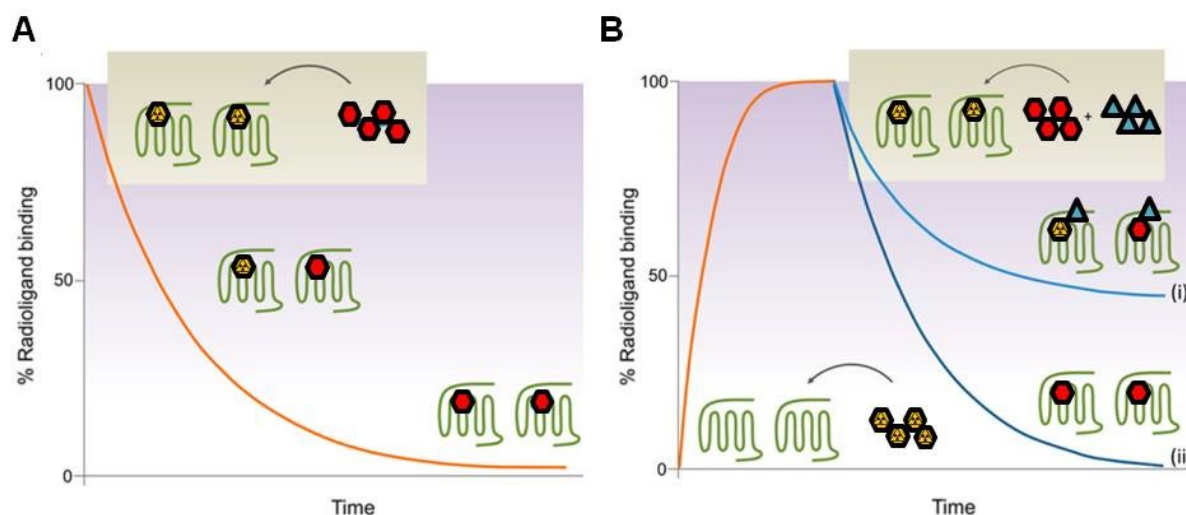


Figure 5: Radioligand-based methods to measure orthosteric and allosteric kinetics at GPCR. **A**, Determining orthosteric ligand dissociation. The receptor-containing material is pre-incubated with radio labeled ligand (yellow hexagon) 100 % radioligand binding, and then a saturating concentration of unlabeled competitor (red hexagon) is added. After a period of incubation, the dissociation of the labeled ligand is complete. Receptors are occupied by the unlabeled ligand. **B**, Determining ligand dissociation in the presence of an allosteric modulator. Incubation of the receptor-containing material with the radio labeled ligand (yellow) until ligand-receptor complex equilibrium is reached (orange curve). An allosteric modulator (cyan triangles) is added, forming the orthosteric-allosteric-receptor complex, together with an excess amount of an unlabeled competitor (red) to start the dissociation of the labeled ligand. After a period of incubation, the allosteric activity is evaluated on the basis of a comparison between the residually bound labeled ligand in the presence (i) or absence (ii) of the allosteric modulator. Picture was taken and modified from (Guo et al. 2017).

Radioligand binding studies detect only changes in alloster-mediated binding affinity but no conformational consequences thereof. In addition, functional assays have to be conducted in order to reveal discrepancies in binding and effect transmission e.g. identification of silent allosteric modulators. Adenosine deaminase has to be applied to the receptor containing material, since adenosine is released by injured membranes or stressed cells. Thus, the investigation of allosteric modulation in the presence of endogenous ligand adenosine is not feasible using this method.

1.3.3 Allosteric modulator PD 81,723

Allosteric modulators have several advantages over orthosteric ligands for drug development. They have no or minor effects in the absence of orthosteric ligand and therefore avoid permanent receptor activation or receptor inhibition. In addition, allosteric modulators will act at the site of endogenous ligand activity, allowing tissue-specific pharmacological treatment. Thus, allosteric modulators show a spatiotemporal mode of action dependent on the orthosteric ligand behavior. As mentioned above, the risk for overdosing is reduced due to saturation of allosteric

effect. Most importantly, allosteric modulator binding sites are less conserved compared to the endogenous binding site among receptor subtypes. This facilitates the development of subtype-selective drugs for receptor families with high sequence identity, like muscarinic receptors or adenosine receptors.

PD 81,723 was identified as allosteric modulator in an A1AR binding screen of the Parke-Davis compound bank (Bruns and Fergus 1990, Bruns et al. 1990). At high concentrations PD 81,723 (> 20 μ M) displayed competitive antagonism. At low concentrations PD 81,723 enhanced the binding affinity of A1AR agonists and slowed down the dissociation of agonist CHA from rat A1AR. The positive allosteric effects of PD 81,723 are selective for the A1AR subtype (Bruns and Fergus 1990, Kollias-Baker et al. 1994, Mizumura et al. 1996). Long term application of PD 81,723 compared to A1AR specific agonist treatment showed minor desensitization and down-regulation of A1ARs (Bhattacharya and Linden 1996), which is a promising finding in terms of drug safety. The binding site of PD 81,723 was proposed to be located in the second extracellular loop (Narlawar et al. 2010). Site-directed mutagenesis studies of human A1AR supported this assumption (Peeters et al. 2012, Kennedy et al. 2014, Nguyen et al. 2016b). Nguyen and co-workers postulated that the allosteric binding site is in close proximity to the orthosteric binding pocket and identified residue E172 as key determinant for allosteric binding.

The therapeutic potential of PD 81,723 was successfully shown *in vivo*, by investigating ischemic damage in heart, CNS and kidney tissues. Ischemic damage is reduced by short intervals of ischemia prior to prolonged phase of ischemia, termed preconditioning. In the presence of PD 81,723 the time required to achieve a preconditioning effect in canine hearts was reduced (Mizumura et al. 1996). A medium dose of PD 81,723, systemically administered to rats prior to 10 min of ischemia, significantly reduced injured hippocampal tissue and improved learning performance compared to vehicle treated group (Meno et al. 2003). PD 81,723 decreased inflammation, necrosis, and apoptosis in kidney ischemic-reperfusion injury without cardiovascular side effects in mice (Park et al. 2012).

Based on PD 81,723 as lead compound (Figure 6), chemists have developed several allosteric modulators (Bruns et al. 1990, van der Klein et al. 1999, Baraldi et al. 2003, Aurelio et al. 2009). T-62, a more potent derivative of PD 81,723 was investigated in clinical trials for neuropathic pain but was terminated due to liver toxicity (Clinical trials.gov NCT00809679).

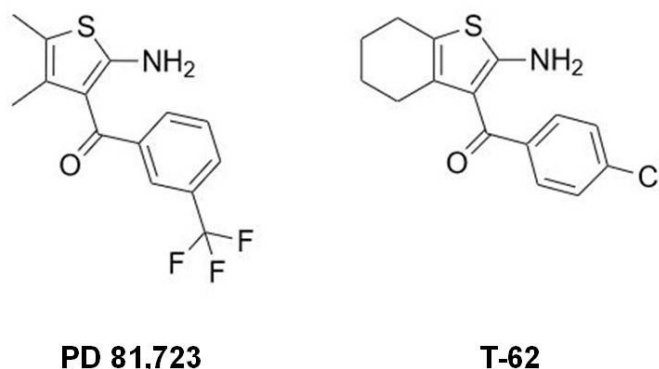


Figure 6: Structures of A1AR positive allosteric modulators. PD 81,723 (2-amino-4,5-dimethylthiophen-3-yl)-[3-(trifluoromethyl)phenyl]methanone and T-62 (2-amino-4,5,6,7-tetrahydro-1-benzothiophen-3-yl)-(4-chlorophenyl)methanone. Chemical structures were drawn with the online tool ChemDraw JS (<https://chemdrawdirect.perkinelmer.cloud/js/sample/index.html>).

Despite the multitude of PD 81,723-based compounds with improved enhancing activity and reduced antagonism (Romagnoli et al. 2015), the progression to clinical trials is modest. Newly synthesized allosteric compounds are characterized and ranked by data derived from radioligand binding studies and functional assays using only synthetic AR agonists. Therefore structure-affinity- and structure-kinetic-relation studies with the endogenous ligand adenosine are missing but are of utmost importance to predict the *in vivo* behavior of allosteric compounds. In addition, species differences of A1AR have to be considered for future screening of candidate series to facilitate the transition from animal testing to clinical trials.

1.4 Fluorescence microscopy

Fluorescence microscopy is a fundamentally important method in many applications in all fields of life science. Fluorescence-based techniques are used in high-throughput screenings of pharmaceutical industry and in basic research to observe the location or interactions of single molecules in living cells. Moreover, conformational changes of single molecules can be recorded by labeling the molecule of interest with two distinct fluorophores capable of resonance energy transfer (RET).

Fluorophores are molecules which absorb light and are thereby elevated from their energetic ground state to the excited state. By spontaneous emission of light, the fluorophore returns to the ground state. Absorption and emission of photons and the occurring energy transfer are usually shown in energy diagrams, termed Jablonski diagrams. To be more precise, the Jablonski diagram in Figure 7 A shows energy levels (black horizontal lines) of electron transitions. A prerequisite for fluorescence are delocalized electrons in π -orbitals. Electrons in π -orbitals are usually oriented in anti-parallel spin, occurring in three singlet-states (S_0 - S_2). Each of these singlet-states consists of vibrational energy levels (0, 1, 2). By absorption of a photon ($h\nu$) an electron is lifted from the energetic ground state (S_0) to a higher vibration-level of an excited state, either to S_1 or to S_2 . Electrons from the S_2 convert to S_1 due to vibration energy loss (internal conversion). The transition from the S_1 state to the ground state can occur with or without emission of a photon (fluorescence or quenching). The energy of the emitting photon is reduced compared to the absorbed photon; accordingly the wavelength of excitation light is shorter than the wavelength of the emitted light. This change in wavelength is called Stokes shift (Lakowicz 2006).

1.4.1 Fluorescence resonance energy transfer

Fluorescence or Förster resonance energy transfer, short FRET, is a photochemical phenomenon which was discovered by Theodor Förster (Förster 1948). It describes the transfer of energy from an excited fluorophore to a second fluorophore, which releases the energy by emitting a photon as illustrated in Figure 7 B. The molecule which transfers the energy is called donor and the absorbing molecule is called acceptor. The energy transfer occurs via dipole-dipole interactions without intermediate photon emission. Three factors influence an efficient energy transfer: 1) the distance of the molecules is within the range of 10 to 100 Angstroms, 2) the

orientation of donor and acceptor dipoles is approximately parallel and 3) the emission spectrum of the donor overlaps the absorption spectrum of the acceptor. The acceptor emits light in a higher wavelength than the donor, which facilitates the measuring of FRET.

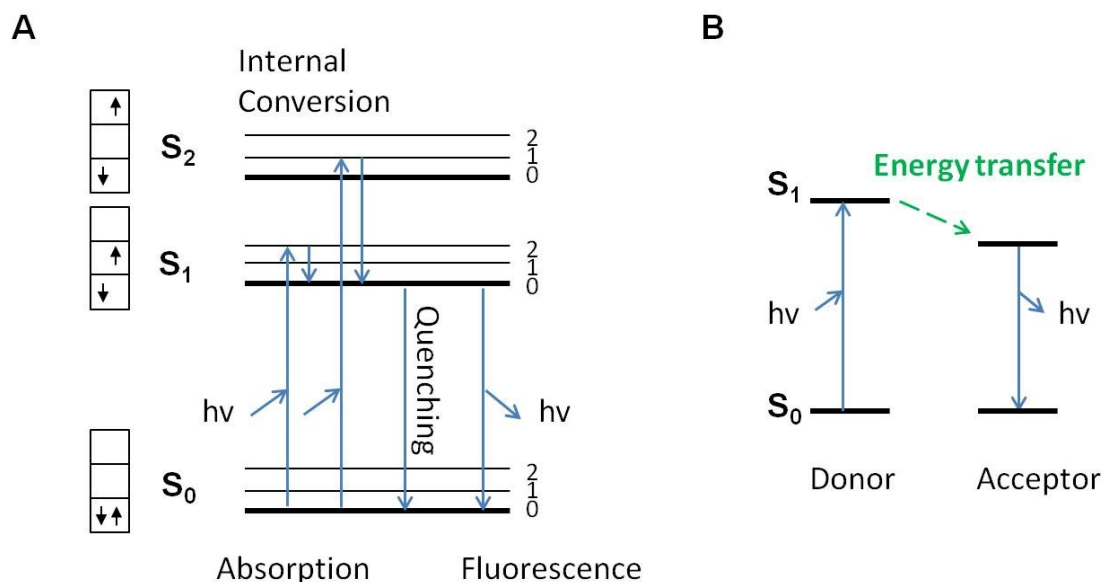


Figure 7: Jablonski diagrams showing energy states of a fluorophore upon excitation and emission of light and energy transfer of two fluorophores. A, excitable electrons of a fluorophore with opposing spin orientation (boxes and black arrows on the left) can occur in singlet states, S_0 , S_1 , and S_2 , which are characterized by vibrational energy levels 0, 1, 2 (black horizontal lines). Upon absorption of a photon ($h\nu$) the electron in the ground state S_0 is excited either to the S_1 or the S_2 excited states. A fast transition without photon emission occurs from the excited S_2 state to the S_1 , this process is called internal conversion. The transition from S_1 to S_0 can occur without (quenching) or with photon emission (fluorescence). Electron transitions are depicted with blue vertical lines. **B,** simplified Jablonski diagram to illustrate fluorescence resonance energy transfer (FRET). The donor molecule is excited to the S_1 state by absorption of a photon. Energy is transferred to a second fluorophore within a distinct distance and with appropriate absorption spectrum. The energy transfer to the second fluorophore, the acceptor, occurs via direct dipole-dipole interactions. Consequently, the acceptor molecule emits a photon.

The FRET technique is exploited for a multiplicity of biochemical applications. This technique enabled analyzing protein-protein interactions as well as ligand-receptor interactions, internal protein conformation changes and protein folding. Moreover, FRET can be used as a nano-meter ruler applied on oligonucleotides to determine distances. Energy transfer can be detected in different ways: 1) Observing the fluorescence intensity level of the donor before and after disrupting the ability of acceptor for FRET, either by photo bleaching or by removal of the acceptor from the range wherein FRET can occur. With this approach the efficiency of FRET can be determined. 2) Observing the fluorescence lifetime (average dwell-time in the excited state, Figure 7 A) of individual donor molecules. The lifetime decays faster in the presence of a quenching or an acceptor molecule. 3) Observing the fluorescence intensity of acceptor and donor; decrease in donor intensity and simultaneous increase in acceptor intensity (see Figure 8 A). This technique is called sensitized emission and is used in this work to monitor conformational changes of A1AR-FRET sensor upon ligand binding (1.4.2). FRET is recorded with an inverted fluorescence microscope equipped with beam splitters and two photon detectors allowing for simultaneous recording of donor and acceptor emission (Figure 8 B).

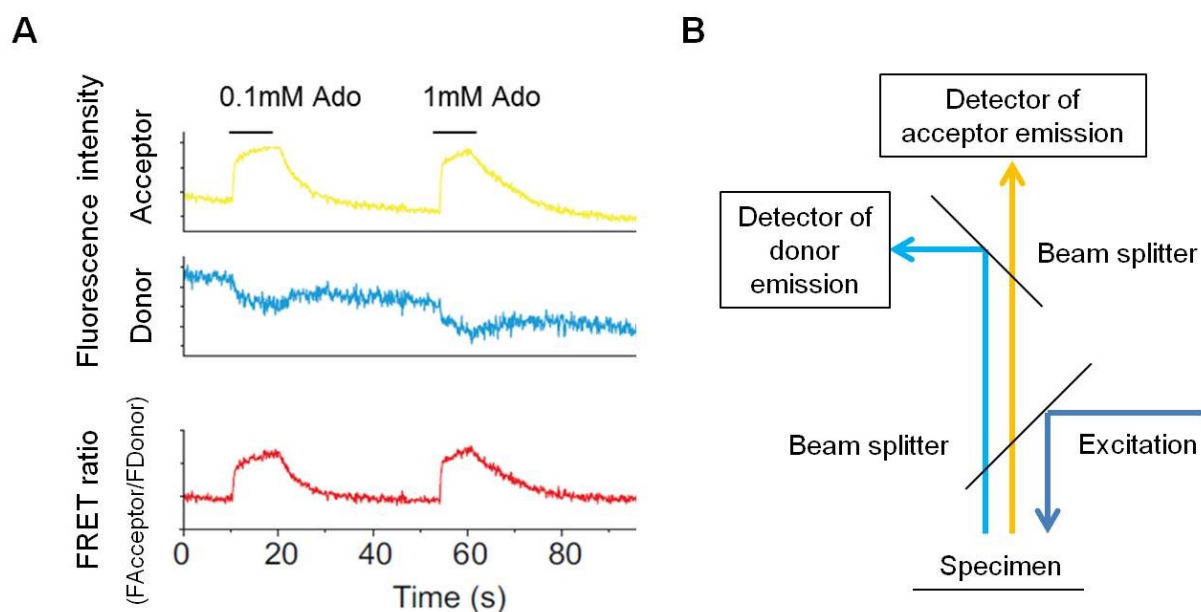


Figure 8: Sensitized emission detection of FRET. **A**, donor (blue) and acceptor (yellow) fluorescence of human A1AR-FRET sensor is simultaneously recorded over time. Ratio of acceptor fluorescence and donor fluorescence (red) is used as read-out of FRET. Upon adenosine (Ado) stimulation the acceptor fluorescence intensity increases and the donor fluorescence intensity decreases. **B**, schematic drawing of inverted fluorescence microscope with excitation and emission pathway. Beam splitter (45° black lines) separate excitation (blue) from emission and donor emission (turquoise) from acceptor emission (yellow).

1.4.2 GPCR FRET sensors in intact living cells

FRET biosensors, which measure intramolecular conformational changes upon GPCR activation, were generated by insertion of fluorescent tags in the third intracellular loop and in the C-terminus of the receptor (Villardaga et al. 2003, Hoffmann et al. 2005, Jensen et al. 2009). In the field of GPCRs the most used acceptor-donor pair is yellow and cyan fluorescent protein, YFP-CFP, and their derivatives. The size of YFP (30 kDa) hampers the binding of the G protein to the receptor and therefore the signaling function of the FRET-sensor is reduced. This limitation was circumvented by a protein labeling technique with a membrane-permeable small fluorescein derivative, called FIAsH (Griffin et al. 1998). FIAsH, fluorescein arsenical hairpin binder, is smaller in size and elicits a higher quantum yield than YFP in living cells (Hoffmann et al. 2005). FIAsH specifically binds the six amino acid sequence, CCPGCC and thereby becomes fluorescent. For the adenosine A2A FRET-sensor it was shown that FIAsH bound to the tetracysteine binding motif encoded in the third intracellular loop preserved the signaling function of the receptor (Hoffmann et al. 2005). Human and rat adenosine A1 adenosine receptor FRET sensors (Stumpf 2015) with the tetracysteine binding motif genetically encoded in the third intracellular loop and the CFP fused to the C-terminus were used in this work.

2 Aims of the study

Regardless of several attempts in the last decades to develop specific agonists to target single subtypes of adenosine receptors, only few drugs and diagnostic tools are on the market. Besides low *in vivo* efficacy, this is often due to severe side effects based on co-activation of all adenosine receptor subtypes.

Allosteric binding sites are less conserved across receptor subtypes, therefore allosteric modulators are promising tools to increase target specificity. The positive allosteric modulator PD 81,723 is specific for the adenosine A1 receptor and enhances the effect of agonists as well as the endogenous ligand adenosine.

Until today, information on allosteric modulation mainly originates from *in vitro* radioligand binding studies using cell lysates. Broken membranes release adenosine and precursors thereof, which complicates the investigation of the endogenous ligand. Contrary to radioligand based methods, fluorescent resonance energy transfer (FRET) techniques allow for real-time recordings of receptor conformational changes or receptor-protein interactions in intact living cells.

The purpose of this work is therefore the investigation of the applicability of the FRET technique to measure positive allosteric modulation on adenosine A1 receptor in the presence of endogenous ligand adenosine. With these FRET measurements two main aims should be addressed:

- Investigate potential differences between human and rat adenosine A1 receptor particularly with regard to affinity and kinetics of PD 81,723.
- Study the role of the second extracellular loop as putative allosteric binding site via mutational analysis.

3 Material and Methods

3.1 Material

3.1.1 Chemicals and reagents

Table 2: Purchased chemicals and reagents

EDT (1,2-Ethanedithiol)	Sigma life science
Adenosine	Sigma life science
Agar	Applichem
Ampicillin	Sigma life science
Ampuwa (H ₂ O for ligand preparation)	Fresenius Kabi Deutschland
Buffers for molecular cloning	New England Biolabs
CaCl ₂	Applichem
CPA (<i>N</i> -Cyclopentyladenosine)	Tocris
DMEM, cell culture grade	PAN-Biotech
DMSO (dimethyl sulfoxide)	Sigma life science
Effectene [®] transfection reagent	Qiagen
Ethanol ≥ 99 %	Sigma life science
FBS	Biochrom AG
FIAsH	Toronto Research Chemicals
G418 (Geneticin Sulfate)	Gibco-ThermoFisher
Glucose	Applichem
H ₂ O ₂ , 30 %	Sigma life science
HDGreen [™] DNA-Dye	Intas Science Imaging Instruments
HEPES	Applichem
Isopropanol ≥ 99 %	Sigma life science
Kanamycin	Applichem
KCl	Applichem
L-Glutamin	Sigma life science
Loading dye, 6x	New England Biolabs
MgCl ₂	Applichem
Myco-1&2 Set	Applichem
NaCl	Applichem
NaOH	Applichem
NECA (5'-N-Ethylcarboxamidoadenosine)	Tocris
PBS	Sigma life science
PD 81,723 (2-amino-4,5-dimethyl-3-thienyl)-[3-(trifluoromethyl)-phenyl]methanone)	Tocris
Penicillin 10000 U/ml, Streptomycin sulfate 10 mg/ml	Sigma life science
Poly-D-Lysine hydrobromide	Sigma life science
Restriction enzymes	New England Biolabs
TAE buffer 10x	Merck, Sigma life science
Theophylline	Sigma life science

Trypsin/EDTA
Tryptone
Universal agarose, peqGOLD
Yeast extract

Gibco-ThermoFisher
Applichem
Peqlab-VWR life science
Applichem

3.1.2 DNA

Table 3: Plasmids used in this work

The denomination FIAsh2 in this list refers to the second position out of two possible positions for the FIAsh-motif insertion in the third intracellular loop. The FIAsh-motif (CCPGCC) was inserted between D221 and P222.

name	resistance gene	source
hA1 in pcDNA3	ampR	Dr. Ulrike Zabel
pc-huA1R- FIAsh2 CFP	ampR	Dr. Ulrike Zabel
pc-huA1R-(S161A)- FIAsh2 CFP	ampR	Dr. Ulrike Zabel
pc-huA1R-(E172A)- FIAsh2 CFP	ampR	Dr. Ulrike Zabel
pc-huA1R-(I175A)- FIAsh2 CFP	ampR	Dr. Ulrike Zabel
pc-huA1R-(S161A M162V)- FIAsh2 CFP	ampR	Dr. Ulrike Zabel
pc-ratA1R	ampR	Dr. Anette Stumpf
pc-ratA1R- FIAsh2 CFP	ampR	Dr. Ulrike Zabel
pc-ratA1R-(S161A)- FIAsh2 CFP	ampR	Dr. Ulrike Zabel
pc-ratA1R-(E172A)- FIAsh2 CFP	ampR	Monika Frank
pc-ratA1R-(I175A)- FIAsh2 CFP	ampR	Monika Frank
pc-ratA1R-(S161A V162M)- FIAsh2 CFP	ampR	Dr. Ulrike Zabel
pGβ-2A-YFP-G2-IRES-Gi1-mTq2 in pEGFP-C1	kanR	Dr.ir. J. Goedhart
pGβ-2A-YFP-G2-IRES-Gi2-mTq2 in pEGFP-C1	kanR	Dr.ir. J. Goedhart
pGβ-2A-YFP-G2-IRES-Gi3-mTq2 in pEGFP-C1	kanR	Dr.ir. J. Goedhart

UZ, AS, MF University of Würzburg; JG University of Amsterdam

3.1.3 Cell lines

Table 4: Cell lines used in this work

The denomination FIAsh3 in this list refers to the third intracellular loop. The FIAsh-binding motif was inserted in the third intracellular loop.

name	source
HEK293	ATCC
HEK 293 human A1 FIAsh3 CFP	Hoffmann-Group
HEK 293 human A1 FIAsh3 CFP S161A	this work
HEK 293 human A1 FIAsh3 CFP E172A	this work
HEK 293 human A1 FIAsh3 CFP I175A	this work
HEK 293 human A1 FIAsh3 CFP S161A M162V	this work
HEK 293 rat A1 FIAsh3 CFP	Hoffmann-Group
HEK 293 rat A1 FIAsh3 CFP S161A	this work
HEK 293 rat A1 FIAsh3 CFP E172A	this work
HEK 293 rat A1 FIAsh3 CFP I175A	this work
HEK 293 rat A1 FIAsh3 CFP S161A V162A	this work

3.1.4 Kits

Effectene transfection reagent was used for stable or transient transfection of HEK293 cells as per manufacturer's instructions.

Plasmid DNA Purification NucleoBond® Xtra Midi from Macherey-Nagel GmbH & Co. KG was used for plasmid preparation.

Cell lines were tested for possible mycoplasma contamination on a regular basis. Myco-1&2 Set from AppliChem was used according to manufacturer's instructions, if stable cell lines were infected.

3.1.5 Medium and buffers

Table 5: Media used for cultivation of *E.coli*

LB-medium	
NaCl	1 % (w/v)
Tryptone	1 % (w/v)
Yeast extract	0.5 % (w/v)
LB-medium solid	
Agar	1g/100 ml LB-medium
Ampicillin	100 µg/ml
Kanamycin	70 µg/ml

Table 6: Buffer used for transformation of chemically competent *E.coli*

KCM buffer	
KCl	100 mM
MgCl ₂	50 mM
CaCl ₂	30 mM

Table 7: Media used for cultivation of HEK293 cells

DMEM+++ (4.5 g/l glucose)		
Penicillin/streptomycin	10 % (w/v)	
L-Glutamine	2 mM	
FBS	10 % (w/v)	
DMEM+++ for freezing		store at -20 °C
DMSO	5 % (w/v)	
FBS	additional 5 % (w/v)	
DMEM+++ for mutant cell lines		
Theophylline	5 mM	add via sterile filtration

Table 8: Composition of physiological buffers used for HEK293 cells

Labeling buffer	concentration	
HEPES	10 mM	
NaCl	150 mM	
KCl	25 mM	
MgCl ₂	2 mM	
CaCl ₂	4 mM	
Glucose	10 mM	add directly before use
pH 7.3		
FRET/measuring buffer		
HEPES	10 mM	
NaCl	140 mM	
KCl	5.4 mM	
MgCl ₂	1 mM	
CaCl ₂	2 mM	
pH 7.3		

3.1.6 Ligand preparation

Adenosine was purchased from Sigma-Aldrich. NECA (5'-N-Ethyl-carboxamidoadenosine), and PD 81,723 (2-amino-4,5-dimethyl-3-thienyl)-[3 (trifluoromethyl)-phenyl]methanone) were purchased from Tocris. FIAsh is commercially available from Toronto Research Chemicals (Canada). Since PD 81,723 is instable in DMSO (Joshi et al. 2004) stock solutions were prepared in EtOH (≥ 99 %).

3.1.7 Equipment

Table 9: Equipment and software used in this work

FRET-Microscope	Zeiss Axiovert 2000
Confocal microscope	Leica TCS SP8
Perfusion system	ALA Scientific
Attofluor cell chamber	Invitrogen, ThermoFisher Scientific
Cover glasses, round 24mm	Hartenstein, Würzburg
Software	
Clampex	Molecular Devices
GraphPad Prism 7.03	Graph pad
Leica LAS AF	Leica
Origin 9 Pro	Origin labs
UCSF Chimera	UCSF Resource for Biocomputing, NIH

3.2 Methods

3.2.1 Molecular biology

3.2.1.1 Polymerase chain reaction

The polymerase chain reaction (PCR) is used to amplify DNA-fragments. The length of a desired fragment is defined by two oligonucleotides, also called primers, which are in part complementary to the DNA strand. One PCR cycle consists of denaturing, annealing and elongation steps. At first, the double stranded-DNA is split in two strands at 94 °C during denaturation. This is followed by the annealing of the oligonucleotides to the complimentary parts on the respective strand at a temperature of about 54 °C. In the final elongation step of the cycle, heat-stable DNA-synthesizing enzymes, called polymerases recognize the strand-oligonucleotide complex and start to complete the DNA molecule by adding free nucleotides to the complementary bases at 72 °C. This cycle is repeated 30 - 35 times to gain an appropriate amount of DNA for further processing.

Table 10: Composition of standard PCR reaction

DNA of interest	100 ng
Buffer 10x	10 µl
Oligonucleotide 1	3 µl
Oligonucleotide 2	3 µl
dNTPs	10 mM
Polymerase	1 µl
	up to 100 µl H ₂ O

3.2.1.2 Electrophoretic separation of DNA

DNA was analyzed for fragment size by separation on a 1 % (w/v) agarose gel, containing HDGreen DNA-Dye (4 µl/100 ml ~50 °C agarose) in 1xTAE-buffer at 120 V for ~ 20 min. The DNA samples were mixed with 6x loading dye as well as the used DNA molecular weight markers, 100 bp DNA Ladder or 1 kb DNA Ladder purchased from New England Biolabs. The stained DNA was detected with UV-light and documented.

3.2.1.3 Transformation of nucleotides in bacteria

To amplify plasmid DNA chemically competent *E.coli* cells (DH5 α cells, made competent by CaCl₂-method) were used. 0.1-1 µg of plasmid-DNA was mixed with

100 µl of ice-cold competent bacteria in 100 µl KCM buffer for 20 min on ice and then for 10 min at room temperature. 1 ml LB-medium was added and the mixture was incubated for 1 h at 37 °C with horizontal shaking (400 rpm). Cells were centrifuged (4000 g for 5 min), the supernatant was discarded and the pellet was resuspended in 50-100 µl LB-medium. The resuspended cells were plated on solid LB plates containing the respective antibiotics.

3.2.1.4 Isolation of nucleotides from bacteria

Plasmid DNA Purification NucleoBond® Xtra EF kit in midi format was used to isolate plasmid DNA from *E.coli*. The principle of the purification is based on an alkaline lysis of bacteria followed by an anion-exchange chromatography. LB-plates with appropriate antibiotics were inspected for isolated colonies, 24 h after transformation and inoculation (3.2.1.3). Single colonies were transferred separately in 3 - 4 ml LB-medium containing antibiotics and incubated for 8 h at 37 °C and 180 rpm. Starter cultures were extended overnight (12 - 16 h, 37 °C, and 180 - 200 rpm) to a volume of 150 ml or 300 ml for less efficient plasmids under antibiotic selection. Bacterial cells were harvested by centrifugation 4,500 - 6,000 x g at 4 °C for 15 min and completely resuspended in buffer containing RNase. Cell suspension was gently mixed with lysis buffer containing SDS at room temperature for 5 min. After neutralization, bacterial cell debris was retained by the use of buffer equilibrated NucleoBond filter. A filter column containing positively charged silica beads to bind the negatively charged DNA backbone was placed underneath the debris filter. Subsequent three washing steps were conducted. One to collect residual lysate out of the bacterial debris filter and after discharge of the retention filter to clear off contaminants and increase the yield of the bound DNA. Release of DNA from silica column filter was achieved by elution with alkaline high salt buffer. Before further processing of the DNA e.g. sequencing or DNA digestion (Table 12) an isopropanol precipitation of DNA was conducted to remove salt and alcohol traces from the detergents used before. After centrifugation of the isopropanol DNA-precipitate mixture (15,000 x g for 30 min at 4 °C), the pellet was washed with 70 % ethanol and solubilized in nuclease-free water or TE-buffer (10 mM Tris/HCl, pH 7.5, 1 mM EDTA). Amplified DNA was stored at - 20 °C.

3.2.1.5 Concentration and purity of nucleotides

To determine DNA concentration and purity of the isolated DNA the spectrophotometer NanoDrop 2000c micro-volume-system was used. A DNA preparation was considered pure when absorption ratio of 260/280 nm was 1.8-1.95. Values lower than 1.8 reflect contamination with protein or other substances absorbing at 280 nm.

3.2.1.6 Molecular cloning

Adenosine A1 receptor FRET-sensors were cloned in the mammalian expression vector backbone pcDNA3 as described in (Stumpf 2015) and (Hoffmann et al. 2005) with CFP fused to C-terminus and an insertion of 6 amino acid sequence (CCPGCC) for FIAsh-binding (3.2.4) in the third intracellular loop. In general; the DNA of interest was amplified and modified with recognition sites for restriction enzymes with PCR techniques (3.2.1.1). The target vector and the DNA amplifications were digested with the appropriate enzyme (Table 12) to generate overlapping ends, followed by a ligation reaction (Table 11) which results in the desired plasmid. After purification, the plasmid was amplified using *E.coli* (3.2.1.3) followed by plasmid isolation (3.2.1.4). In general, the plasmid was digested with two enzymes, one recognizing a restriction site within the DNA insert and one cutting in the vector backbone (Table 12). The plasmid of successful control digestions were sequenced to ensure the exact DNA insertion in the vector. The DNA was send to Eurofins Genomics Germany GmbH for sequencing by the Sanger method.

Table 11: Ligation of DNA of interest and vector backbone with overlapping ends

DNA-Insert	5 ng	
Vector	30 ng	
10x T4-DNA-Ligase-buffer	1 µl	
T4-DNA-Ligase	1 µl	
H ₂ O, endonuclease free	20 µl	16 °C o/n

Table 12: Digestion of DNA by restriction enzymes, general composition

DNA	1 µg	
enzyme 1	1 µl	
enzyme 2	1 µl	
appropriate buffer	5 µl	
H ₂ O, endonuclease free	50 µl	1 h, 37 °C

3.2.2 Cell culture

Human embryonic kidney 293 (HEK293) cells were cultured in DMEM⁺⁺⁺ medium in 5 % CO₂ and at 37 °C. All steps were carefully conducted under antiseptic conditions and all solutions and media were used at room temperature. Cells were sub-cultured when they reached around 90 % confluency. Briefly, cells were washed with PBS and detached from the 10 cm-dish surface by adding 1 ml of Trypsin-EDTA. Cells were collected in the appropriate amount of medium and transferred to a new 10 cm-dish with freshly applied medium. Cells were frozen in chilled DMEM⁺⁺⁺ medium containing 10 % of DMSO (Table 7). The cell suspension in the precooled cryo-tubes were frozen at -20 °C for three hours and then transferred to -80 °C for permanent storage. Before freezing and during maintaining of the cells the cultures were tested for contamination with mycoplasma using PCR (3.2.1.1) on a regular basis. The supernatant of 100 µl medium of a confluent plate and a positive control (95 °C for 5 min) was used as DNA template (2 µl of the samples) and assayed with mycoplasma-detecting oligonucleotides, MGSO and GPO from MWG Biotech GmbH. Cells were thawed in fresh medium and after 3 - 4 hours the medium was exchanged to remove residual DMSO. This step is crucial due to the cytotoxicity of DMSO. Stable cell lines were maintained in DMEM⁺⁺⁺ medium containing 0.2 g/l G418. For confocal- or FRET-microscopy, cells were seeded in the desired cell density on autoclaved borosilicate 24 mm round glass cover slips placed in 6 well-plates. Mutant strains were incubated with DMEM⁺⁺⁺ containing 5 mM theophylline 24 h prior to experiment (Stumpf 2015).

3.2.3 Transient and stable transfection of HEK293 cells

The effectene transfection kit from Qiagen was used for transfection of HEK293 cells. At the day of transfection the cells had a confluency of 60 %. Right before the application of the transfection mixture the cells were washed with PBS and covered with 9 ml of fresh medium in a 10 cm-dish. The appropriate amount of DNA diluted in the provided transfection buffer (Table 13) was incubated with the enhancer solution for 5 min after 1 s of brief vortexing. In the next step the effectene reagent was added. After mixing for 10 s, the mixture was incubated for 10 min at room temperature. Fresh DMEM⁺⁺⁺ medium was added to the mixture (up to 1 ml), and pipetted up and down twice, and added drop-wise to the seeded cells. If cytotoxicity occurred after 12 - 16 h, cells were washed with PBS and fresh medium was applied. Around 48 h post-transfection the cells were analyzed for fluorescence expression.

Table 13: Transfection of HEK293 cells with Effectene transfection kit

Master mix	6-well plate	10 cm-dish	
Plasmid DNA	3 µg G _i -sensor 1 µg A1AR	2 µg A1AR	
EC buffer	300 µl	300 µl	
Enhancer	19.2 µl	16 µl	vortex 1 s, incubate 5 min
Effectene	37 µl	32 µl	vortex 10 s, incubate 15 min
DMEM	600 µl	600 µl	carefully pipette 2x

To generate stably transfected cells, 48 h after transfection cells were treated with selection medium containing a high concentration of antibiotic (0.8 g/l G418). In parallel to the transfection procedure a 10 cm-dish was seeded with non-transfected HEK293 cells. The daily treatment with high-antibiotic medium was continued until all non-transfected cells in the control 10 cm-dish were dead. At this time point the transfected cells grew in colonies. Colonies which were clearly distinguishable from their adjacent colonies were carefully picked and separated in a multi-well plate with a mild selection medium (0.5 g/l G418). Again cells were analyzed for fluorescence two days after reseeding. For ensuring to produce a monoclonal cell line a further separation step was necessary. Cells were detached and resuspended in appropriate amount of medium and cell number was determined using Countess II FL Automated Cell Counter (ThermoFischer Scientific). The cell suspension was diluted in an appropriate amount of selection medium to seed statistically 0.5 cells per well of a 96-well plate. After three to four days the cells were surveyed daily for morphology and fluorescence. Again, the best cells were selected and raised in cell number for culturing and confocal analysis.

3.2.4 FIAsH-labeling

The labeling of FRET receptor sensors expressed in HEK293 cells with the small fluorophore FIAsH was conducted as described in (Hoffmann et al. 2005). The confluency of the cells should not be less than 60 % at the time of FIAsH-labeling procedure. All incubation steps were carried out at 37 °C and 7 % CO₂. Cells expressing receptor FRET-sensor (containing the FIAsH-binding motif), were washed with label buffer (Table 7). 0.5 µM FIAsH and 12.5 µM EDT (1.2-ethanedithiol) in label buffer was applied to the cells and incubated for 1 h. Non-specifically bound FIAsH was removed by incubation with 250 µM EDT in label buffer for 10 min. Cells

were washed twice with label buffer and fresh DMEM⁺⁺⁺ medium was added for recovery (37 °C, 5 - 10 min).

3.2.5 FRET measurements

FRET experiments were performed as previously reported (Hoffmann et al. 2005). Cells were seeded on cover slips ($\varnothing = 24$ mm coated for 30 min with poly-D-lysine) 48 h before the experiment. Cover slips were placed in an “Attofluor” chamber and covered with measuring buffer. The holder was placed on the FRET microscope (Zeiss Axiovert 200, oil immersion 63 × objective) equipped with a polychrome IV lamp (TILL photonics, Germany). Emission of CFP (480/20 nm filter) and FIAsh (535/15 nm filter), were monitored simultaneously (beam splitter DCLP 505 nm) upon excitation at 436 nm. Recording frequency was 10 Hz with 20 ms illumination out of 100 ms. Fluorescence was detected by photodiodes (TILL photonics), digitalized using an analog-digital converter (Digidata 1440 A, Axon Instruments) and recorded with Clampex 9.0 software (Molecular Devices, LLC). For data analysis and correction OriginPro 9 was used (3.2.7). During the experiment, cells were perfused with measuring buffer (140 mM NaCl, 5.4 mM KCl, 2 mM CaCl₂, 1 mM MgCl₂, 10 mM HEPES, pH 7.3) supplemented with the ligand in indicated concentrations using a pressure-controlled perfusion system (ALA Scientific).

3.2.6 Confocal analysis

Confocal microscopy was performed using a Leica TCS SP8 inverted scanning microscope with a 63 x oil immersion objective lens. Cells expressing adenosine receptors tagged with CFP were seeded onto cover slip glasses placed in six-well plates. Cover slips were embedded in an “Attofluor” chamber and covered with measuring buffer prior to scanning. Fluorescence was detected using a 442 nm diode laser.

3.2.7 Data analysis

Statistical and graphical analyses were performed using Graph Pad Prism software. For calculation of EC₃₀ values the online tool “Compute EC anything from EC₅₀” from Graph Pad Prism (<https://www.graphpad.com/quickcalcs/Ecanything1.cfm>; accessed 2019) was used. Data were analyzed by ANOVA and appropriate posttests or by its non-parametric equivalent Kruskal-Wallis test and by Student’s unpaired two-tailed t-test or non-parametric Mann-Whitney test as indicated for every figure. Significance

levels are given as: #P < 0.05, ##P < 0.01, ###P < 0.001, ####P < 0.0001. Data represent the mean \pm SEM unless otherwise stated.

The raw data of simultaneous recordings of 480 nm (CFP) and 535 nm (FIAsH) fluorescence intensity were corrected for donor emission technically co-recorded in acceptor emission channel (bleed trough) and for direct excitation of acceptor by light of 436 nm (cross talk). For bleed trough correction, the intensity recordings of 535 nm were subtracted by correction factor 1 multiplied by the 480 nm intensity recordings per time point (Equation 1). Correction factor 1 can be determined by recording the fluorescence intensity of cells expressing only donor in the 535 nm-channel. To correct for cross talk, direct excitation of the acceptor with a wavelength of 490 nm was recorded (${}_{490}F_{\text{Accept}}$) at the end of each FRET experiment and multiplied with correction factor 2 (Equation 1). Correction factor 2 can be determined by recording the fluorescence intensity of cells expressing only acceptor, excited by light of 436 nm, in the 535 nm-channel. These correction factors are dependent on the used filters, microscope and excitation light source. The bleed trough of 535 nm emission in the 480 nm-channel was insignificantly small and therefore negligible. The output FRET signal is the ratio of the corrected acceptor and the donor fluorescence intensity per time point (Equation 2). FRET data processing as well as the correction of decrease in FRET intensity overtime (photobleaching of the fluorophores) was conducted in Origin 9 Pro.

FRET signal correction:

$$F_{\text{Accept}} - (F_{\text{Donor}} * \text{correction factor 1}) - (\text{correction factor 2} * {}_{490}F_{\text{Accept}}) = \text{correct } F_{\text{Accept}} \quad (1)$$

$$\text{correct } F_{\text{Accept}} / F_{\text{Donor}} = \text{FRET ratio} \quad (2)$$

Kinetic fits were conducted with Clampfit 10.7 (Molecular Devices, LLC) using the equation:

$$f(t) = A * e^{-t/\tau}$$

Tau (τ) is the time constant of either association or dissociation, A is the amplitude of FRET signal and t is the time from the starting point of FRET signal change to the plateau for association and to baseline for dissociation.

4 Results

4.1 Investigation of rat and human adenosine A1 receptor

Intramolecular fluorescence resonance energy transfer-based techniques are highly suitable to measure conformational changes of GPCRs *in vitro* and *in vivo* (Hoffmann et al. 2005). With the FRET sensors developed for human and rat A1 adenosine receptor (Stumpf 2015) the conformational change stimulated by orthosteric ligands in combination with the positive allosteric modulator PD 81,723 was monitored in HEK293 cells. The differences in protein sequence of human and rat adenosine A1 receptor are highlighted in Figure 9. The collected response of receptors expressed at the surface of single cells was recorded over time with a recording frequency of one data point per 100 milliseconds. This read-out allows the investigation of real-time kinetics of adenosine receptors in living cells.

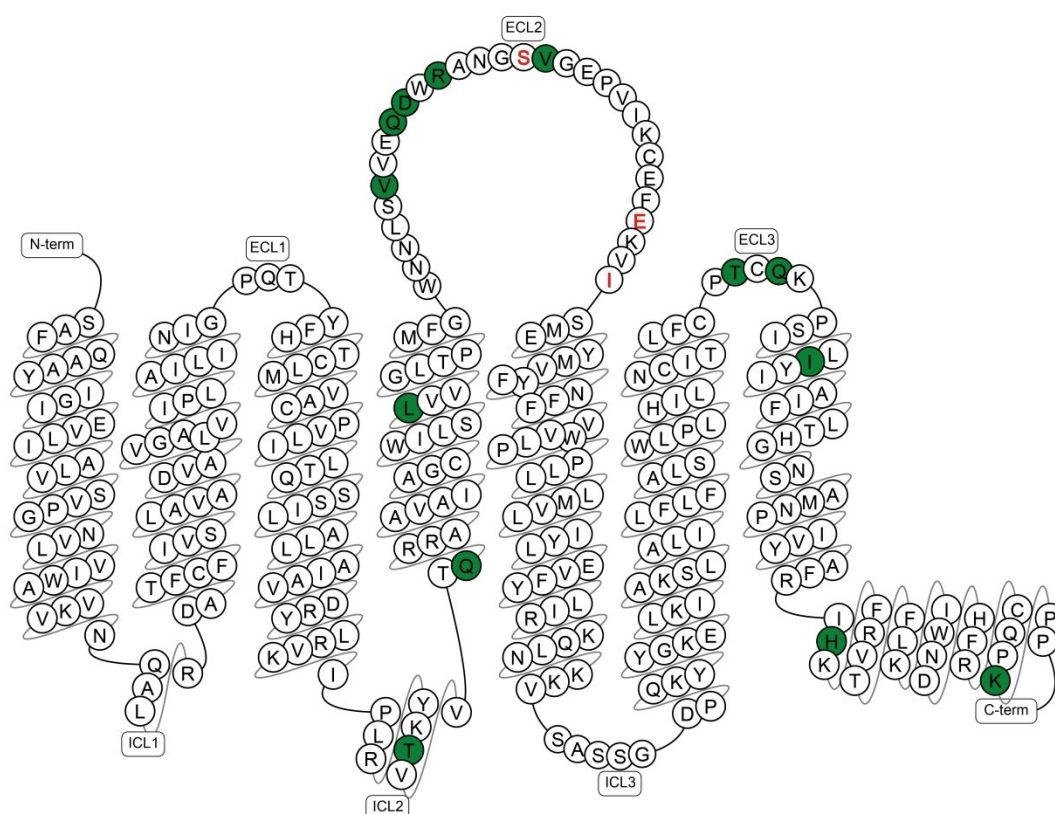


Figure 9: Protein sequence of rat adenosine A1 receptor. Sequence of rat adenosine A1 receptor represented as snake plot. Amino acids which are distinct in the sequence of human adenosine A1 receptor are highlighted in green (alignment of human and rat A1AR, see appendix Figure 28). Amino acids in red letters are potentially important for allosteric modulator binding or exerting its enhancing effects (Nguyen et al. 2016b). These amino acids were investigated in this work, see 4.2. The snake plot was generated from www.gpcrdb.org.

4.1.1 Orthosteric characterization of rat A1 FIAsh3 CFP sensor

Drug candidates are likely to elicit different pharmacologic properties depending on the molecular structure of the target protein. Among species, the molecular structure of the drug binding site may vary substantially, although high sequence similarity of target proteins suggests compatibility. Considering this, it is highly important for the drug discovery and development process to include species in an early phase of basic research. Species should be chosen, which will be relevant for animal testing later on in the preclinical research phase. Therefore this work focuses on the investigation of allosteric modulation of human and rat adenosine A1 receptors. The stable cell line expressing rat A1 FIAsh3 CFP receptor (working group Prof. Hoffmann) was investigated for affinity of the endogenous ligand adenosine, as well as the synthetic agonists CPA and NECA, Figure 10.

The rat receptor FRET sensor was well expressed at the cell membrane and the cells maintained a morphologically healthy form. Cells were assayed with different concentrations of ligand directly referenced by 100 μ M of the respective ligand. The measured FRET changes were plotted in percent of 100 μ M of ligand and a sigmoid curve was fitted using GraphPad Prism. EC₅₀ values resulting from the fit curve are represented in Table 14 as well as the EC₅₀ values of human A1 FIAsh3 CFP receptor (unpublished data from working group of Prof. C. Hoffmann, (Stumpf 2015)).

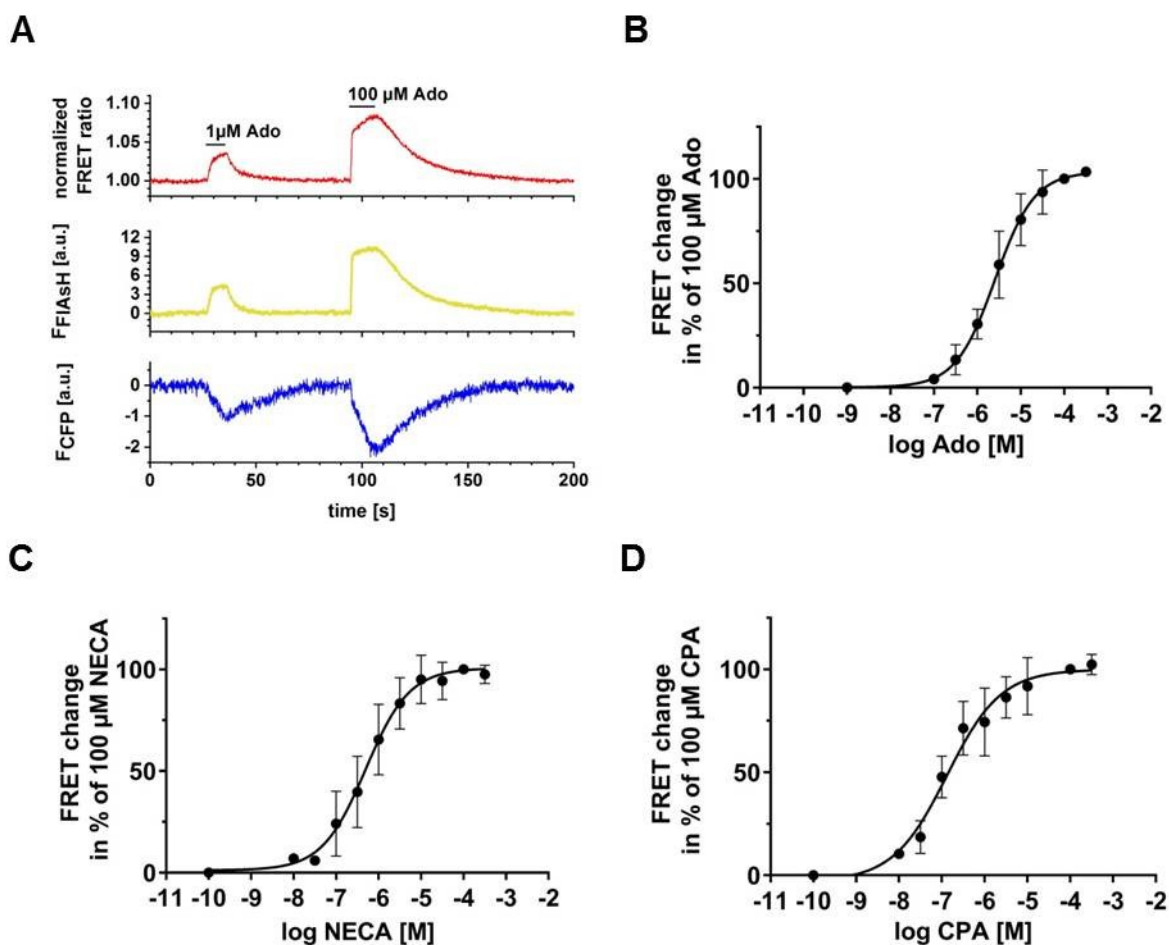


Figure 10: Orthosteric characterization of rat A1 FIAsh3 CFP receptor FRET sensor. **A**, representative FRET trace showing adenosine-induced changes in CFP (F_{CFP} , blue) and FIAsh (F_{FIAsh} , yellow) fluorescence intensities over time as well as the normalized FRET ratio (F_{FIAsh}/F_{CFP} , red) of single cells expressing rat A1AR FRET sensor. Black horizontal bars indicate duration of ligand application. FRET traces were corrected for photo bleaching. Concentration response curves of orthosteric ligands, **B**, adenosine **C**, NECA and **D**, CPA for rat A1AR. Data points represent the mean \pm SD of $n \geq 30$ individual cells from five independent experiments. Determined EC_{50} values are listed in Table 14.

Table 14: EC_{50} values of orthosteric agonists for rat and human A1 wt FRET sensor.

The EC_{50} values of Ado, NECA and CPA for rat adenosine A1 receptor as well as the EC_{50} value of CPA for human adenosine A1 receptor were determined in this work. The EC_{50} values of Ado and NECA for human A1AR were determined in a previous doctoral study in the working group of Professor Hoffmann (Stumpf 2015). Data were obtained from $n \geq 24$ individual cells from at least four independent experimental days. Confidence intervals 95 % are presented in brackets.

	Ado	NECA	CPA
rat A1AR	2.6 μ M (2.2 - 3.1)	0.5 μ M (0.4 - 0.7)	0.13 μ M (0.09 - 0.2)
human A1AR	6.4 μ M (3.8 - 10.3)	2.6 μ M (1.2 - 3.4)	0.32 μ M (0.2 - 0.45)

4.1.2 Orthosteric kinetics of rat and human A1 FIAsh3 CFP receptor

Cell lines stably expressing human or rat adenosine A1 receptors were further characterized for their kinetic properties in response to adenosine. The equilibrium states of occupied and unoccupied receptor during the FRET experiment are depicted in Figure 11 A. The orthosteric ligand is applied to the unoccupied receptor (R) and the equilibrium is shifted to the active orthosteric-receptor complex state (OR*). By washing the cells with buffer solution the orthosteric ligand is removed from the equilibrium reaction, which subsequently shifts the equilibrium to the inactive receptor state (R). The kinetics of adenosine were calculated from FRET signals induced by 100 μ M adenosine (saturating concentration). FRET traces were corrected for photo bleaching and fitted with a mono-exponential equation using Clampfit software as described in 3.2.7. The curve for association was fitted from the starting point of FRET signal change to the plateau of the FRET signal, dissociation kinetic was fitted from starting point of FRET signal decrease to the plateau of the FRET signal baseline (Figure 11 B). The resulting kinetic parameters were reported as tau values. The mean association kinetic was determined for human A1AR as 396.9 ± 15 ms and for rat A1AR as 442.4 ± 45.5 ms. The mean dissociation of adenosine occurred within 5.4 ± 0.6 s and 8.3 ± 0.9 s from human and rat adenosine A1 receptor respectively, Figure 11 C, D.

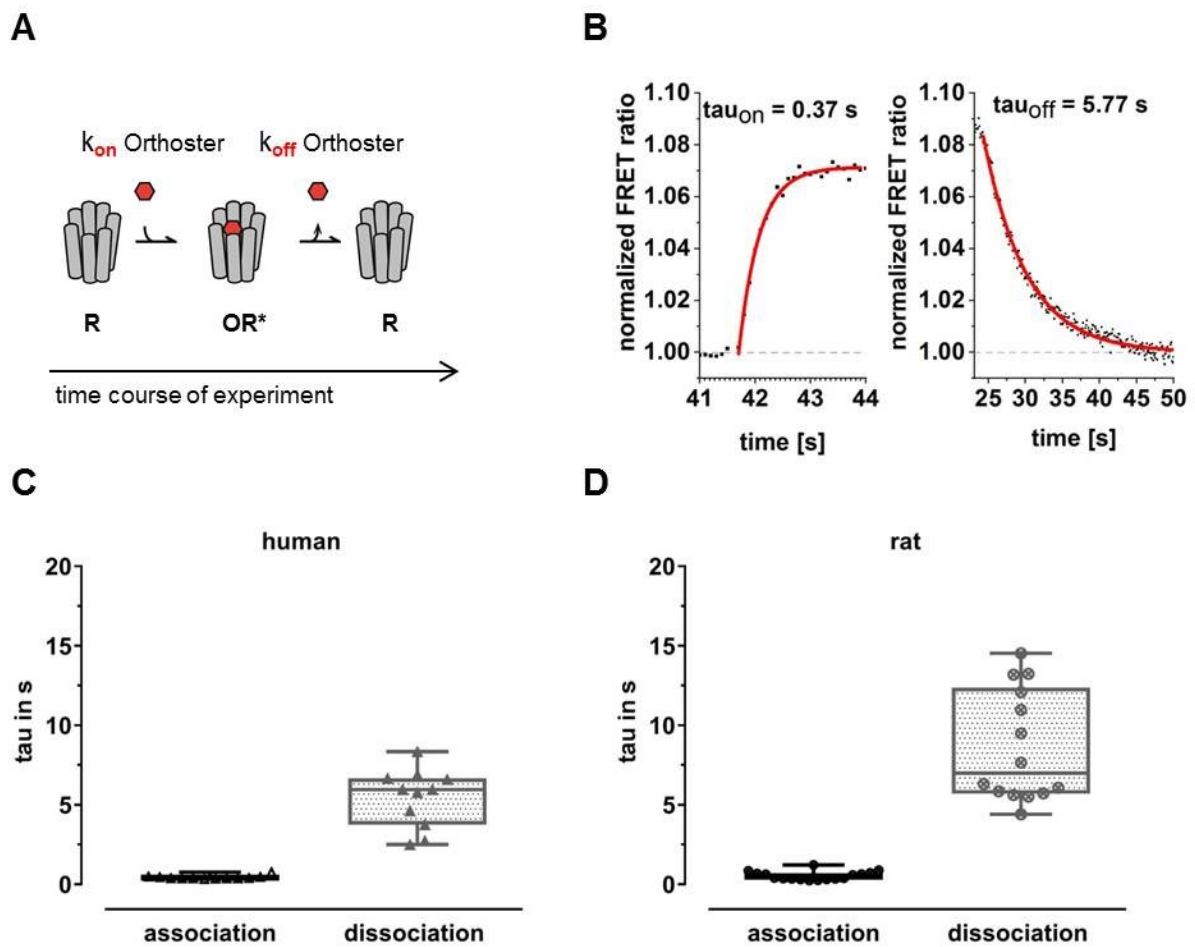


Figure 11: Orthosteric kinetics of human and rat A1 FIAsh3 CFP receptor. **A**, pictogram shows separate states of ligand receptor occupancy during the experiment. The empty inactive receptor (R) is binding the orthosteric ligand (red hexagon) forming an activated orthoster-receptor-complex (OR*). Orthosteric ligand dissociates from OR* and receptor returns to the inactive state (R). **B**, kinetic determination of human A1AR activation by 100 μ M adenosine (left panel) and receptor deactivation (right panel) using the software Clampfit. The data points were fitted with the mono-exponential equation noted in 3.2.7 (red curve), resulting in time constant τ . **C**, **D**, association and dissociation of 100 μ M adenosine for human and rat A1 wt. Single τ values are represented in box plots. Median is indicated by vertical line and whiskers are defined by the minimal and maximal τ value. Every data point represents an individual cell, $n \geq 11$ from at least three independent experimental days.

4.1.3 Measuring procedure of allosteric modulation at adenosine A1 receptors

Classical allosteric modulators are not able to induce a response in the absence of orthosteric ligand (Christopoulos 2002). This was confirmed for PD 81,723 as shown for the human adenosine A1 receptor (Figure 12). No significant FRET response was recorded with 30 μM of PD 81,723 or vehicle (0.03 % EtOH) compared to the signal induced by 10 μM adenosine.

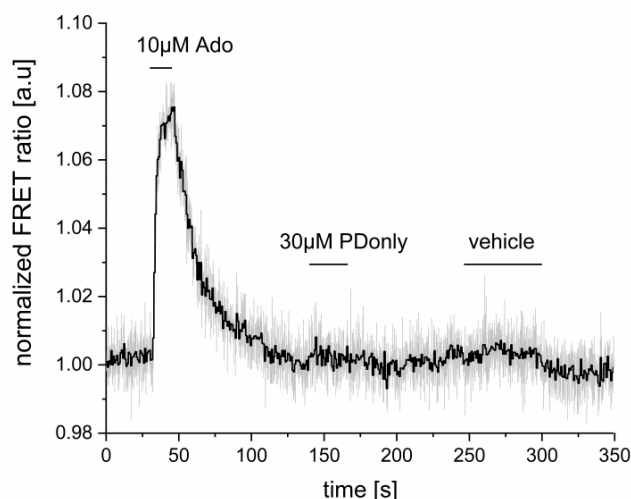


Figure 12: In the absence of orthosteric ligand PD 81,723 mediates no receptor response. FRET ratio of human adenosine A1 receptor. The receptor is responding to stimulation with 10 μM adenosine. 30 μM PD 81,723 and vehicle show no FRET response. Black horizontal bars indicate duration of ligand application.

To measure allosteric effects on adenosine receptors, a suitable concentration of orthosteric ligand had to be determined to operate in the optimal measuring window to monitor maximal allosteric effects. For probing a positive allosteric modulator the concentration of orthosteric ligand has to be lower than the EC_{50} of the orthosteric concentration-response curve to avoid underestimation of the allosteric effect (Christopoulos 2002). On the other hand the concentration has to be high enough to induce a FRET change clearly distinguishable from baseline fluctuations (noise). For adenosine, a concentration around the EC_{30} was found to give solid and reliable FRET responses. EC_{30} of orthosteric ligand was used for all experiments investigating PD 81,723 affinity (4.1.4, 4.1.6) as well as in kinetic measurements (4.1.8). Due to the fact that PD 81,723 was not able to induce a FRET change on its own (Figure 12) it was necessary to apply a mixture of orthosteric ligand and PD 81,723 to the cells.

For this purpose, a measurement protocol was developed (Figure 13).

- Step 1: Application of orthosteric ligand solution with the concentration of interest until plateau formation of the FRET response occurred.
- Step 2: Application of a solution consisting of orthosteric ligand in the very same concentration as in step 1 and allosteric modulator, until plateau formation of the FRET response occurred.
- Step 3: Application of buffer solution without any ligand, until FRET response decreased back to baseline levels.

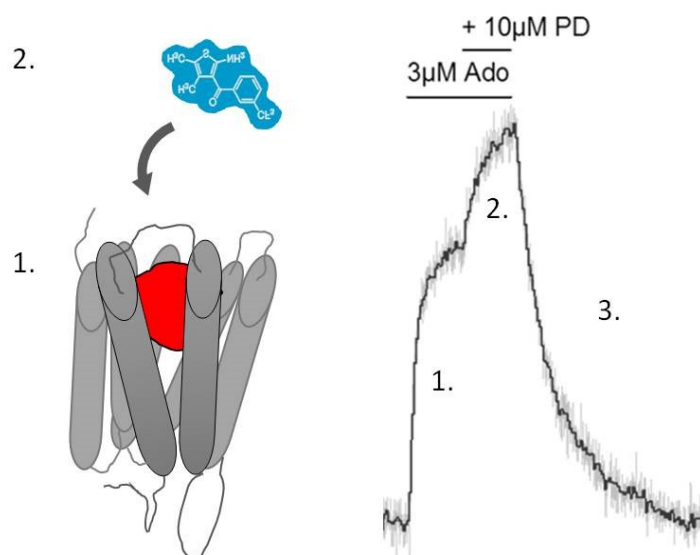


Figure 13: Measurement scheme for determining allosteric effects. Left, pictogram of receptor bound to orthosteric ligand (red) represents the state of step 1. Allosteric modulator molecule (blue) is added in the second step. Right, the FRET signal increases upon orthosteric ligand application (EC_{30} of adenosine) and forming a plateau in step 1. In step 2 the FRET signal is further enhanced by application of allosteric modulator (PD 81,723) and forming a plateau. The FRET signal decreases upon washing with buffer and reaching baseline again, step 3.

4.1.4 Determination of PD 81,723 affinity for adenosine-occupied receptor

Traditional methods, like radioligand binding studies, are not feasible to determine allosteric modulator affinity in combination with endogenous ligand adenosine. This limitation is based on the requirement for the presence of adenosine deaminase in membrane preparations, since destroyed membranes release considerably amounts of adenosine.

The affinity of the positive allosteric modulator PD 81,723 was investigated for the first time in the presence of endogenous ligand adenosine in living cells. With the established scheme for measuring allosteric effects for adenosine A1 receptor (as described in 4.1.3) the affinity of PD 81,723 was investigated by increasing concentrations of allosteric modulator up to 30 μM PD 81,723. Higher concentrations of allosteric modulator showed no reproducible and reliable FRET signals. The lowest concentration of allosteric modulator used here was 0.3 μM PD 81,723, which still generated FRET changes clearly distinguishable from noise of the FRET trace. The receptors were assayed with the respective EC_{30} concentration of adenosine, 3 μM Ado for human A1AR and 1 μM Ado for rat A1AR. EC_{30} values were calculated by the use of an online tool provided by GraphPad with the help of the respective hill slope values and EC_{50} concentrations (<https://www.graphpad.com/quickcalcs/Ecanything1.cfm>; accessed 2019). The enhancing effect of PD 81,723 was calculated and plotted as percentage of adenosine signal amplitude in a concentration dependent manner (Figure 14). The resulting EC_{50} concentration for the enhancing effect of PD 81,723 was 2.1 μM for human and 2.9 μM for rat adenosine A1 receptor. This data indicates that the affinity of PD 81,723 towards human and rat adenosine A1 receptors is not substantially different. Interestingly, the enhancing effect of PD 81,723 is higher for rat adenosine A1 receptor at maximal concentrations of allosteric modulator.

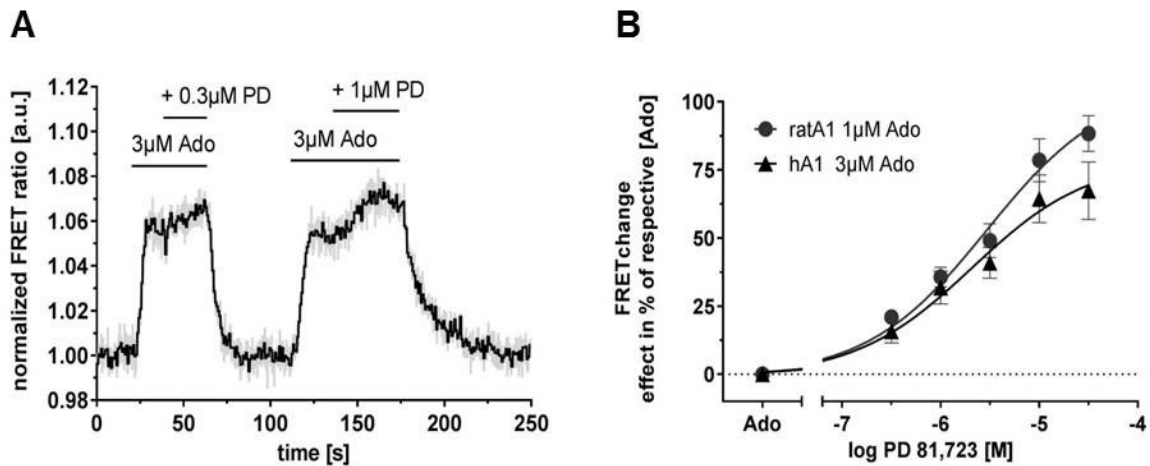


Figure 14: Determination of allosteric modulator affinity. **A**, normalized FRET trace over time showing FRET ratio (FIAsH/CFP) of single cells expressing human A1AR FRET sensor. FRET trace was corrected for photo bleaching and normalized to the first data point of the recording. Affinity was determined using the EC_{30} concentration of adenosine (human A1AR 3 μ M, rat A1AR 1 μ M) and varying concentrations of PD 81,723. **B**, modulator enhancement was plotted in percentage of signal evoked by EC_{30} concentration of adenosine (normalized as 0 %) for human A1AR (triangle) and rat A1AR (circle). The affinity of PD 81,723 was determined for human A1AR as 2.1 μ M and for rat A1AR as 2.9 μ M. Data represent the mean \pm SEM of human $n = 40$ or rat $n = 33$ individual cells from six independent experiments.

Positive allosteric modulators are known to have the property to prolong the dissociation time of orthosteric ligand (Christopoulos 2002). In Figure 15 A the prolongation effect of PD 81,723 on the human adenosine A1 receptor stimulated with 3 μ M Ado is clearly demonstrated. This is further visualized in Figure 15 B by normalizing the amplitudes of the signal decay curve of 0 μ M, 10 μ M and 30 μ M PD 81,723 to 1 and setting the start of signal decay to $t = 0$ s. The prolongation effect increases in dependency of the concentration of PD 81,723. This prolonged dissociation might be the reason for the increased affinity of the orthosteric ligand to its target receptor in the presence of the allosteric modulator, Figure 16. The interplay of kinetics and affinity is further investigated in the following chapters. But first, the impact of allosteric modulator on adenosine concentration-response curve was investigated to elucidate an additional characteristic of allosteric modulators, termed cooperativity.

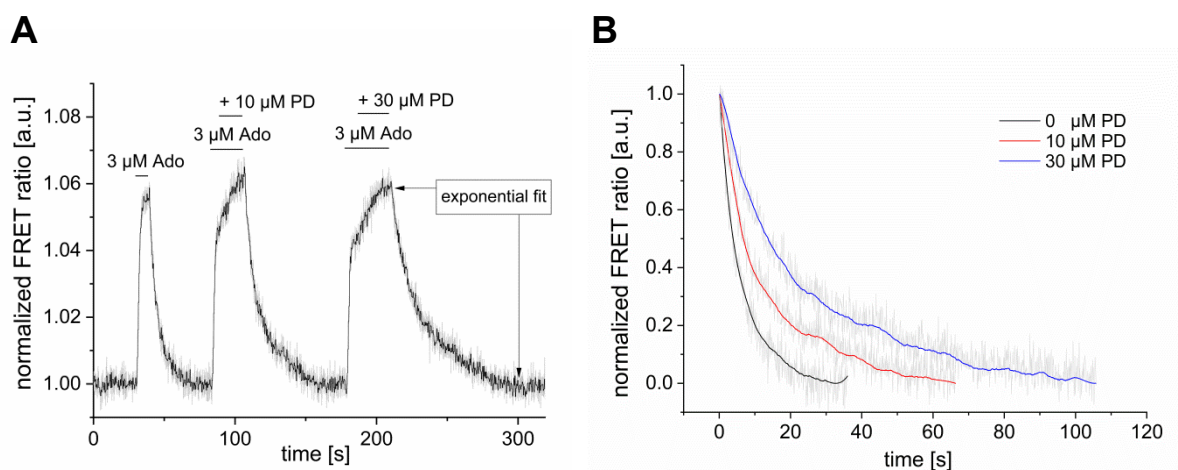


Figure 15: Prolonged dissociation time in the presence of allosteric modulator. Left panel, normalized FRET trace over time showing FRET ratio (FIAsH/CFP) of single cells expressing human A1AR FRET sensor, arrows indicate area for exponential fitting. Right panel, visualization of the prolongation effect by comparing the FRET signal decay of 3 μM adenosine without allosteric modulator 0 μM PD (black), with 10 μM PD (red) and with 30 μM PD (blue). Amplitudes of the decay curves were normalized to 1 [ordinate] and to $t = 0$ s [abscissa].

4.1.5 Influence of allosteric modulator on orthosteric affinity

The term cooperativity describes the strength of interference of the allosteric binding site with the orthosteric binding site. In order to measure cooperativity, the influence of the allosteric modulator on the concentration-response curve of the orthosteric ligand is surveyed. The aim of the following experiments was to learn if there is a difference in cooperativity of rat and human adenosine A1 receptors, although the affinity of PD 81,723 towards both receptors was in an identical micro molar range.

To investigate to which extent the affinity of adenosine is changed in the presence of allosteric modulator, the concentration of adenosine was increased, while a high concentration of PD 81,723 was used and kept constant (10 μM PD 81,723). The application of the solutions was described above (4.1.3). In Figure 16 C, D absolute FRET change values were plotted against the concentration of adenosine represented on logarithmic scale. Absolute FRET values represent the difference from baseline to the plateau of the FRET signal either induced solely by adenosine (grey) or in the presence of PD 81,723 (black). In the presence of PD 81,723 the affinity of adenosine was enhanced 2.4-fold for the human receptor and 1.6-fold for rat adenosine A1 receptor compared to adenosine affinity in the absence of PD 81,723. Interestingly, allosteric enhancement still occurred at saturating concentrations of adenosine. The data confirmed that PD 81,723 acts as a PAM by

shifting the EC₅₀ value of adenosine to the left, thus enhancing adenosine affinity for human and rat A1AR.

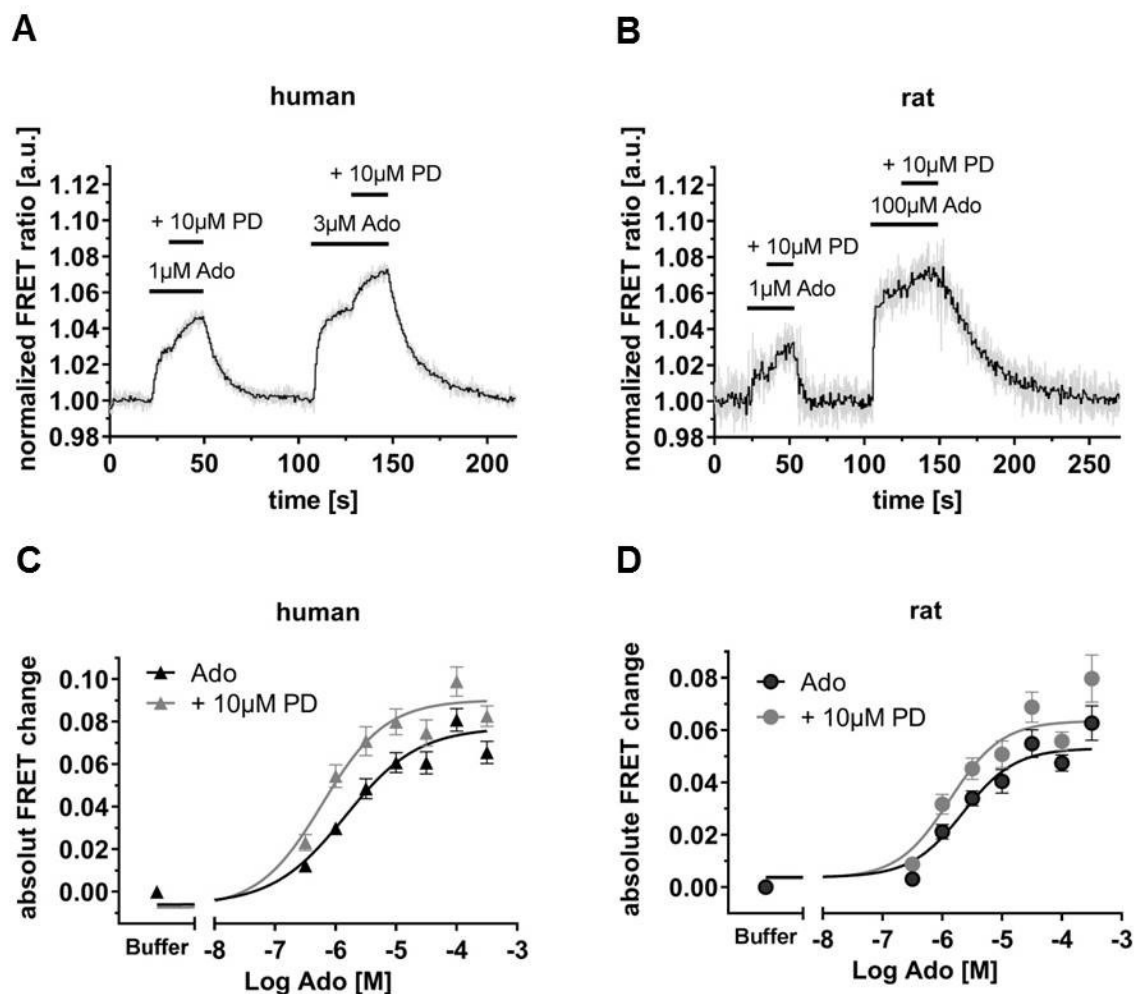


Figure 16: Influence of allosteric modulator on orthosteric concentration-response curve. **A, B,** normalized FRET trace over time showing FRET ratio (FIAsH/CFP) of single cells expressing human A1AR and rat A1AR FRET sensor, respectively. Influence of allosteric modulator was measured by varying concentrations of Ado and constant concentration of 10 μM PD 81,723. **C, D,** adenosine response in the presence of 10 μM PD 81,723 (grey) compared to the adenosine response without PD 81,723 (black). **C,** for human A1AR a 2.4-fold shift and **D,** for rat A1AR a 1.6-fold shift was determined. Absolute FRET change values (plateau of signal - baseline) were plotted. Data represent the mean ± SEM of human $n = 52$ individual cells from eight independent experiments or rat $n = 37$ individual cells from seven independent experiments. Curves are significantly different ($p < 0.0001$) by two-way ANOVA and Bonferroni's comparison test.

4.1.6 Probe dependency of allosteric modulator PD 81,723

The impact of the orthosteric ligand on the affinity of the allosteric modulator is dependent on the structure of the used orthosteric ligand (denoted probe). To study this phenomenon, called probe dependency, NECA as non-specific adenosine receptor agonist was used instead of adenosine. The experimental setup to

determine allosteric modulator affinity (as described in 4.1.4) was used here with 1 μM NECA, see Figure 17. 1 μM NECA corresponds to the EC_{30} concentration of NECA for human adenosine A1 receptor (Stumpf 2015).

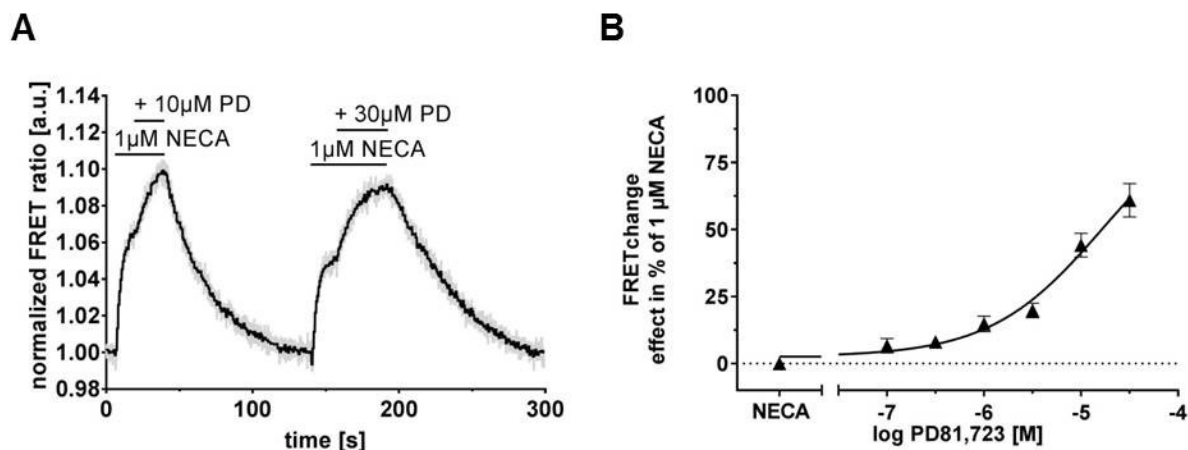


Figure 17: Probe dependency of PD 81,723. **A**, normalized FRET trace over time showing FRET ratio (FIAsH/CFP) of single cells expressing human A1AR FRET sensor. FRET trace was corrected for photo bleaching and normalized to the first data point of the recording. PD 81,723 affinity was determined using the EC_{30} concentration of NECA (1 μM) and varying concentrations of PD 81,723. **B**, modulator enhancement was plotted in percent of signal evoked by EC_{30} concentration of NECA (normalized as 0 %) for human A1AR. The resulting EC_{50} value for PD 81,723 was determined as 9.4 μM . Data represent the mean \pm SEM of $n = 19$ individual cells measured at four independent experimental days.

Of note, in Figure 17 B the saturation of the concentration-response curve was not reached with the highest feasible concentration of PD 81,723. For NECA the determined EC_{50} value of PD 81,723 was 4.5-fold increased ($\text{EC}_{50} = 9.4 \mu\text{M}$) compared to the EC_{50} value for the adenosine-occupied human adenosine A1 receptor ($\text{EC}_{50} = 2.1 \mu\text{M}$). This reduced affinity of PD 81,723 for NECA-occupied receptors in contrast to Ado-occupied receptors indicates the importance of surveying adenosine levels in participants of clinical trials. This data shows a clear probe dependency of PD 81,723 and proves again the ability of the FRET method as an appropriate measurement tool for allosteric modulation. The focus of this work is on the interaction of endogenous adenosine and PD 81,723 therefore probe dependency with other agonists was not further elucidated.

4.1.7 Visualization of allosteric modulation on G protein level

Allosteric effects were observed by monitoring conformational changes of the receptors, as demonstrated in the previous chapters. The enhancing effect of PD 81,723 on the adenosine receptor might have an impact on the behavior of downstream G proteins. In addition to modulating affinity PD 81,723 might influence

efficacy as well. Hence, the question for enhancing effects of PD 81,723 on G protein activation arose. For this purpose, HEK293 cells were transfected with untagged human A1AR and $G\alpha_{i3}$ protein FRET-sensor (van Unen et al. 2016). The $G\alpha_i$ -subunit is tagged with a CFP derivative (mTurquoise) and the γ -subunit is tagged with an YFP variant (Venus) as acceptor fluorophore. Upon conformational change of the receptor, induced by adenosine, G proteins are activated and subunit rearrangement occurs (Figure 18 A). The rearrangement of the subunits either increases the distance or the orientation of the fluorophores towards each other, which leads to a decrease in FRET ratio during ligand application (Figure 18 B). An enhancing effect of PD 81,723 was observed in combination with 0.1 μM adenosine. With higher concentrations of adenosine the enhancing effect of PD 81,723 was not observed. The difference of adenosine concentration to measure allosteric modulation at the receptor (3 μM) and on the G protein level (0.1 μM) is based on the signal amplification along the signal transduction cascade. The enhancing effect of PD 81,723 on G protein behavior was not further investigated since the off-kinetics of the FRET signal were slow and the requirement for lower concentrations of adenosine hampered reproducibility.

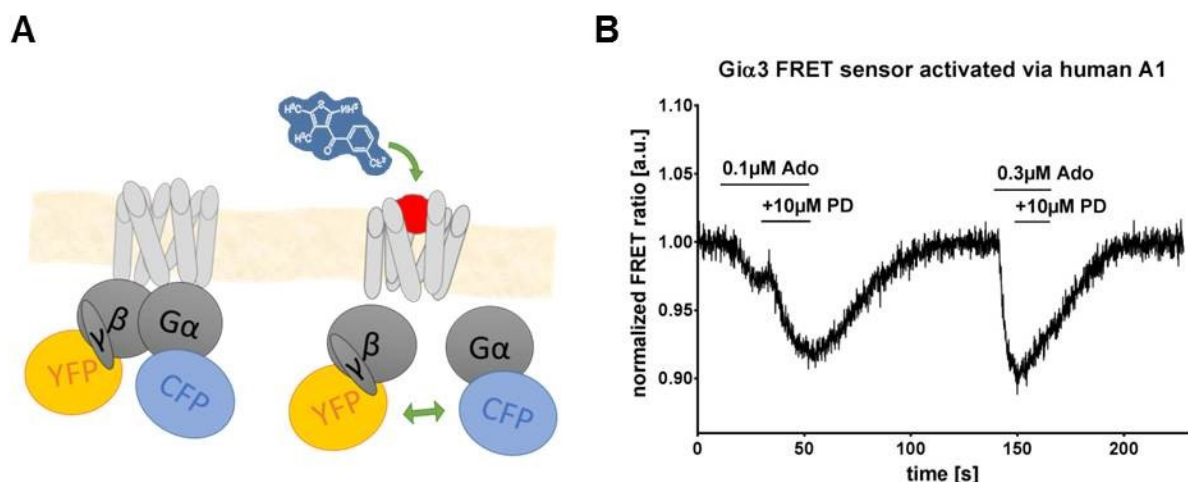


Figure 18: G protein-based FRET sensor and allosteric enhancement at G protein level. **A**, pictogram shows principle of G_i -protein FRET sensor (van Unen et al. 2016). Upon ligand binding the G protein is activated and by reorganizing the subunits. The distance between the fluorescent tags of the G protein-based FRET-sensor increases. The resulting FRET ratio is decreasing. **B**, normalized FRET trace over time showing FRET ratio (YFP/CFP) of single cells expressing $G\alpha_{i3}$ -FRET sensor. The FRET sensor was co-transfected with untagged human adenosine A1 receptor. Enhancing effect of PD 81,723 on the G protein behavior is clearly visible for 0.1 μM Ado but not for 0.3 μM Ado.

4.1.8 Determination of allosteric kinetics

The influence of allosteric modulator on the dissociation kinetics of orthosteric ligands is quite often the only kinetic read-out in the field of allosteric studies. To shed light on the allosteric mechanism of slowing down the receptor deactivation upon ligand dissociation (Figure 15) a set of three kinetic experiments was designed. First, receptor deactivation upon dissociation of PD 81,723, second dissociation of adenosine, and third dissociation of both ligands, adenosine along with PD 81,723, were monitored via conformational change, see Figure 19.

In this study, the dissociation of PD 81,723 from the adenosine-occupied receptor in active conformation was monitored for the first time (Figure 19 B). The procedure is schematically depicted in Figure 19 A. The orthosteric ligand is applied to the unoccupied receptor until equilibrium of binding and unbinding is stabilized (OR*). This state of equilibrium is shifted by the application of allosteric modulator to the state of alloster-orthoster-receptor (OAR*) equilibrium. The dissociation of allosteric modulator from the OAR* state is induced by removing allosteric modulator from the reaction and the receptor returns to the OR* state. In Figure 19 B the dissociation of PD 81,723 was initiated by washing the receptor bound to adenosine and PD 81,723 with a solution only containing adenosine and thereby removing PD 81,723 from the receptor. Consequently, the FRET signal decreases to the level of receptor bound to adenosine, Figure 19 B. By washing with buffer, thereby removing adenosine, the receptor is returning to the inactive state and the FRET signal decreases to baseline levels. The dissociation of PD 81,723 from the adenosine-occupied receptor was determined by fitting the decaying FRET signal from the OAR* plateau to the OR* plateau (cyan curve) with the mono-exponential equation described in 3.2.7 resulting in time constant, tau. Single dissociation tau values of human and rat adenosine A1 receptor are represented in Figure 20.

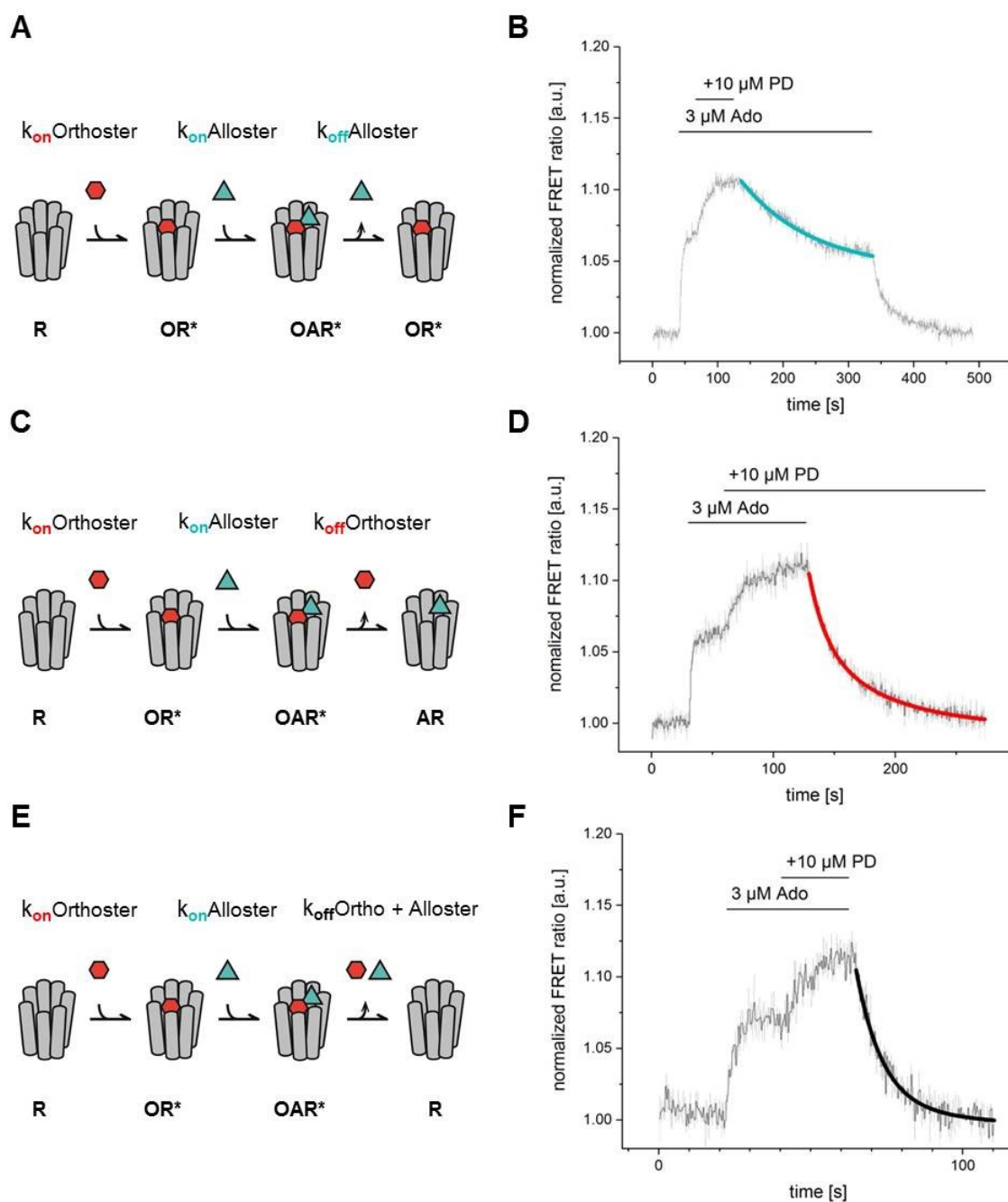


Figure 19: Experimental procedure for determination of orthosteric and allosteric kinetics. **A, C, E**, pictograms show separate states of ligand receptor occupancy. The empty inactive receptor (R) is binding the applied orthosteric ligand (red hexagon) forming an activated orthoster-receptor-complex (OR*). Allosteric modulator (cyan triangle) binds to the OR* forming an orthoster-alloster-receptor-complex (OAR*). **B, D, F**, representative FRET traces, showing FRET ratio (FIAsH/CFP) of single cells expressing human adenosine A1 receptor. FRET traces were corrected for photo bleaching and normalized to the first data point of the recording. Black horizontal lines indicate duration of ligand application. **A**, allosteric modulator dissociates from OAR*-complex resulting in OR*-complex. **B**, dissociation of allosteric modulator was achieved by washing with 3 μ M Ado and thereby removing PD 81,723 from Ado-bound receptor. Fit curve for obtaining off-kinetics of alloster (tau) is indicated in cyan **C**, orthosteric ligand dissociates from OAR*-complex resulting in inactivated alloster-receptor-complex (AR). **D**, dissociation of orthoster was achieved by washing with 10 μ M PD 81,723 and thereby removing Ado from PD 81,723-bound receptor. Fit curve for obtaining off-kinetics (tau) of orthoster is indicated in red. **E**, orthoster and allosteric modulator dissociate from OAR* resulting in empty inactive receptor R. **F**, simultaneous dissociation of Ado and PD 81,723 by washing with buffer. Fit curve for obtaining off-kinetics (tau) of orthoster and alloster is indicated in black.

The allosteric modulator might sterically block the exit trajectory of the orthosteric ligand from the receptor binding pocket and thereby causing a prolonged dissociation time (as shown in Figure 15). To elucidate this assumption the dissociation of orthosteric ligand in the presence of allosteric modulator at the receptor (Figure 19 C) as well as simultaneous dissociation of orthosteric ligand and allosteric ligand (Figure 19 E) were investigated. In Figure 19 F, the dissociation of adenosine in the presence of PD 81,723 at the receptor was observed by washing the Ado-PD-receptor complex with buffer solution only containing 10 μ M of PD 81,723 and thereby removing adenosine from the equilibrium reaction. The simultaneous dissociation of both molecules was achieved by washing the receptor bound to Ado and PD with buffer solution resulting in unoccupied inactive receptor, see Figure 19 D. The quantitative outcome of the above described set of experiments is represented in Figure 20 and in Table 15.

Table 15: Orthosteric and allosteric dissociation kinetics from OAR* of human and rat adenosine A1 receptors. Dissociation of 10 μ M PD 81,723 from OAR* is significantly different from simultaneous dissociation of adenosine and PD 81,723 from OAR*. Dissociation of 3 μ M adenosine from OAR* was not significantly different from simultaneous dissociation of adenosine and PD 81,723 from OAR* (# $P < 0.05$ Kruskal-Wallis test). Tau values are presented as median in seconds, 25 % and 75 % percentile are presented in brackets. Data were collected on at least three independent experimental days, $n \geq 7$ individual cells per condition.

Dissociation from OAR*	human A1AR tau [s]	rat A1AR tau [s]
10 μ M PD	156.9 (89.9 - 184.8) #	93.3 (63.7 - 112.3) #
3 μ M Ado	16.0 (13.5 - 30.5)	28.3 (19.5 - 33.3)
3 μ M Ado + 10 μ M PD	20.1 (5.1 - 22.9)	11.8 (9.8 - 25.2)

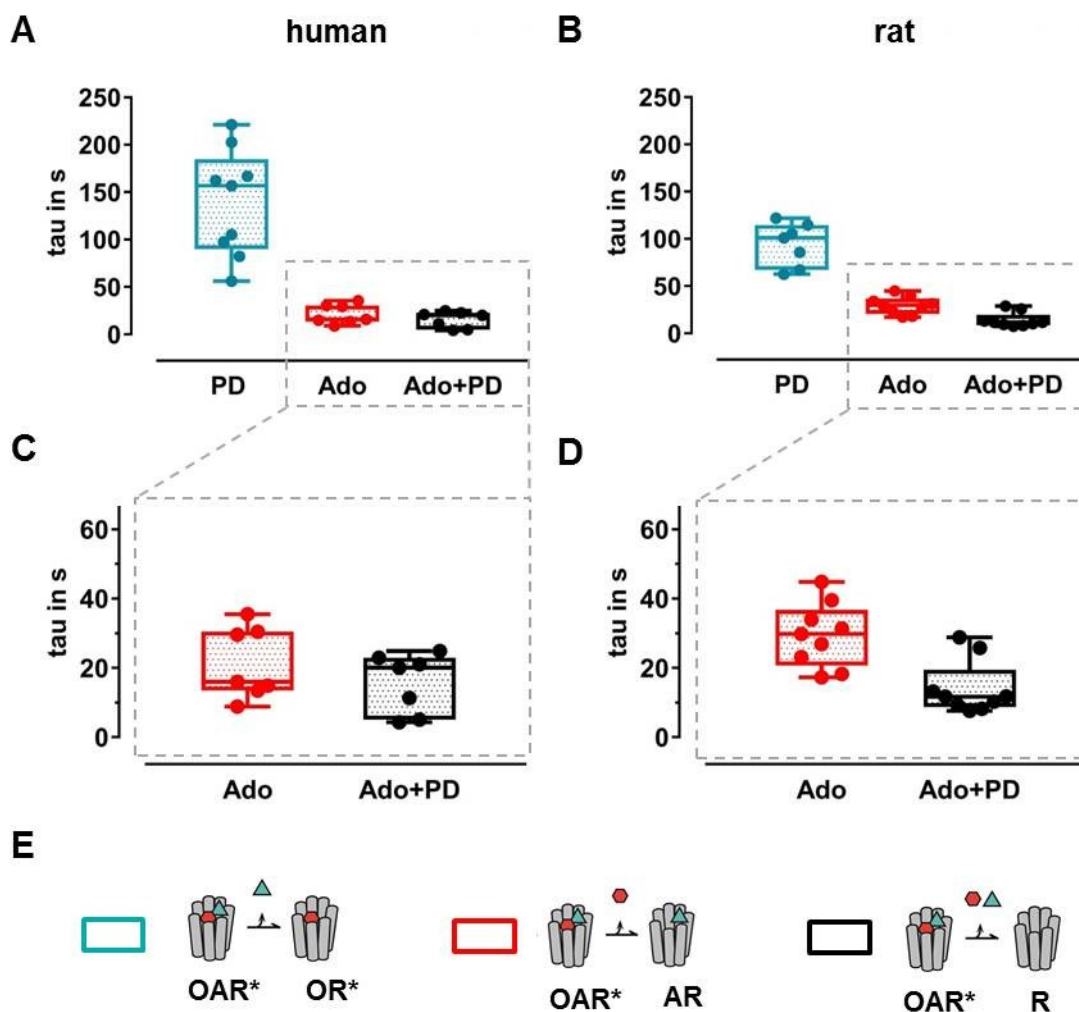


Figure 20: Orthosteric and allosteric dissociation kinetics from OAR*. Single tau values are represented in box plots. Median is indicated by vertical line and the whiskers are defined by minimal and maximal tau value. The tau values were determined as visualized in Figure 19. **A, C**, dissociation from human A1AR **B, D**, dissociation from rat A1AR. **A, B**, dissociation of PD 81,723 from OAR* (cyan) is reduced compared to dissociation of adenosine (red) and dissociation of both ligands simultaneously (black). **C, D**, the dissociation of adenosine from OAR* in the presence of PD 81,723 at the receptor (red) is marginally reduced over simultaneous dissociation (black). **E**, pictograms illustrate the respective molecular events at the receptor. Data were collected from $n \geq 7$ individual cells measured on at least three independent experimental days (means \pm SEM are reported in appendix Table 28, Table 29).

The kinetic data of all three experiments are presented in Figure 20, which allows examining two comparisons. First, the significant slower dissociation of PD 81,723 (cyan) from adenosine-occupied receptor (OR*) in contrast to the dissociation of adenosine along with PD 81,723 (black) demonstrate that the receptor surface formed by the bound orthosteric ligand represents a highly attracting target for the allosteric modulator. Second, the comparison of adenosine dissociation from PD 81,723-occupied receptor (AR) with the simultaneous dissociation of adenosine

and PD 81,723 resulted in slightly slower dissociation of adenosine over simultaneous dissociation, but no significant difference was found. This data might indicate that adenosine is not sterically blocked by PD 81,723. The present work is unique in measuring the active receptor bound to adenosine and PD 81,723 and especially for determining the deactivation kinetics of the receptor upon dissociation of allosteric modulator. With these measurements additional information on the dissociation kinetics of the allosteric modulator itself can be obtained, which was lacking to date. These findings could be of high interest for the improvement of allosteric drug candidates. Altogether, the kinetic data obtained in this work revealed that the adenosine-bound adenosine A1 receptor is a high affinity target for PD 81,723 and the prolonged dissociation might be rather caused by energetic stability of the complex than by steric interactions of orthoster and allosteric modulator.

4.2 Investigation of mutations in the putative allosteric binding site

4.2.1 Orthosteric characterization of mutants in the second extracellular loop

Extracellular loops contribute to the binding site for allosteric modulators, due to their high sequence variability in the evolution of GPCRs. This proposal was investigated in the field of adenosine receptors by mutational analysis (Peeters et al. 2012, Nguyen et al. 2016a, Kennedy et al. 2014). In the present work, three amino acid residues (S161, E172 and I175) in the second extracellular loop were substituted by alanine to elucidate their influence on orthosteric and allosteric behavior. E172 and I175 are in the vicinity of the orthosteric binding pocket whereas S161 is the most distant to the orthosteric ligand binding site (Figure 21 A). Stable cell lines expressing the single mutant FRET sensors were generated for rat and human A1AR. The mutants showed reduced membrane expression of the CFP-tagged receptor, which hampered the detection of FRET (Figure 21 B, left panel). The membrane localization of adenosine receptor mutants can be improved by overnight treatment with theophylline, an AR antagonist (Stumpf 2015, Malaga-Diequez et al. 2010). Cells expressing rat E172A showed reduced receptor expression and less membrane localization compared to the cells pre-treated with theophylline (Figure 21 B, right panel). Cells were carefully washed with measuring buffer (Table 8) to clear off any residual theophylline just before the experiment. Without theophylline treatment insufficient or no FRET signals were detected for the mutant cell lines except for human E172A; expressing sufficient receptor sensor at the membrane.

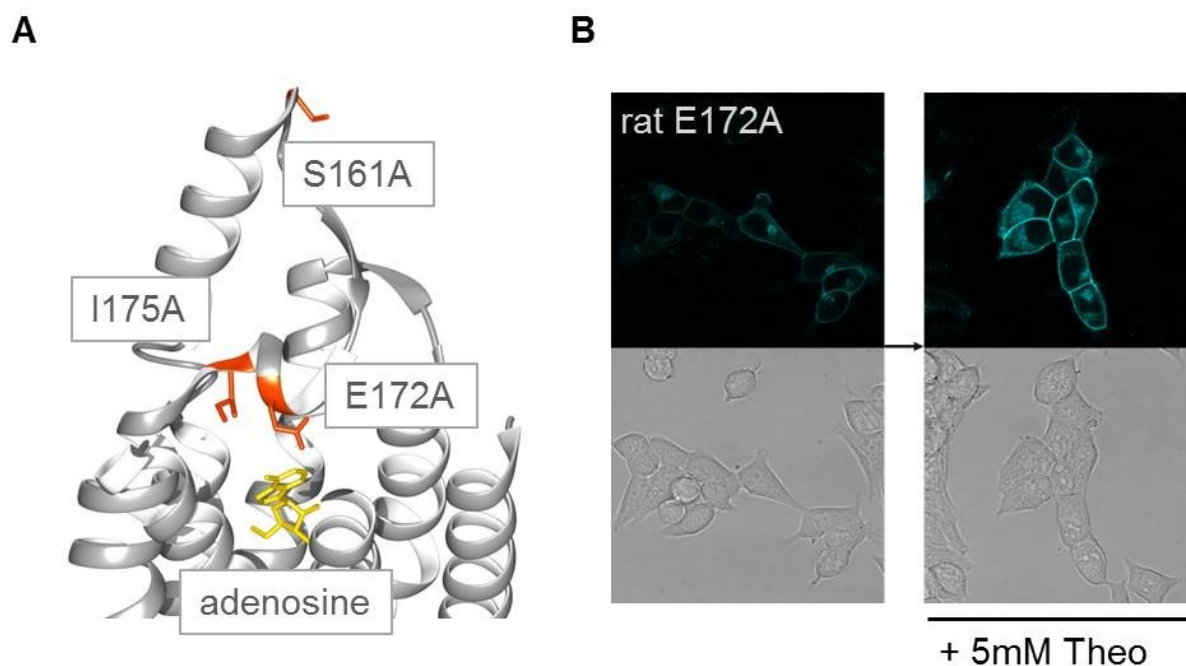


Figure 21: Modifications of the second extracellular loop and membrane localization of mutant receptor sensor. **A**, active structure of human adenosine A1 receptor bound to adenosine (yellow), PDB code: 6D9H showing amino acid residues (orange) chosen for alanine exchange. **B**, confocal images of cells stably expressing rat A1 FIAsh3 CFP E172A. **Top panels** show CFP emission upon excitation at 442 nm, **bottom panels** show cell morphology. **Left panel** shows expression of rat E172A without theophylline treatment, and **right panel** shows membrane localization of rat E172A after 24 h incubation with 5 mM theophylline. Images of membrane expression of human and rat mutants are represented in appendix Figure 29 and Figure 30.

4.2.1.1 Adenosine affinity of mutants in the second extracellular loop

The mutant cell lines of human and rat adenosine A1 receptors were characterized for adenosine affinity as described in 4.1.1. Concentration-response curves of mutant cell lines are represented in appendix, Figure 32. EC_{50} values are listed in Table 16 including the EC_{50} values of rat and human A1AR wt. E172A and I175A showed a decrease in affinity for adenosine, while S161A increased the affinity compared to wt for both species. The reduction in affinity for E172A and I175A over wt turned out to be in good correlation with the spatial orientation of both amino acids towards adenosine in the recently published crystal structure of A1AR in the active conformation bound to adenosine (Draper-Joyce et al. 2018), see Figure 21 A.

Table 16: EC₅₀ values of adenosine for human and rat ECL2 mutants compared to wt. Cell lines were investigated for adenosine response as described in 4.1.1. The EC₅₀ value of adenosine for human A1AR was determined in a previous doctoral study in the working group of Professor Hoffmann (Stumpf 2015). Data represent the mean in μM of $n \geq 18$ individual cells for human, $n \geq 14$ individual cells for rat from at least four independent experiments. Confidence intervals 95 % are presented in brackets. (#P < 0.05 one-way ANOVA and Dunnett's multiple comparisons test)

Mutation	human		rat	
	EC ₅₀ [μM] of Ado		EC ₅₀ [μM] of Ado	
wt	6.4	(3.8 - 10.3)	2.6	(2.2 - 3.1)
S161A	2.9	(1.5 - 5.4) #	1.1	(0.5 - 2.6) #
E172A	12.5	(10.0 - 15.6) #	14.8	(3.6 - 30.2) #
I175A	15.6	(12.6 - 19.3) #	10.5	(5.1 - 25.9) #

4.2.1.2 Orthosteric kinetics of mutants in the second extracellular loop

To investigate the kinetics of the mutant cell lines the association of adenosine to the unoccupied receptor ($R+O \rightarrow RO^*$) and the dissociation of adenosine from the activated receptor ($RO^* \rightarrow R+O$) were analyzed as described in 4.1.2. The computed tau values of the mutants were plotted in comparison to the kinetics of wt (Figure 22). The time constants of dissociation for E172A and I175A were decreased for both human and rat adenosine receptor compared to S161A and wt, see Figure 22 C, D. Ligands with fast dissociation kinetics have a short interaction-time with the receptor, which can result in reduced affinity. The decrease in dissociation time of E172A and I175A might therefore explain the decreased affinity (see respective EC₅₀ values in Table 14).

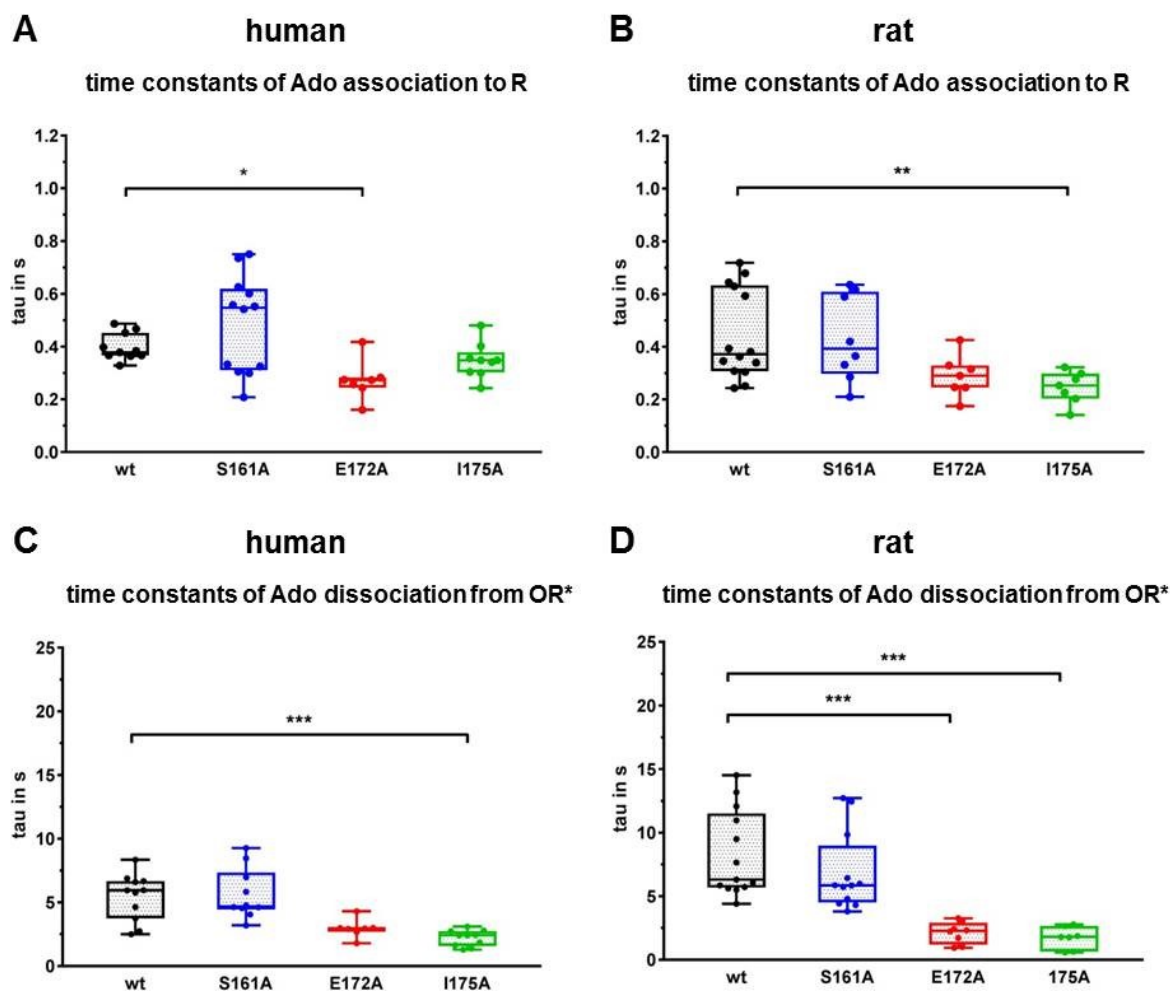


Figure 22: Influence of mutations in the second extracellular loop on the kinetics of adenosine. **A, B**, receptor activation upon association of 100 μ M adenosine to the unoccupied receptor of **A**, human A1AR **B**, rat A1AR. **C, D**, dissociation of 100 μ M adenosine from adenosine-receptor complex OR* of **C**, human A1AR and **D**, rat A1AR. Single tau values are represented in box plots. Median is indicated by vertical line and the whiskers are defined by the minimal and maximal tau value. Data were collected from at least three independent experimental days, $n \geq 7$ individual cells. Statistical significance was calculated by using Kruskal-Wallis test (* $P < 0.05$, ** $P < 0.01$, *** $P < 0.001$). Means \pm SEM in milliseconds are reported in appendix, Table 23, Table 24.

4.2.2 Allosteric characterization of mutants in the second extracellular loop

4.2.2.1 PD 81,723 affinity of mutants in the second extracellular loop

Affinity of PD 81,723 for the mutants in the second extracellular loop was experimentally determined as described in 4.1.4. EC_{30} values for each mutant were calculated by the use of an online tool provided by GraphPad (<https://www.graphpad.com/quickcalcs/Ecanything1.cfm>; accessed 2019) with the help of the respective hill slope values and EC_{50} concentrations determined in 4.2.1.1. Concentration-response curves represented in Figure 23 show the highest

relative enhancement for human E172A and the smallest enhancement for rat E172A. The resulting affinity values are represented in Table 17. A significantly increased affinity over human wt was found for human S161A, whereas the affinities of rat wt and rat S161A were not significantly different. This finding indicates a species-dependent difference in the binding process of the allosteric modulator.

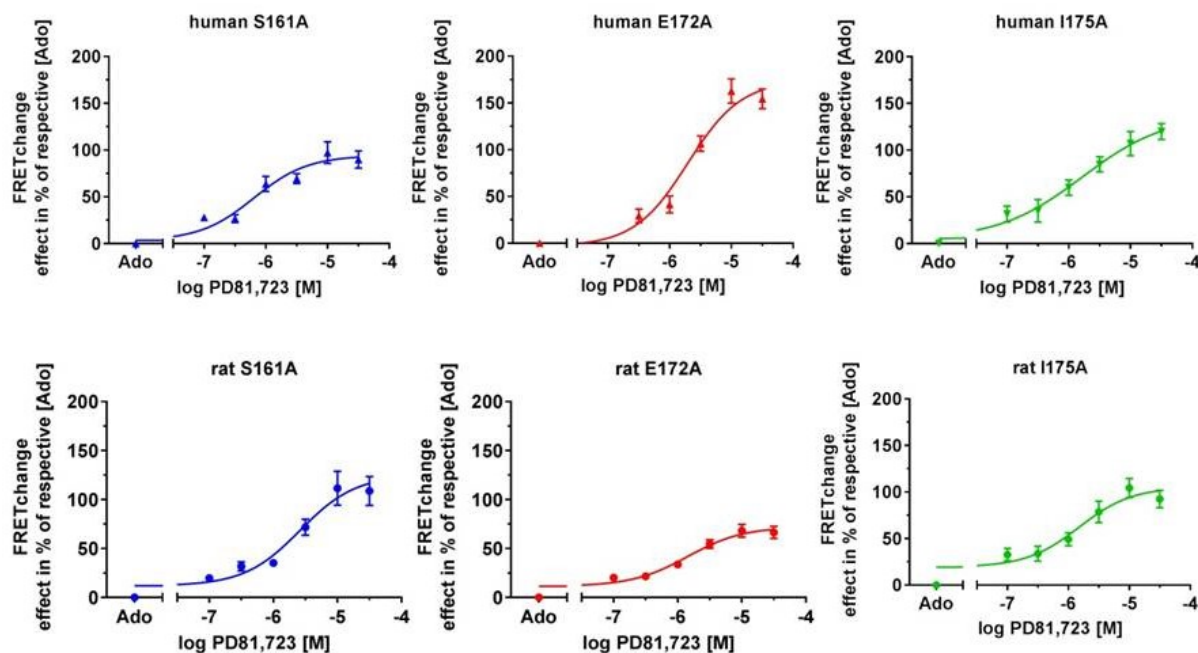


Figure 23: Affinity of PD 81,723 for human and rat mutants of second extra cellular loop. Top panel, human A1AR mutants, S161A (blue curve) was investigated for PD 81,723 affinity by the use of 2 μ M Ado. E172A (red curve) was assayed with 4 μ M Ado and I175A (green curve) with 5 μ M Ado. **Bottom panel,** rat A1 mutants, S161A (blue curve) was assayed for PD 81,723 affinity by the use of 0.5 μ M Ado. E172A (red curve) was investigated with 7 μ M Ado and I175A (green curve) with 5 μ M Ado. EC_{50} values of PD 81,723 are summarized in Table 17. Data represent the mean \pm SEM of $n \geq 16$ individual cells for rat and $n \geq 24$ individual cells for human measured on at least four independent experimental days.

Table 17: EC₅₀ of PD 81,723 for human and rat ECL2 mutants compared to wt. Cell lines were investigated for PD 81,723 affinity as described in 4.1.4 and 4.2.2.1. Resulting EC₅₀ values are represented in μM , 95 % confidence intervals are represented in brackets. Human S161A shows a significantly increased affinity over human wt, while rat S161A was not significantly different from rat wt (# $P < 0.05$ one-way ANOVA and Dunnett's multiple comparisons test). Data were obtained from $n \geq 24$ individual cells for human and $n \geq 16$ individual cells for rat measured on at least four independent experimental days.

Mutation	human EC ₅₀ [μM] of PD 81,723		rat EC ₅₀ [μM] of PD 81,723	
wt	2.08	(0.25 - 17.1)	2.96	(0.5 - 17.6)
S161A	0.64	(0.21 - 2.5) #	2.61	(0.89 - 7.57)
E172A	1.96	(1.1 - 3.6)	1.43	(0.58 - 3.46) #
I175A	1.65	(0.22 - 12.2)	1.50	(0.51 - 4.44) #

4.2.2.2 Influence of PD 81,723 on orthosteric affinity of mutants in the second extracellular loop

The influence of PD 81,723 on the concentration-response curve of adenosine was investigated for human and rat adenosine A1 receptor wt and demonstrated positive cooperativity of PD 81,723 for adenosine (see 4.1.5). The described experimental procedure was repeated for human and rat A1AR mutants of the second extracellular loop. Rat I175A showed an overall lower maximal response to adenosine, the FRET change is not substantially higher than 5 % (Figure 24, bottom panel green curves). Calculated fold shifts of the resulting EC₅₀ values are listed in Table 18. The strongest impact of PD 81,723 on the EC₅₀ values was found for human wt and for rat E172A and I175A. EC₅₀ values determined from absolute FRET change values are represented in appendix Table 22. The data shows that all mutants preserved the ability for positive cooperation of adenosine and allosteric modulator.

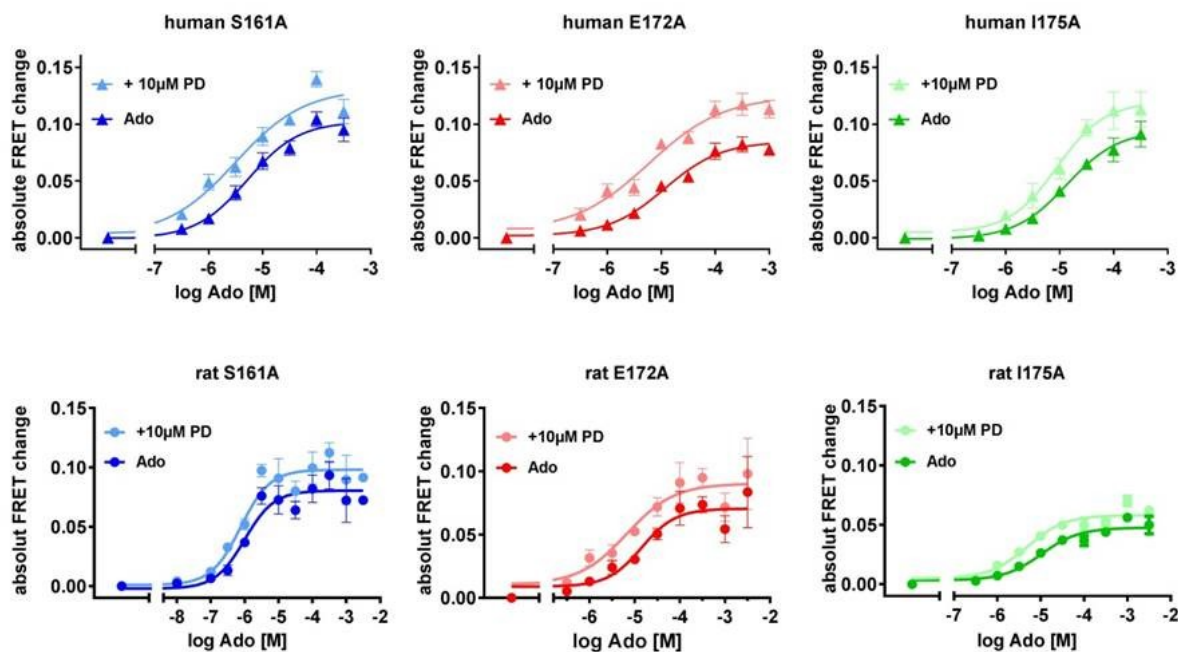


Figure 24: Influence of allosteric modulator on orthosteric concentration-response curve of mutants in the second extracellular loop. Adenosine response in the presence of 10 μ M PD 81,723 (light color) compared to the adenosine response without PD 81,723 (intensive color). **Top panels,** represent human A1AR mutants, **bottom panels,** represent rat A1AR mutants, S161A in blue, E172A in red and I175A in green. Fold shifts are summarized in Table 18. Data represent the mean \pm SEM of absolute FRET change values of $n \geq 30$ individual cells for human and $n \geq 25$ individual cells for rat measured on at least five independent experimental days. Curves are significantly different ($P < 0.0001$) by two-way ANOVA and Bonferroni's comparison test.

Table 18: Influence of mutants on the ability of PD 81,723 to shift the concentration-response curve of adenosine. EC_{50} values (listed in appendix, Table 22) were used for calculating the fold change of EC_{50} in the presence of the allosteric modulator PD 81,723. For statistical analysis an unpaired two-tailed t-test was performed using $\log EC_{50} \pm SD$ (## $P < 0.01$, #### $P < 0.0001$). Data were obtained from $n \geq 30$ individual cells for human and $n \geq 25$ individual cells for rat measured on at least five independent experimental days.

Mutation	human EC_{50} fold shift	rat EC_{50} fold shift
wt	2.40 ####	1.65 ####
S161A	1.65 ####	1.32 ##
E172A	1.97 ####	2.13 ####
I175A	1.51 ####	2.15 ####

4.2.2.3 Allosteric kinetics of mutants in the second extracellular loop

To elucidate the influence of the mutations in the second extracellular loop on the kinetic behavior of allosteric modulator PD 81,723, mutant cells lines were investigated for association and dissociation of PD 81,723 as described in 4.1.2. The determined tau values of the mutants were compared to wt kinetics (Figure 25). For rat A1AR no significant differences were detected (Figure 25 B, D). Human A1AR showed faster dissociation kinetics for E172A and I175A (Figure 25 C) compared to human wt. The association of PD 81,723 for human S161A was faster than for wt and the dissociation from S161A was slightly slower than wt (Figure 25 A, C). Increased association kinetics and decreased dissociation kinetics of a ligand results in an increased residence time at the receptor. This, together with the increased affinity determined for human S161A but not for rat S161A (Table 17) lead to the question as to what point these differences arise.

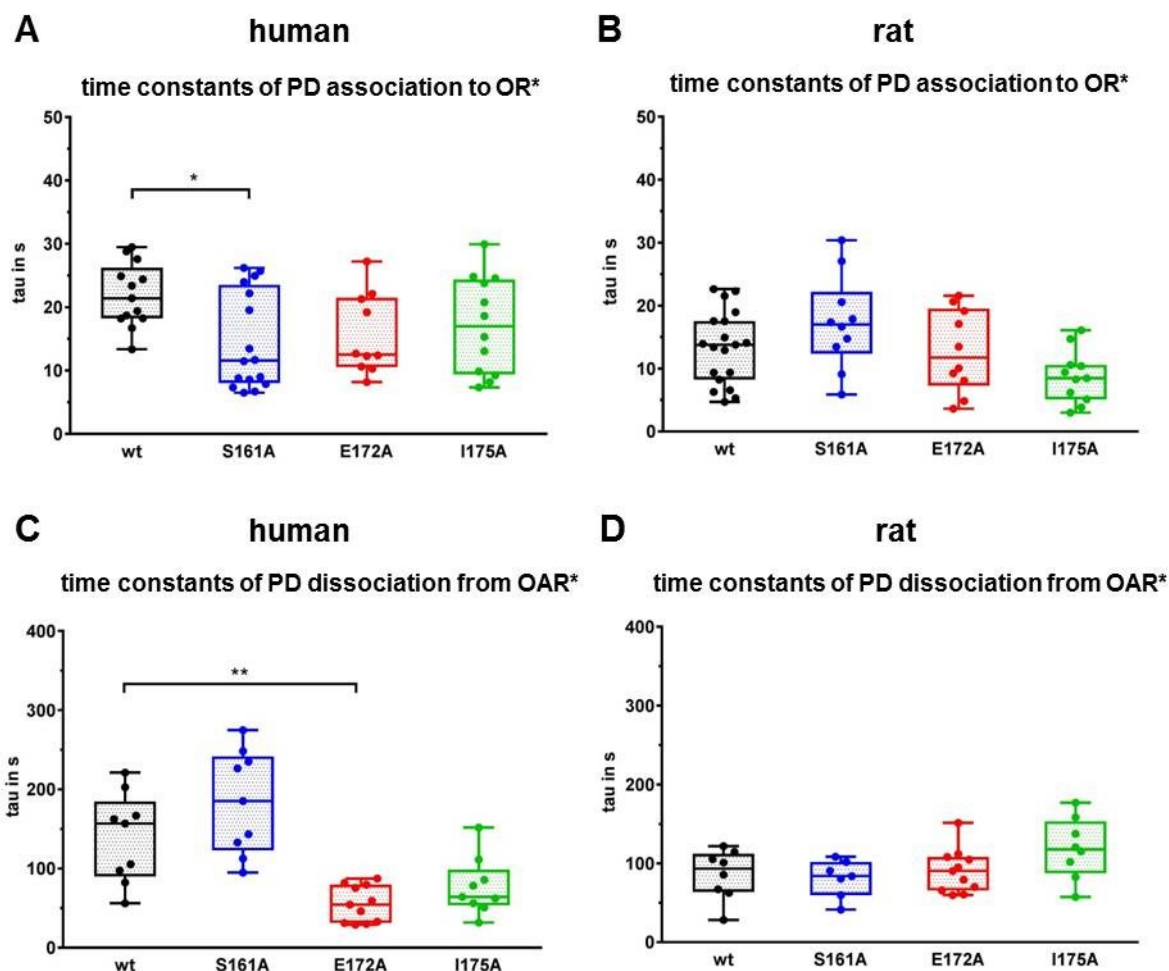


Figure 25: Influence of mutations in the second extracellular loop on the kinetics of PD 81,723. **A, B**, association of PD 81,723 to human A1AR **A** and rat A1AR **B**. **C, D**, dissociation of PD 81,723 from human receptors occupied by adenosine **C** and from rat receptors occupied by adenosine **D**. Single tau values are represented in box plots. Median is indicated by vertical line and the whiskers are defined by the minimal and maximal tau value. Statistical significance was calculated by using the Kruskal-Wallis test (* $P < 0.05$, ** $P < 0.01$). Data were obtained from $n \geq 8$ individual cells measured on at least three independent experimental days (means \pm SEM are reported in appendix, Table 27, Table 28, Table 29).

By inspecting the crystal structure of active adenosine A1 receptor (Draper-Joyce et al. 2018) as well as the amino acid sequence of rat A1AR four distinct amino acids in the helix of the second extracellular loop were revealed A151, R154, A155, A157. Furthermore, the adjacent amino acid of S161 at position 162 was found to be a methionine in the human sequence whereas a valine was found in rat A1AR sequence. To investigate the influence of amino acid at position 162 on PD 81,723 behavior two double mutants were generated on the base of S161A; human A1 FIAsh3 CFP S161A M162V and rat A1 FIAsh3 CFP S161A V162M. Both mutant receptors were well expressed at the cell membrane after overnight incubation with

theophylline as described in 4.2.1., see Figure 26. The double mutant cell lines were characterized for adenosine and PD 81,723 affinity as described before in chapter 4.1.1 and 4.1.4. The EC_{50} values of adenosine are listed in appendix Table 20. The calculated EC_{30} values of adenosine were used to determine the affinity of PD 81,723 for human S161A M162V ($EC_{50} = 2.6 \mu\text{M}$) and for rat S161A V162M ($EC_{50} = 2.1 \mu\text{M}$).

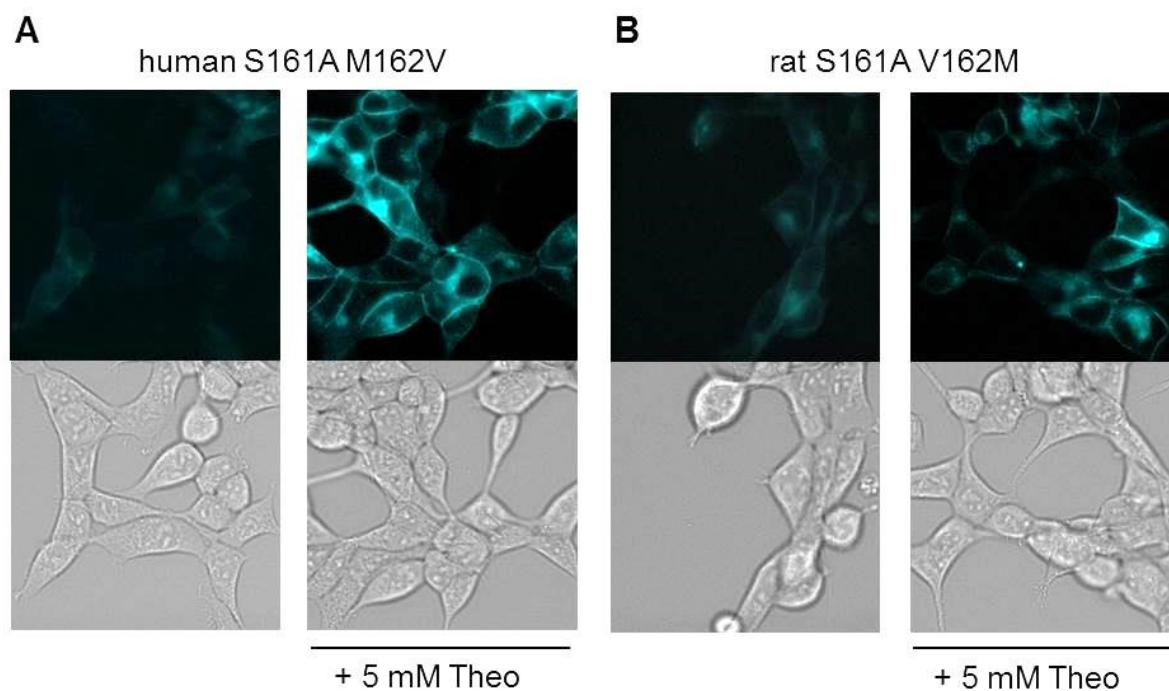


Figure 26: Membrane localization of double mutant receptor FRET sensor. A, cells expressing human A1 FIAsh3 CFP S161A M162V show reduced membrane expression without theophylline **left panel**, compared to cells after 24 h incubation with 5 mM theophylline **right panel**. **B,** cells expressing rat A1 FIAsh3 CFP S161A V162M show reduced membrane expression without theophylline **left panel**, compared to cells after 24 h incubation with 5 mM theophylline, **right panel**.

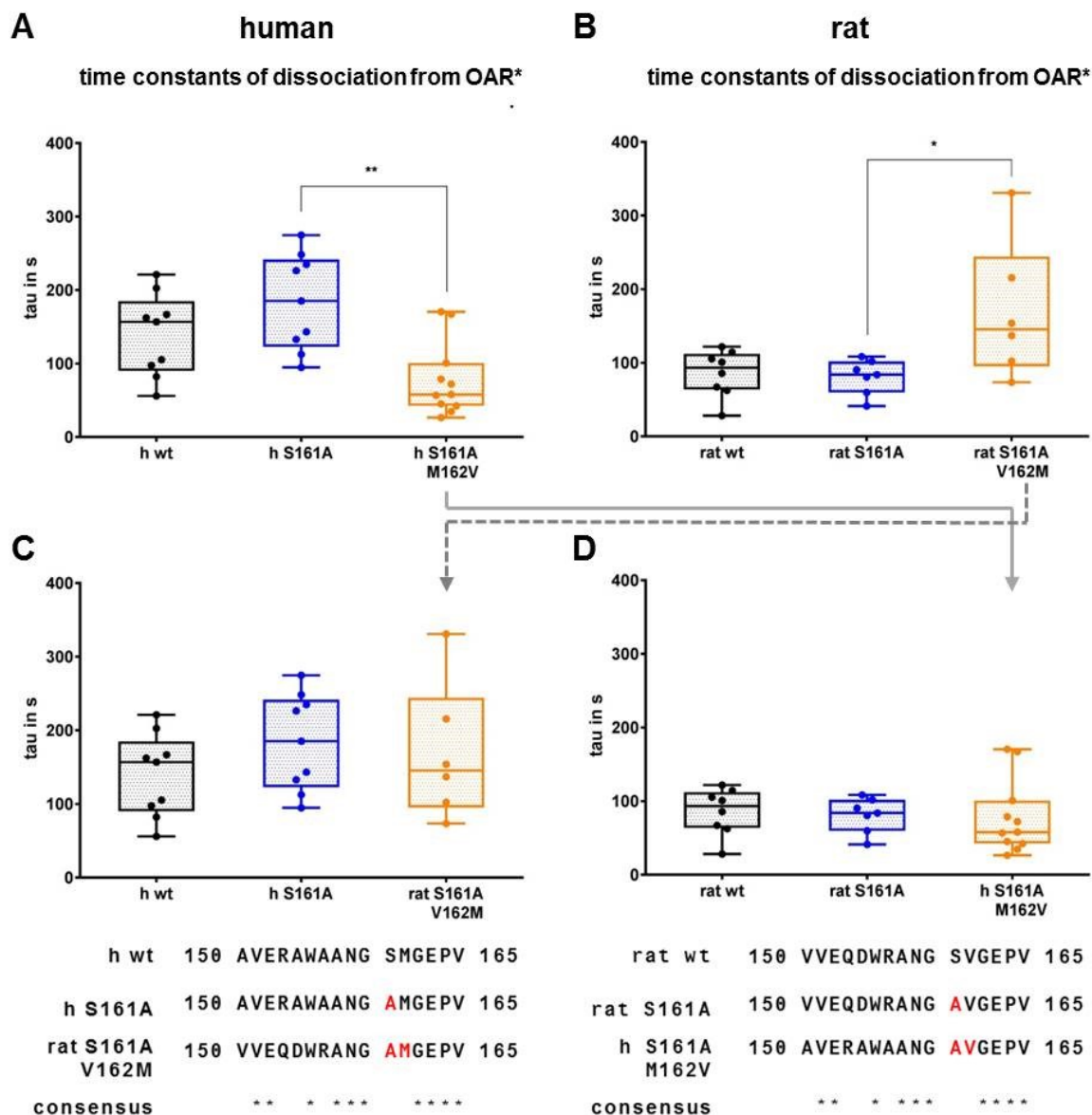


Figure 27: Kinetic rescue of human S161A by S161A M162V. **A**, dissociation of human wt, human S161A and human S161A M162V **B**, comparison of dissociation time constants of rat wt, rat S161A and rat S161A V162M. **C, D, top** visualization of the kinetic rescue by exchanging the human and rat double mutant. **C**, graph represents human wt and human S161A in comparison to rat S161A V161M **D**, graph shows rat wt and rat S161A in comparison to human S161A M161V. **C, D, bottom**, alignments show sections of the second extracellular loop, mutational changes are highlighted in red letters. Single tau values are represented in box plots. Median is indicated by vertical line and the whiskers are defined by the minimal and maximal tau value. Statistical significance was calculated by using the Kruskal-Wallis test (* $P < 0.05$, ** $P < 0.01$). Data were obtained from $n \geq 6$ individual cells measured on at least three independent experimental days (means \pm SEM are reported in appendix, Table 28, Table 29).

The dissociation of PD 81,723 from human double mutant was faster compared to wt and S161A and the dissociation of PD 81,723 from rat double mutant was slower compared to rat wt and rat S161A (Figure 27 A, B and Table 19). By exchanging amino acids from one species to the other at position 162 the human S161A mutant was made rat-like and the rat S161A became human-like. This equalization of the species is visualized by exchanging the kinetics of the rat double mutant in the graph presenting human wt and human S161A and vice versa (Figure 27 C, D). The alignments in the bottom panel of Figure 27 C and D show the mutational changes in red letters at position 161 and 162 but also the other four differing amino acids in the second extracellular loop are visible (see consensus row). In Figure 27 C, D the dissociation time constants of double mutants are in the same range as the S161A of the other species (not significantly different by Mann-Whitney test). This shows that the human double mutant, exchanged for the rat amino acid valine, indeed behaved like rat S161A and rat double mutant behaved like human S161A. This data suggests that interactions with the residue at position 162 are important for the kinetic behavior of allosteric modulators.

Table 19: Dissociation of 10 μ M PD 81,723 from OAR*. The kinetics of the double mutant were significantly different from respective wt and respective S161A (# $P < 0.05$, ## $P < 0.01$ Mann-Whitney test). Tau values are presented as median in seconds, 25 % and 75 % percentile are presented in brackets. Data were obtained from $n \geq 6$ individual cells measured on at least three independent experimental days. For curve fitting the mono-exponential equation ($f(x) = A * e^{(-t/\tau)}$) was used.

human	wt	S161A	S161A M162V
tau [s]	156.9 (89.9-184.8) #	185.2 (122.8-241.6) ##	58.1 (42.4-100.9)
rat	wt	S161A	S161A V162M
tau [s]	93.3 (63.7-112.3) #	83.8 (59.7-101.8) #	145.4 (95.2-244.3)

5 Discussion

Adenosine receptors (A1, A2A, A2B and A3), widely distributed throughout the human body, are involved in multiple physiological and pathophysiological processes. Several attempts have been made to target specific adenosine receptor subtypes. Numerous compounds have been identified with varying affinity amongst AR subtypes (Müller and Jacobson 2011). Most of these compounds are still not on the market as approved drugs. This limitation is due to two major reasons; first, being insufficient efficacy, which is in part because of dose-limiting toxicity in chronic application and, second being manifold on- or off-target side effects (Yan et al. 2003). Positive allosteric modulators (PAM) potentiate the effects induced by receptor agonists and act in a spatial and temporal manner defined by the agonist behavior. In addition, allosteric modulators display improved subtype-selectivity as a result of less conserved allosteric binding sites across receptor subtypes. Furthermore, the use of subtype-specific PAMs has a high potential for reducing accompanying side effects due to a reduced demand for agonist dose (Dhalla et al. 2003). Application of decreased doses of agonists would be preferable as this will reduce the risk of dose-limiting toxicity and dose-limiting adverse effects as well. In the field of adenosine receptors, adverse side effects are in part mediated by co-activation of AR subtypes in the same or other tissues (Yan et al. 2003). Reduction in these side effects of adenosine agonists might be achieved by increasing subtype-specificity with the positive allosteric modulator PD 81,723, which is selective for adenosine A1 receptor subtype (Bruns and Fergus 1990). Therefore it is of utmost interest to gain detailed insights on allosteric mechanisms at the A1AR in terms of affinity and kinetics. The impact of single amino acids in the putative allosteric binding site on the allosteric behavior can provide valuable knowledge for drug development in medical chemistry.

5.1 Orthosteric and allosteric characterization of human and rat adenosine A1 receptor

5.1.1 Orthosteric characterization

Studies on adenosine receptors using standard methods like radioligand binding cannot investigate effects of endogenous ligand adenosine. Radioligand binding experiments use membrane preparations, which release uncontrollable amounts of adenosine and therefore addition of adenosine deaminase, becomes necessary (Seibt et al. 2013). Thus radioligand binding is unsuitable for determining adenosine affinity. This shortcoming can be overcome by the use of fluorescently tagged receptors in intact cells. With FRET (fluorescence resonance energy transfer)-based techniques ligand binding can be observed indirectly by recording conformational changes. Although radioligand binding assays detect direct ligand binding, binding might lead only to small conformational changes on the extracellular part of the receptor and not necessarily lead to an activation of the receptor and consequently no downstream signaling would occur. Innovative FRET sensors have been developed, which detect conformational movements of the intracellular part of the receptor upon ligand binding and consequent biologic response. Thus, one could say such FRET sensors can measure 'effective' ligand binding. Recently developed FRET sensors are highly suitable to monitor conformational changes in real time as demonstrated for several GPCRs (Stumpf and Hoffmann 2016, Messerer et al. 2017, Wright et al. 2018). In the present work an established FRET sensor design was applied to the adenosine A1 receptor. The adenosine A1 FRET sensor consists of a FIAsh binding motif introduced into the sequence of the third intracellular loop and a CFP genetically encoded at the receptor C-terminus (1.4.2). The FIAsh-based FRET sensors, designed as described above, maintained the signaling properties of the receptor (Hoffmann et al. 2005).

In the present work, HEK293 cells stably expressing the above described A1AR FRET sensor (Stumpf 2015), were used to investigate orthosteric and allosteric ligand interactions at human and rat adenosine A1 receptors in real-time. The generation of stable cell lines ensured consistent expression levels and reproducible results of the FIAsh-labeling procedure. The novel rat adenosine A1 receptor FRET sensor was first characterized for orthosteric ligand affinity. The endogenous ligand adenosine, the synthetic agonists CPA and NECA were also tested. NECA is a high-

affinity agonist but unspecific for all four adenosine receptor subtypes, while CPA is known to have an increased affinity for A1AR compared to the other AR subtypes. The affinities determined in this study were reflect the known tendencies in specificity (Ado > NECA > CPA), but the values of CPA and NECA are not comparative with values found in the benchmark literature, (Klotz 2000). The authors reported a calculated K_i -value for CPA as 2.3 nM for the human A1AR derived from competition binding assays with radio labeled [^3H]NECA in the presence of GTP [receptor in high affinity state] (Klotz et al. 1989). The fact that CPA affinity determined from the FRET measurements was reduced 100-fold (320 nM CPA) is based on the assay in use. In the field of adenosine receptors, the 'gold standard' to determine ligand affinities is radioligand binding. Most radioligand binding studies are based on membrane preparations. Destroyed membranes yield higher affinity and faster dissociation kinetics than intact cells (Hara et al. 1998, Fierens et al. 2002). Furthermore, in radioligand binding experiments with GPCRs, an excess of GTP is applied to the membrane fractions, thereby manipulating the coupling state of G proteins to the receptors, which results in significant affinity-shifts. One can doubt the comparativity of such experimental conditions with physiologic conditions. Radioligand binding affinities obtained from competition binding assays with antagonist DPXPC in intact CHO cells (Cordeaux et al. 2004) were in line with the values found in the present work: for NECA an affinity of 1.7 μM and for CPA an affinity of 0.67 μM was determined ($\text{EC}_{50}\text{FRET}$: 2.6 μM NECA and 0.32 μM CPA).

Affinities for the endogenous orthosteric ligand adenosine have been seldom determined by radioligand binding studies (Libert et al. 1992, Cohen et al. 1996). This is a consequence of the fact that externally added adenosine deaminase (ADA) is necessary to control endogenous release of adenosine. Therefore most affinity data is derived from functional read-outs like adenylyl cyclase assays (Yan et al. 2003). Fluorophore based techniques, like the whole cell FRET approach used in this work, are highly suitable to measure adenosine affinities in the absence of ADA (Stumpf 2015). Cooper and co-workers determined the affinity of endogenous adenosine in a competition assay for human A1AR as 38 μM and for rat A1AR as 29 μM using a bioluminescent approach (BRET between fluorescent antagonist CA200645 and Nluc-A1). Furthermore the authors also identified adenosine binding affinities using BRET between a fluorescent adenosine (ABA-X-BY630) and human A1AR tagged with Nano-luciferase as 0.77 μM and for rat as 0.95 μM in a saturation binding assay

(Cooper et al. 2019). The adenosine affinities identified by the used FRET approach, 6.4 μM for human A1AR (Stumpf 2015) and 2.6 μM for rat A1AR, fall quite well within the range determined by Cooper and coworkers.

Most ligands identified by *in vitro* screening assays showed sufficient efficacy or affinity for clinical trials, but failed because of severe side effects or lack of *in vivo* efficacy (Waring et al. 2015). An alternate approach for the prediction of *in vivo* performance is the analysis of kinetic data of drug candidates. For drug discovery, kinetics will become a key aspect. Depending on the disease pattern, a short or long residence time (1.1.3) is preferable. A dependency of prolonged residence time and high affinity is not necessarily given for all GPCRs (Louvel et al. 2014), that is why researchers should carefully inspect both properties before excluding a promising candidate from animal testing only by its *in vitro* affinity. Although residence time was defined only by the dissociation rate, researchers become more and more aware of the correlation of both association and dissociation for *in vivo* systems (Sykes et al. 2019).

Ideally, affinity data obtained from radioligand-based saturating experiments are expected to be consistent with the dissociation constant K_D calculated from another set of radioligand experiments as illustrated in Figure 5, chapter 1.3.2. By calculating a kinetic $K_{D \text{ FRET}}$, the kinetic data of adenosine can be correlated with the affinity data of adenosine reported in this work. The Kinetic $K_{D \text{ FRET}}$ for adenosine was calculated (Table 25, appendix), assuming that the equations used for radioligand binding data as described in 1.1.3 are as well valid for the FRET data obtained in this work. Observed association kinetics, (k_{obs}), reported using the human and rat FRET sensors were 10-fold and 20-fold faster than dissociation kinetics (k_{off}) for 100 μM adenosine (Figure 11; Table 25, appendix). The calculated $K_{D \text{ FRET}}$ was 7.88 μM for the human A1AR and 5.65 μM for rat A1AR, which are in good agreement with the human EC_{50} of 6.4 μM and rat EC_{50} of 2.6 μM determined by affinity FRET measurements as described in 4.1.1. This proves that the FRET method delivers equal output as radio labeled applications, in providing information on the affinity as well as association and dissociation rate constants of a ligand. One could argue that intramolecular FRET sensors are only detecting indirect ligand binding. Nevertheless, striking advantage of FRET measurements is that the state of active receptor is observed; an effective binding is measured on-line with this technique. Generation of

radioactive labeled ligands is time consuming and expensive. Moreover, there is also no limitation in the choice of ligands to investigate with such a FRET-based sensor, in contrast to radioligand binding assays. In general, FRET sensors can report ligand binding under physiologic conditions *in vivo*. Furthermore, the FRET-pair design used in this study maintains G protein signaling function of the adenosine A1 receptor (Stumpf 2015). Radioligand binding assays have to be accompanied by additional time consuming second-messenger assays to prove functional binding, whereas intramolecular FRET sensors monitor on-line effective binding.

5.1.2 Allosteric characterization

Orthosteric affinity in the presence of allosteric modulator is well studied in the field of allosteric modulation, but affinity data of the allosteric modulator for its target is rather seldom investigated. In the present work, the affinity of PD 81,723 to human and rat adenosine A1 receptor in combination with endogenous ligand adenosine was determined for the first time. Adenosine concentrations in the lower micro molar range (3 μM hA1AR; 1 μM ratA1AR) were identified to exhibit an optimal measuring window for positive allosteric effects. Interestingly, Kollias-Baker and colleagues also used 3 μM adenosine to investigate positive allosteric effects in perfused guinea pig hearts (Kollias-Baker et al. 1994). This beautifully underlines the *in vivo* relevance of the present work and demonstrates the strength of a FRET approach to mirror physiologically relevant concentrations.

The affinity of allosteric modulator PD 81,723 was experimentally determined to be in between 0.1 μM to 30 μM PD 81,723. Concentrations exceeding 30 μM PD 81,723 showed no reproducible FRET enhancement of the adenosine signal. In some cases 100 μM PD 81,723 initiated signal enhancement for couple of hundred milliseconds followed by a fast decrease to baseline or below, even in the continuous presence of Ado and PD 81,723. 100 μM of PD 81,723 also yielded a visible yellow color, possibly interfering with the excitation of CFP. Yellow color of a solution containing molecules with conjugate double bonds indicates light absorption in the wavelength area of blue light (e.g. β -carotene absorbs at 460 nm). In addition, this behavior reflects the evolving competitive antagonism of PD 81,723. The antagonistic behavior for high concentrations of PD 81,723 has been observed in radioligand binding assays by Bruns and co-workers (Bruns and Fergus 1990). These authors had determined a affinity of 9.83 μM for PD 81,723 by observing the dissociation of radio

labeled CHA from rat whole brain membranes dependent on increasing concentrations of PD 81,723 (Bruns et al. 1990). Similarly, another study identified an EC_{50} value of 14.7 μM for PD 81,723 determined in a dissociation assay of CPA from rat brain cortex membranes (van der Klein et al. 1999). In addition, the *in vivo* action of endogenous adenosine was enhanced by PD 81,723 as qualitatively demonstrated for isolated guinea pig hearts (Kollias-Baker et al. 1994).

In the present work, the affinity of PD 81,723 for human and rat adenosine receptor was determined for the first time in combination with endogenous agonist adenosine. Human and rat receptors displayed no considerable difference in affinity for PD 81,723. The affinity of PD 81,723 for the adenosine-occupied receptor was determined in the lower micro molar range, whereas PD 81,723 showed five-fold reduction in affinity for the NECA-occupied human adenosine A1 receptor in the present work. The application of PD 81,723 in combination with adenosine or NECA showed a clear difference in the saturation of the concentration response curve of PD 81,723. The enhancing effect of allosteric modulator did not reach saturation with 30 μM PD 81,723 at NECA-bound receptor (Figure 17), which is problematic in regard to the evolving antagonism of PD 81,723 at higher concentrations. The application of PD 81,723 in combination with adenosine has a broader therapeutic window compared to the use of other agonists, which require higher PD 81,723 concentrations to reach the half maximal effect. This difference and dependence of affinity of PD 81,723 on different probes (CHA, CPA, and NECA) should be considered in the design of clinical trials aiming to dose allosteric modulators in combination with synthetic adenosine agonists. The evidence for probe dependency is an explicit characteristic for allostery and indicates the sensitivity of allosteric modulator for distinct receptor conformations.

An allosteric modulator can influence the properties of a conformationally linked orthosteric binding site. The cooperativity of the allosteric site with the orthosteric site was investigated by monitoring the conformational change induced by varying concentrations of adenosine and consequent enhancement by 10 μM PD 81,723. The resulting concentration-response curves show that PD 81,723 increases the affinity of adenosine for human and rat A1AR, displaying a positive cooperativity as anticipated for PAMs (Figure 16). PD 81,723 showed a stronger influence on the EC_{50} of adenosine at human A1AR than at rat A1AR, indicating an improved cooperativity at human A1AR. This finding is in accordance with an increased affinity

of PD 81,723 for human A1AR (Figure 14). The cooperativity shift for adenosine is relatively low compared to affinity shifts of other adenosine agonists (Guo et al. 2014), which further supports the identified probe dependency.

In this study, the data is represented in absolute FRET change values per tested concentration. This representation displayed the left-ward shift (EC_{50}) as well as the upward-shift of the concentration-response curve for high adenosine concentrations (E_{max}) in the presence of PD 81,723. Surprisingly, the response to saturating concentrations of adenosine was further enhanced by PD 81,723, which allows for two valid assumptions. First, this finding might indicate that receptors which were not responsive before became available for adenosine binding in the presence of PD 81,723, or second, the FRET efficiency for each adenosine-activated receptor sensor increased.

A change in FRET efficiency, either by a change in the distance or by the relative orientation of the fluorescent tags towards each other, is indicative of a different conformation at the intracellular site of the receptor triggered by allosteric binding. An enhancement in conformational change would prove that allosteric modulators regulate not only affinity but also efficacy. Therefore, the allosteric behavior would not solely be explainable by increased orthosteric binding, but by a more efficacious signal transmission within the receptor and subsequent increased G protein coupling. Unfortunately, the G protein activation assay was not suitable to address the question of improved signaling by allosteric modulator, as described in chapter 4.1.7. For future investigations, a G protein coupling assay might be more successful. The kinetics of the coupling would be expected to be faster in the presence of the allosteric modulator. In addition, single molecule FRET-sensors would only detect the effect of allosteric modulator on the G protein coupling independent of increasing receptor numbers.

The first interpretation, that more receptors are activated, is supported by the finding of increased maximal agonist binding (B_{max}) in the presence of PD 81,723 in radioligand binding experiments (Baraldi et al. 2003) or in BRET experiments using fluorescent A1AR agonists (Cooper et al. 2019). The authors of the latter study concluded that the presence of positive allosteric modulators switches the receptors from inactive to active states. The allosteric enhancement of E_{max} , identified in the present work, might also imply the existence of a receptor reserve for A1AR. Receptor reserve defines a fraction of receptors, which were not activated by the

agonist concentration required to provoke a full response of the cell. This might also indicate that PD 81,723 switches inactive or irresponsive receptors from the reserve to the field of action.

5.1.3 Kinetic aspects of allosteric modulation

In addition to 'probe dependency' and 'cooperativity', a further characteristic of allosteric ligands is the regulation of orthosteric kinetics. It has been observed by several research groups, that the dissociation of orthosteric ligands is slowed down in the presence of positive allosteric modulators. Kinetic data of allosteric modulation is often derived from radioligand binding studies (1.3.2) using simple fitting models which do not consider receptor dynamics as a part of ligand binding kinetics (Copeland 2011). The impact of PAMs on orthosteric ligand dissociation is well-known in the field (Guo et al. 2014), but the dissociation kinetics of allosteric modulators itself have not been investigated so far. The kinetic behavior of PD 81,723 for adenosine-bound human and rat adenosine A1 receptor was determined in this work for the first time. In contrast to kinetic data derived from radioligand assays, FRET biosensors can monitor receptor activation and deactivation kinetics using *in vivo* conditions. The FRET setup used in this work enabled the simulation of an open system by ligand application and removal in milliseconds (as described in 3.2.5).

The decay in FRET response upon washout of PD 81,723, in the constant presence of adenosine at the receptor, was slowed down manifold compared to simultaneous washout of adenosine and PD 81,723. The dissociation of PD 81,723 from human adenosine A1 receptor bound to adenosine was 1.6-fold slower compared to rat A1AR, but the dissociation of PD 81,723 from the active receptor conformation compared to adenosine-PD 81,723-receptor complex dissociation was reduced by factor eight for both species (human: 7.8-fold, rat: 7.9-fold). Additionally, data on association of PD 81,723 to the adenosine-activated receptor was also collected from these experiments (Table 27, appendix). Thus a kinetic K_D was calculated by the ratio of dissociation and association of 10 μ M PD 81,723 (Table 30, appendix).

Kinetic $K_{D \text{ FRET}}$ and experimentally determined EC_{50} of PD 81,723 were found to be in good relation with each other:

Human A1AR: $EC_{50} = 2.1 \mu\text{M}$ and $K_D = 1.84 \mu\text{M}$

Rat A1AR: $EC_{50} = 2.9 \mu\text{M}$ and $K_D = 1.87 \mu\text{M}$

This correlation indicates that the equations for orthosteric binding are also valid for potentially complex allosteric binding events and that PD 81,723 recognizes the adenosine-occupied receptor as a discrete binding scaffold. In comparing a series of drug candidates, the kinetic $K_{D \text{ FRET}}$ of an allosteric modulator is a valuable parameter. The experimental determination leading to $K_{D \text{ FRET}}$ delivers information on association, dissociation and affinity of an allosteric compound under investigation. To sum it up, FRET faithfully reports 'effective' orthosteric and allosteric ligand association and dissociation kinetics by monitoring adenosine A1 receptor dynamics in single living cells.

It has been hypothesized that PD 81,723 increases agonist binding by slowing down the dissociation kinetics of adenosine receptor agonists (Bruns et al. 1990, Mizumura et al. 1996, Guo et al. 2014). However, for a deeper understanding of allosteric mechanism the question arises if the prolonged dissociation is the reason for the increase in affinity or if the prolonged dissociation is a consequence of the increased affinity. An explanation for prolonged dissociation of orthosteric ligand in the presence of an allosteric modulator might be caused by a direct steric hindrance of the orthosteric molecule by the allosteric modulator. Steric hindrance was observed for the muscarinic acetylcholine receptor M2; at which the orthosteric ligand is locked in the binding pocket by a lid of aromatic residues. The binding of a PAM further stabilized the lid closure (Kruse et al. 2013, Burger et al. 2018).

In order to elucidate the question on steric hindrance at A1AR, two washout experiments were conducted. One situation is comparable with the batch experiments described in literature, in which an infinite dilution is applied to membranes pre-incubated with orthosteric ligand and allosteric modulator ($OAR \rightarrow O+A+R$). The second set of washout experiments illuminates the dissociation of orthosteric ligand from the receptor in the presence of allosteric modulator ($OAR \rightarrow O+AR$). The receptor deactivation upon dissociation of both adenosine and PD 81,723 was compared to the dissociation of adenosine from the Ado-PD-receptor

complex in the continuous presence of PD 81,723. The dissociation of adenosine was not significantly different from simultaneous dissociation of adenosine and PD 81,723. This indicates that direct steric hindrance of PD 81,723 does not slow down the exit of adenosine from human and rat adenosine A1 receptor.

In comparing the results of the three washout experiments (Figure 20) an evident difference could be seen in the dissociation kinetics of PD 81,723 from the active adenosine-receptor complex. The significantly slower dissociation of PD 81,723 might be due to rebinding events of PD 81,723 to the active conformation of the adenosine-bound receptor (OR*). This proves that OR* is a high affinity target for allosteric modulators and might indicate that OAR* is a favourable energetic state for the orthosteric ligand. Energetic stable complexes are less likely to dissociate. Recently published MD simulations of human A1AR predicted that NECA exhibited less movements within the orthosteric binding vestibule in the presence of allosteric modulators (Miao et al. 2018). Hence, it can be hypothesized, that PD 81,723 binds to the active receptor conformation (receptor occupied by A1AR agonists) and stabilizes the orientation of the ECL2 towards the central binding vestibule. Thereby the space for orthosteric ligand dynamics would be reduced, which would result in a favourable energetic state and the complex would require more time to dissociate. The present study is unique in measuring the active conformation of the adenosine-PD 81,723-receptor (OAR*) complex and especially for determining the deactivation kinetics of the adenosine-occupied receptor upon dissociation of PD 81,723. The findings of the three washout experiments demonstrated, that the dissociation of PD 81,723 is the time-limiting step of the dissociation of the Ado-PD-receptor complex and that this behavior is driven by affinity rather than by steric hindrance.

5.2 Investigation of putative allosteric binding site

Quite notable information has emerged on allosteric modulators and lead allosteric compounds in the last three decades (Bruns et al. 1990, Baraldi et al. 2000, Aurelio et al. 2009, Valant et al. 2014). Allosteric binding sites are less conserved across species and receptor subtypes, but to date it is not fully understood which amino acid residues are involved in the binding process of allosteric modulators for A1AR. Further mutagenesis studies coupled with affinity and kinetic investigations will be important to identify the entry and exit trajectories of allosteric modulators to the binding sites.

The putative allosteric binding site in the adenosine A1 receptor is presumably located in the second extracellular loop (Narlawar et al. 2010, Peeters et al. 2012). The second extracellular loop (ECL2) of human A1AR was investigated in detail by Nguyen and co-workers. The authors conducted an alanine scan of all residues in the ECL2 and characterized the mutants for orthosteric binding (Nguyen et al. 2016a) as well as allosteric affinity for the unoccupied receptor, allosteric cooperativity and allosteric efficacy (Nguyen et al. 2016b). Supported by their results, three residues with interesting profiles were selected for investigation of the putative allosteric binding site in this work: The authors identified for S161A an increase in PD 81,723 binding to the unoccupied receptor, a decrease in allosteric binding cooperativity with NECA and a decrease in allosteric ligand efficacy. I175A showed a ten-fold increase in PD 81,723 binding to the unoccupied and therefore inactive receptor but did not affect the other parameters. Of all mutants under investigation E172A showed a decrease in PD 81,723 binding to the inactive receptor and showed an increase in NECA cooperativity on cAMP inhibition assay (Nguyen et al. 2016b).

5.2.1 Orthosteric characterization of mutants in the second extracellular loop

The focus of this work is on the adenosine-occupied and therefore active receptor conformation, which reflects the situation of a stressed or injured tissue *in vivo*. The chosen residues were exchanged in adenosine A1 receptor FRET sensors for alanine to delineate their influence on the behavior of PD 81,723 in terms of affinity and kinetics. Human and rat mutant A1ARs containing single alanine substitutions were expressed in HEK293 cells. The mutant cell lines showed lower membrane expression compared to wt. Incubation for 24 h with 5 mM theophylline resulted in clear membrane localization of the CFP-tagged receptors and the FRET efficiency

was in the same range as wt receptors. The rescue of adenosine A1 receptor mutants with theophylline was shown for the human A1AR by A. Stumpf (Stumpf 2015). The phenomenon of pharmacochaperoning at adenosine receptors was investigated by Malaga and co-workers. They concluded that the occupancy of the binding pocket by a small molecule might correct for improper receptor folding allowing the receptor to migrate from the endoplasmic reticulum to the plasma membrane (Malaga-Diequez et al. 2010).

The orthosteric characterization of the mutants showed that the affinity of adenosine was reduced for E172A and I175A. This finding is in accordance with the localization of both residues in the proximity of the adenosine binding site (Figure 21, Figure 31). Similarly, the kinetic investigation of these mutants showed a faster dissociation of adenosine as well as a faster association compared to wt receptor (Figure 22), indicative of an improved accessibility of the orthosteric binding site by adenosine. Thus, E172 and I175 might function as gate keeper amino acids for the orthosteric binding pocket of human and rat A1AR. Nguyen and co-workers also found a decreased affinity of subtype-unspecific agonist NECA for human E172A and I175A (Nguyen et al. 2016a).

S161A, located distant to the orthosteric binding pocket, displayed no significant difference in on- and off-rate of adenosine in both species, although the affinity of adenosine was increased for human and rat S161A by a factor of two (Table 16). The positive influence of S161A on the affinity of adenosine is interesting since S161 is part of the consensus glycosylation motif NXS and indeed the adjacent amino acid N159 is the predicted N-glycosylation amino acid in the ECL2 (UniProt 2019). Since adenosine A1 receptor has been shown to be a glycoprotein (Klotz and Lohse 1986) the mutation of S161 may influence the glycosylation process of A1AR. The question arises if the presence of glycosyl-modification has an influence on the spatial conformation of the second extracellular loop and therefore on ligand binding. For other GPCRs such as histamine H2 and muscarinic M2 receptor, it has been shown that the presence of N-glycosylation does not alter receptor functionality (Fukushima et al. 1995, van Koppen and Nathanson 1990). S161A adenosine receptor shows clear membrane localization after theophylline incubation with an equal extent as E172A and I175A. This demonstrates that an intact glycosylation motif is not crucial for A1AR folding and maintenance of a functional form in the membrane. The effect of S161A on the affinity of adenosine is solely explainable by the change of the

amino acid sequence and the spatial outcome in the second extracellular loop thereof.

5.2.2 Allosteric characterization of mutants in the second extracellular loop

In order to identify the impact of single amino acids in the second extracellular loop on allosteric behaviour, alanine exchange mutants were investigated for affinity, cooperativity and kinetics of PD 81,723. At high concentrations, PD 81,723 showed the strongest FRET signal enhancement for human E172A: a 150 % enhancement of the adenosine response (Figure 23, chapter 4.2.2.1). The stronger impact of allosteric modulator on the orthosteric ligand in the absence of negatively charged residue E172 is indicative of an attenuating function in the communication of both binding sites in human A1AR. This interpretation is not valid for rat E172A. In contrast the enhancing effect of PD 81,723 for rat E172A is even less than for rat wt, displaying 68 % and 88 % enhancement respectively. The hypothesis, that E172 is important for the transmission of allosteric effect, is supported by the outcome of the cooperativity experiments (4.2.2.2). The extent of the shift of the adenosine concentration-response curve in the presence of PD 81,723 was decreased for human E172 compared to human wt. In contrast, the shift by rat E172 compared to rat wt was increased (Table 18). With regard to affinity (Table 17), the EC_{50} value of PD 81,723 at human E172A receptor was not significantly different to wt, whereas EC_{50} value for rat E172A was two-fold decreased compared to rat wt. This discrepancy might be caused by an altered structural interplay of different extracellular amino acids in rat and human A1AR; five amino acids in the ECL2 as well as two amino acids in the ECL3 (Figure 9). Human E172 is likely to form hydrogen bonds with PD 81,723, as it was predicted by MD simulations for human A1AR (Nguyen et al. 2016b). The formation of hydrogen bonds with PD 81,723 might be different in rat A1AR. However, E172 has the same orientation relative to the orthosteric binding pocket in human and rat since the affinities found for adenosine were comparable in both species. The data represented in this work indicates that the binding pose of PD 81,723 in the extracellular binding vestibule towards E172 might be different for human and rat A1AR.

Another important finding was revealed by the analysis of allosteric affinity for the adenosine-occupied mutant receptors. Human S161A receptor occupied by adenosine was identified as the most affine target for PD 81,723 amongst all investigated adenosine A1 receptors. Interestingly, the EC_{50} of the homolog rat A1AR

mutant was not significantly different from rat wt. For both species the cooperativity of PD 81,723 with adenosine at S161A receptor was slightly reduced compared to wt receptor (Table 18). This indicates that residue S161 is important for the binding process of PD 81,723 to human A1AR but might not directly interfere in the communication of allosteric and orthosteric site. This might indicate that the distant region of the ECL2 is involved in the initial approaching phase of allosteric binding, but PD 81,723 elicits its cooperative effects from a final binding position in the proximity of the orthosteric binding site.

The investigation of allosteric modulator kinetics for the rat mutant receptors revealed no apparent changes (Figure 25). On the contrary, human S161A occupied by adenosine displayed significantly faster association and slightly reduced dissociation kinetics of PD 81,723. In general, increased association and a decreased dissociation might result in a longer residence time of PD 81,723 at the human S161A receptor and therefore display higher affinity. In total, human and rat S161A show clear differences in allosteric affinity and kinetics. In the second extracellular loop, human and rat A1AR differ in five amino acids (Figure 9). The recently published human A1AR crystal structure (Draper-Joyce et al. 2018) was able to resolve the second extracellular loop which then revealed a short helix structure. Four of the five differing residues are located within this helix but the fifth one, methionine 162, is located outside. In rat adenosine A1 receptor a valine is expressed at position 162. To address the question whether the species discrepancy can be explained by the adjacent residue at site 162, two double mutants were generated. The human double mutant, consisting of A161 and V162, showed a significant faster dissociation compared to human S161A and human wt (Table 19). Complementary, dissociation of rat S161A V162M was significantly slower than rat S161A and rat wt. The human S161A mutant was converted to a 'rat like' version by exchanging M162 for the rat valine in this region of the loop and the dissociation kinetics were then compared to rat S161A (Figure 27). Indeed no apparent difference was found in the dissociation constants and the same holds true for the rat double mutant compared to human S161A.

The influence of methionine on the phenotype of human S161A is further supported by the decrease in PD 81,723 affinity for the human double mutant to the affinity level of rat S161A (human S161A M162V 2.57 μ M, rat S161A 2.61 μ M). This proves the significance of residue 162 on the identified species discrepancy and demonstrates

an impact on allosteric kinetics. Data from Kennedy and colleagues indicated an important role of S161 and M162 in the allosteric binding process to human A1AR (Kennedy et al. 2014). They exchanged residues N159, G160, S161, and M162 for alanine in one construct and determined a decreased allosteric activity of their positive allosteric ligand ATL525. A single mutation construct containing M162 exchanged for canine G162 showed a reduction of ATL525 activity (canine A1AR wt exhibits minor allosteric modulator activity than human A1AR). This might indicate that the identified effect of residue 162 on PD 81,723 kinetics is independent of the presence of serine or alanine at position 161.

The difference in dissociation of PD 81,723 from the double mutants compared to the respective wt (Figure 27 A, B and Table 19) indicates an important role of residue 162 to regulate the kinetic behavior of allosteric modulators. However, it is important to investigate the role of single mutation, human M162A and rat V162A, on the allosteric behavior of PD 81,723, particularly in regard to dissociation kinetics of the allosteric modulator. The outcome of these experiments would be helpful to explore the role of the second extracellular loop in allosteric ligand binding processes.

6 Conclusions and outlook

Adenosine receptors (A1, A2A, A2b and A3) are highly distributed throughout the human body. The positive allosteric modulator PD 81,723 exerts its regulatory effect exclusively on the adenosine A1 receptor and is therefore strictly subtype-specific. Despite several years of research on allosteric modulation of A1AR, little information exists on the interactions of PD 81,723 with the endogenous ligand adenosine. Therefore detailed investigations, in terms of affinity and kinetics, are important to understand the interaction of positive allosteric modulators with physiological or pathophysiological levels of adenosine *in vivo*.

Microscopy of living cells expressing human or rat adenosine receptor FRET sensors allowed real-time monitoring of ligand-induced conformational receptor dynamics under physiological conditions. This approach enabled the investigation of allosteric modulation in combination with adenosine, in contrast to radioligand assays.

In this work, an experimental procedure was developed and the affinity of PD 81,723 as well as the cooperativity with adenosine was successfully determined for human and rat adenosine A1 receptor. The dependence of the allosteric effect on the probe (bound agonist) was found to differ by a five-fold decrease in PD 81,723 affinity for NECA compared to adenosine. This finding indicates a broader therapeutic window of allosteric modulators for adenosine-occupied receptors. Endogenous adenosine levels in the tissue should be considered by pharmacologists in predicting *in vivo* affinities and efficacy in a combined administration of allosteric modulator and synthetic adenosine agonists.

Positive allosteric regulation on A1AR is most often characterized by the prolongation of agonist dissociation from the receptor. Kinetic data, as presented in this work, suggests that another mechanism than steric hindrance of adenosine by PD 81,723 induces the phenomenon of prolonged dissociation. For the first time the “pure” unbinding kinetics of PD 81,723 from the adenosine-occupied-receptor complex were observed. The change in active receptor conformation upon dissociation of PD 81,723 was 8-fold slower compared to simultaneous dissociation of adenosine and PD 81,723. This is indicative of a rebinding process of PD 81,723 to the active conformation and therefore demonstrates that the receptor occupied by adenosine is a high affinity target for allosteric modulators. Investigation of additional A1AR

allosteric enhancers for their dissociation kinetics using such a FRET-based approach can provide valuable and more physiological structure-kinetic relationships for medicinal chemists. In addition it would be interesting to elucidate the influence of A1AR pre-stimulation with PD 81,723 on the association kinetics of adenosine. This would provide further insight on orthosteric affinity enhancement in the presence of allosteric modulator *in vivo*.

The alanine substitution of S161 in the second extracellular loop, putative allosteric binding site, showed an increased PD 81,723 affinity compared to wild-type for the human A1AR. On the contrary, rat S161A displayed no significant difference in PD 81,723 affinity compared to rat wt. The mutation of S161 in human A1AR resulted in a faster association and a slower dissociation of PD 81,723, which indicates a prolonged residence time. This discrepancy in species-dependent behavior was a result of the adjacent residue M162 (rat V162). The generated double mutants, consisting of human S161A V162M and rat S161A M162V, revealed that the dissociation of PD 81,723 is highly dependent on the interaction with residue at site 162. To further elucidate the role of residue 162 for PD 81,723 binding, single mutants (alanine as well as bulkier and charged residue substitutions) can be investigated in terms of affinity and dissociation kinetics. Together with MD simulations, data provided by these suggested experiments will help to understand the binding process of allosteric modulators via the second extracellular loop of A1AR.

Taken together, human and rat A1AR FRET-sensors allowed real-time recording of allosteric enhancement of the endogenous ligand adenosine under physiological conditions. This work provides affinity (EC_{50}) of PD 81,723 for human and rat A1AR, provides evidence for probe dependency of PD 81,723 with NECA, reveals the mechanism of prolonged dissociation of adenosine in the presence of PD 81,723 and indicates the importance of residue at site 162 located in the second extracellular loop for the kinetic behavior of PD 81,723.

7 Appendix

AA1R_HUMAN	1	MPPSISAFQAAAYIGIEVLI	60
AA1R_RAT	1	MPPYISAFQAAAYIGIEVLI	60
AA1R_HUMAN	61	LVIPLAILINIGPQTYFHTCLMVACPVLI	120
AA1R_RAT	61	LVIPLAILINIGPQTYFHTCLMVACPVLI	120
AA1R_HUMAN	121	PRRAAVAIAGCWILSFVVGLTPMFGWNNLSAVERAWA	180
AA1R_RAT	121	QRRRAVAIAGCWILSLVVGLTPMFGWNNLSVVEQDWR	180
AA1R_HUMAN	181	VYFNFFVWVLPPLLMLVIYLEVFYLIRKQLNKKVSASSGDPQKYYGKELKIAKSLALIL	240
AA1R_RAT	181	VYFNFFVWVLPPLLMLVIYLEVFYLIRKQLNKKVSASSGDPQKYYGKELKIAKSLALIL	240
AA1R_HUMAN	241	FLFALSWLPLHILNCITLFCPSCHKPSILTYIAIFLTHGNSAMNPIVYAFRIQKFRVTFI	300
AA1R_RAT	241	FLFALSWLPLHILNCITLFCPTCQKPSILTYIAIFLTHGNSAMNPIVYAFRIHKFRVTFI	300
AA1R_HUMAN	301	KIWNDFRCQPA	326
AA1R_RAT	301	KIWNDFRCQPK	326

Figure 28: Protein sequence alignment of hA1AR and ratA1AR. High similarity of amino acids is highlighted in dark grey and no similarity in white. Alignment was conducted with UniProt: a worldwide hub of protein knowledge Nucleic Acids Res. 47: D506-515 (2019).

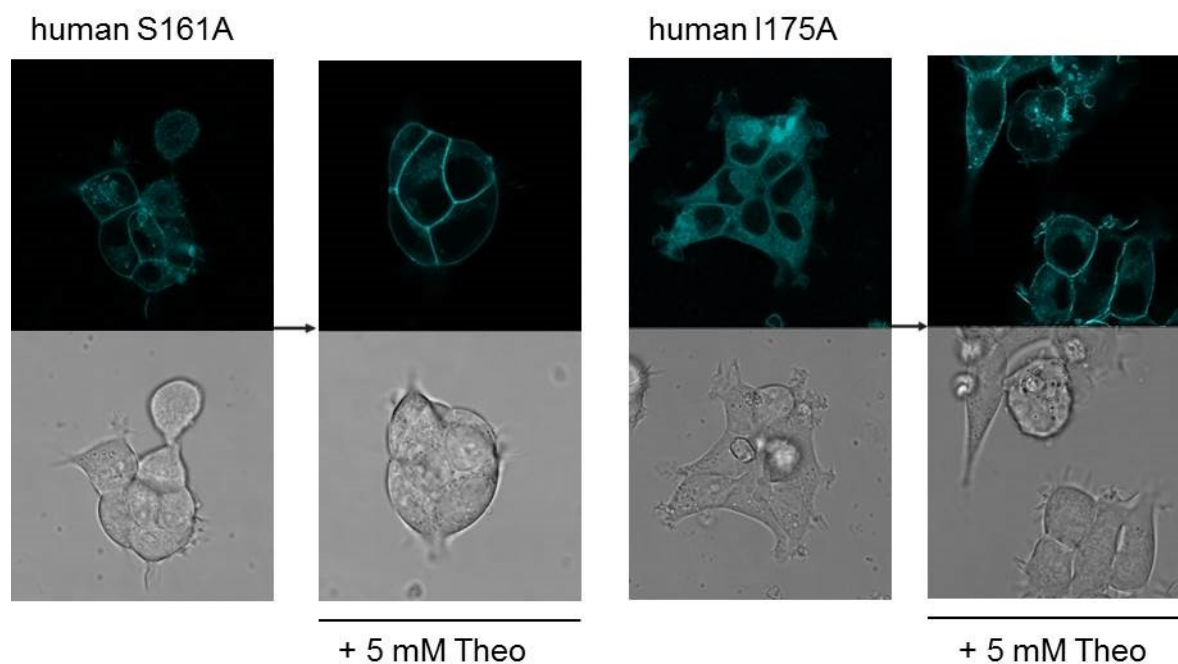


Figure 29: Human mutant A1AR FRET sensor membrane localization before and after 24 h of 5 mM theophylline incubation. Membrane localization of human A1 E172A FRET sensor was similar to human A1 wt FRET sensor. Incubation with theophylline was not necessary to detect proper FRET signals, but for comparability all mutant and wt cell lines were treated with theophylline.

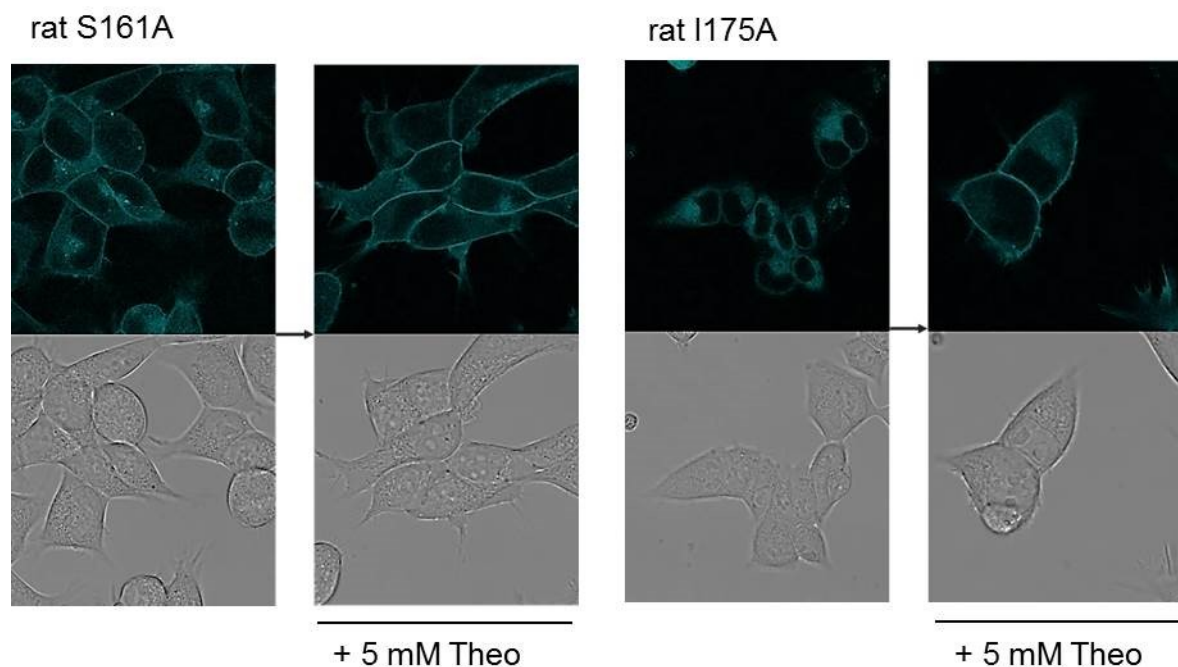


Figure 30: Rat mutant A1AR FRET sensor membrane localization before and after 24 h of 5 mM theophylline incubation. Rat A1 E172A expression is represented at Figure 21, B.

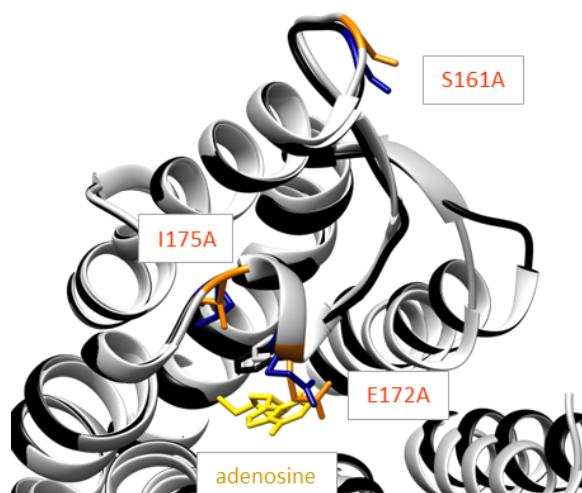


Figure 31: Superimposed active (grey) and inactive (black) backbones of human A1AR (PDB code: 6D9H, 5UEN). Adenosine is represented in yellow, mutant residues of the active structure in orange and mutant residues of the inactive structure in blue.

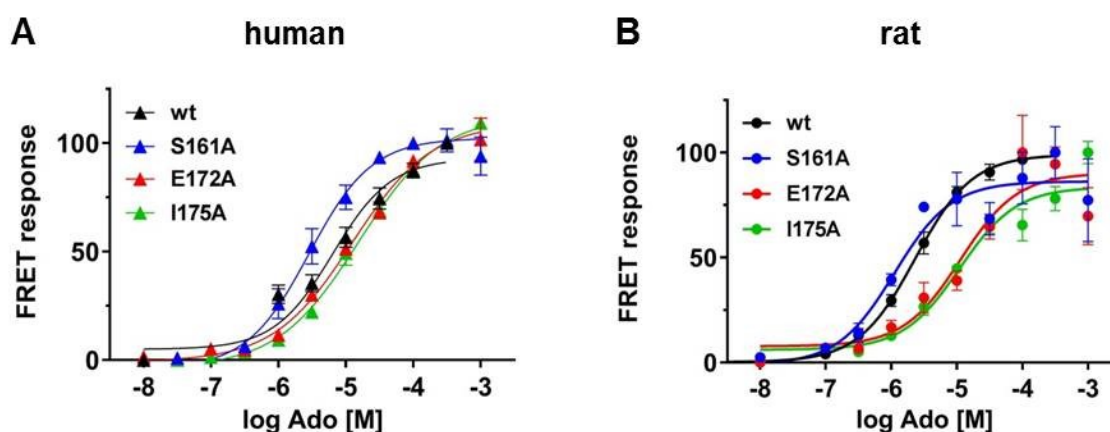


Figure 32: Influence of mutants in the second extracellular loop on concentration-response curves of adenosine. Cell lines were investigated for adenosine response as described in 4.1.1. The concentration response curve of adenosine for human A1AR was determined in a previous doctoral study in the working group of Professor Hoffmann (Stumpf 2015). Data represent the mean of $n \geq 18$ individual cells for human, $n \geq 14$ individual cells for rat from at least four independent experiments. SEM is indicated by error bars.

Table 20: EC₅₀ values of adenosine for human and rat A1AR wt and mutants.

Cell lines were investigated for adenosine response as described in 4.1.1. The EC₅₀ value of adenosine for human A1AR was determined in a previous doctoral study in the working group of Professor Hoffmann (Stumpf 2015). Data represent the mean in μM of $n \geq 18$ individual cells for human and $n \geq 14$ individual cells for rat from at least four independent experiments. Confidence intervals 95 % are indicated. (# $P < 0.05$ one-way ANOVA and Dunnett's multiple comparisons test, compared to wt)

human	EC ₅₀ [μM]	95 %CI	
wt	6.4	3.8 - 10.3	
S161A	2.9	1.5 - 5.4	#
E172A	12.5	10.0 -15.6	#
I175A	15.6	12.6 -19.3	#
S161A M162V	3.21	2.4 - 4.4	#
rat	EC ₅₀ [μM]	95 %CI	
wt	2.6	2.2 -3.1	
S161A	1.1	0.5 - 2.6	#
E172A	14.8	3.6 - 30.2	#
I175A	11.1	5.1 - 25.9	#
S161A V162M	4.22	2.9 - 6.1	#

Table 21: EC₅₀ values of PD 81,723 for human and rat A1AR wt and mutants.

Cell lines were investigated for PD 81,723 affinity as described in 4.1.4 and 4.2.2.1. Data represent the mean \pm SEM of $n \geq 24$ individual cells for human and $n \geq 16$ individual cells for rat measured on at least four independent experimental days. Confidence intervals 95 % are indicated. (# $P < 0.05$ one-way ANOVA and Dunnett's multiple comparisons test, compared to wt)

human	EC ₅₀ [μM]	95 %CI	
wt	2.08	0.25 - 17.1	
S161A	0.64	0.21 - 2.5	#
E172A	1.96	1.1 - 3.6	
I175A	1.65	0.22 - 12.2	
S161A M162V	2.57	0.74 - 7.5	
rat	EC ₅₀ [μM]	95 %CI	
wt	2.96	0.5 - 17.6	
S161A	2.61	0.89 - 7.57	
E172A	1.43	0.58 - 3.46	#
I175A	1.50	0.51 - 4.44	#
S161A V162M	2.11	0.46 - 7.28	

Table 22: Influence of mutants on the ability of PD 81,723 to shift the concentration-response curve of adenosine. A concentration of 10 μM PD 81,723 was used with increasing concentrations of adenosine. Absolute FRET values were plotted and fitted to calculate EC_{50} values. EC_{50} values were used for calculating the fold change of EC_{50} in the presence of the allosteric modulator PD 81,723. For statistical analysis an unpaired two-tailed t-test was performed using $\log \text{EC}_{50} \pm \text{SD}$ (## $P < 0.01$, #### $P < 0.0001$). Data represent the mean \pm SEM of $n \geq 30$ individual cells for human and $n \geq 25$ individual cells for rat measured on at least five independent experimental days.

mutation	human EC_{50} [μM]		fold shift	rat EC_{50} [μM]		fold shift
	Ado	+ PD81,723		Ado	+ PD81,723	
wt	1.45	0.60	2.40 ####	2.22	1.34	1.65 ####
S161A	5.21	3.15	1.65 ####	1.00	0.76	1.32 ##
E172A	11.58	5.86	1.97 ####	14.23	6.67	2.13 ####
I175A	13.52	8.94	1.51 ####	10.50	4.88	2.15 ####

Table 23: Association and dissociation kinetics of 100 μM adenosine to and from human A1AR. Mean and SEM of tau values are represented in milliseconds. Numbers of successful fit curves are indicated, representing individual cells.

Association of 100 μM Ado to human A1, tau [ms]	wt	S161A	E172A	I175A
Mean	396.9	486.1	272.7	346.8
SEM	15.0	53.1	28.8	22.3
Number of values	11	12	7	9
Dissociation of 100 μM Ado from human A1, tau [ms]	wt	S161A	E172A	I175A
Mean	5433.0	5635.1	2942.0	2202.9
SEM	551.7	627.9	276.8	197.9
Number of values	11	10	7	10

Table 24: Association and dissociation kinetics of 100 μM adenosine to and from rat A1AR. Mean and SEM of tau values are represented in milliseconds. Numbers of successful fit curves are indicated, representing individual cells.

Association of 100 μM Ado to rat A1, tau [ms]	wt	S161A	E172A	I175A
Mean	442.4	431.5	289.4	245.7
SEM	45.5	57.6	30.0	23.3
Number of values	14	8	7	7
Dissociation of 100 μM Ado from rat A1, tau [ms]	wt	S161A	E172A	I175A
Mean	8260.4	6847.7	2120.3	1723.5
SEM	939.5	890.3	301.8	327.0
Number of values	13	12	8	7

Table 25: Calculation of kinetic K_D FRET of 100 μ M adenosine. Mean tau values in seconds were used from Table 23 and Table 24. Equations are explained in chapter 1.1.3. k_{on} is dependent on the used ligand concentration (here: 0.0001 M).

100 μ M Ado		human A1AR	rat A1AR
tau association	[s]	0.40	0.44
k_{obs} (= 1/tau)	[s ⁻¹]	2.52	2.26
tau dissociation	[s]	5.43	8.26
k_{off} (= 1/tau)	[s ⁻¹]	0.18	0.12
k_{on} (= $k_{obs} - k_{off} / 0.0001$)	[s ⁻¹ /M]	23348.31	21413.78
K_D (= k_{off} / k_{on})	[M]	7.88E-06	5.65E-06

Table 26: Association of EC_{30} of Ado to OR*. Data in milliseconds were obtained from kinetic experiments as described in 4.1.8 and in 4.2.2.3. Numbers of successful fit curves are indicated, representing individual cells.

Association of EC_{30} of Ado to human A1, tau [ms]	wt	S161A	E172A	I175A	S161A M162V
Mean	2345	3012	1501	1503	3307
SEM	166.1	294.4	260.2	138.1	534.6
Number of values	16	19	14	15	14
Association of EC_{30} of Ado to rat A1, tau [ms]	wt	S161A	E172A	I175A	S161A V162M
Mean	2641	3146	1341	1539	2282
SEM	262.6	286.8	154.8	317.7	346.9
Number of values	23	13	9	10	10

Table 27: Association of 10 μ M PD 81,723 to the human receptor occupied by adenosine (EC_{30}). Mean and SEM of tau values are represented in seconds. Data represent the mean \pm SEM of $n \geq 11$ individual cells for human and $n \geq 10$ individual cells for rat measured on at least three independent experimental days. For curve fitting the mono-exponential equation ($f(x) = A * e^{(-t/\tau)}$) was used.

Association of 10 μ M PD 81,723 to OR*	wt	S161A	E172A	I175A	S161A M162V
human tau [s]	21.89 \pm 1.4	14.63 \pm 1.9	14.88 \pm 1.9	17.13 \pm 2.2	36.07 \pm 4.3
Association of 10 μ M PD 81,723 to OR*	wt	S161A	E172A	I175A	S161A V162M
rat tau [s]	13.34 \pm 1.3	17.31 \pm 2.4	12.78 \pm 2.1	8.74 \pm 1.25	28.45 \pm 2.3

Table 28: Dissociation kinetics from OAR* of human A1AR. Dissociation of 10 μM PD 81,723 from OAR* is significantly different from simultaneous dissociation from OAR*. Dissociation of 3 μM adenosine from OAR* was not significantly different from simultaneous dissociation from OAR* (# $P < 0.05$ Kruskal-Wallis test). Tau values are presented in seconds. Data represent the mean \pm SEM of $n \geq 5$ individual cells measured on at least three independent experimental days. For curve fitting the mono-exponential equation ($f(x) = A * e^{(-t/\tau)}$) was used.

Dissociation from OAR* tau [s]	human wt	S161A	E172A	I175A	S161A M162V
10 μM PD	139.0 \pm 18.8 [#]	183.7 \pm 21.8 [#]	55.2 \pm 6.9 [#]	76.9 \pm 12.0 [#]	77.6 \pm 15.0 [#]
3 μM Ado	21.24 \pm 3.9	36.19 \pm 2.7	7.4 \pm 1.3	7.6 \pm 1.1	8.9 \pm 0.6
3 μM Ado + 10 μM PD	15.65 \pm 3.3	26.48 \pm 3.7	5.6 \pm 0.6	6.6 \pm 1.1	11.2 \pm 2.6

Table 29: Dissociation kinetics from OAR* of rat A1AR. Dissociation of 10 μM PD 81,723 from OAR* is significantly different from simultaneous dissociation from OAR*. Dissociation of 3 μM adenosine from OAR* was not significantly different from simultaneous dissociation from OAR* (# $P < 0.05$ Kruskal-Wallis test). Tau values are presented as Mean \pm SEM in seconds. Data represent the mean \pm SEM of $n \geq 5$ individual cells measured on at least three independent experimental days. For curve fitting the mono-exponential equation ($f(x) = A * e^{(-t/\tau)}$) was used.

Dissociation from OAR* tau [s]	rat wt	S161A	E172A	I175A	S161A V162M
10 μM PD	85.8 \pm 11.1 [#]	80.9 \pm 8.9 [#]	90.6 \pm 8.4 [#]	118.8 \pm 13.8 [#]	168.8 \pm 37.9 [#]
3 μM Ado	29.4 \pm 3.1	37.3 \pm 5.1	7.6 \pm 0.7	6.8 \pm 1.5	9.98 \pm 0.9
3 μM Ado + 10 μM PD	14.1 \pm 2.6	16.8 \pm 2.2	4.6 \pm 0.5	5.2 \pm 0.5	5.4 \pm 1.0

Table 30: Calculation of kinetic K_D FRET of 10 μM PD 81,723. Mean tau values in seconds were used from Table 27, Table 28, Table 29. Equations are explained in chapter 1.1.3. k_{on} is dependent on the used concentration of ligand (here: 0.00001 M).

10 μM PD 81,723		human A1AR	rat A1AR
tau association	[s]	21.89	13.34
k_{obs} (= 1/tau)	[s ⁻¹]	0.05	0.07
tau dissociation	[s]	139	85.8
k_{off} (= 1/tau)	[s ⁻¹]	0.01	0.01
k_{on} (= $k_{obs} - k_{off} / 0.00001$)	[s ⁻¹ /M]	3848.87	6330.75
K_D (= k_{off} / k_{on})	[M]	1.87E-06	1.84E-06

8 References

- Abbracchio MP, Burnstock G. 1994. Purinoceptors: are there families of P2X and P2Y purinoceptors? *Pharmacol Ther*, 64 (3):445-475.
- Anderson CM, Xiong W, Geiger JD, Young JD, Cass CE, Baldwin SA, Parkinson FE. 1999. Distribution of equilibrative, nitrobenzylthioinosine-sensitive nucleoside transporters (ENT1) in brain. *J Neurochem*, 73 (2):867-873.
- Aurelio L, Valant C, Flynn BL, Sexton PM, Christopoulos A, Scammells PJ. 2009. Allosteric modulators of the adenosine A1 receptor: synthesis and pharmacological evaluation of 4-substituted 2-amino-3-benzoylthiophenes. *J Med Chem*, 52 (14):4543-4547.
- Baraldi PG, Zaid AN, Lampronti I, Fruttarolo F, Pavani MG, Tabrizi MA, Shryock JC, Leung E, Romagnoli R. 2000. Synthesis and biological effects of a new series of 2-amino-3-benzoylthiophenes as allosteric enhancers of A1-adenosine receptor. *Bioorg Med Chem Lett*, 10 (17):1953-1957.
- Baraldi PG, Romagnoli R, Pavani MG, Nunez Mdel C, Tabrizi MA, Shryock JC, Leung E, Moorman AR, Uluoglu C, Iannotta V, Merighi S, Borea PA. 2003. Synthesis and biological effects of novel 2-amino-3-naphthoylthiophenes as allosteric enhancers of the A1 adenosine receptor. *J Med Chem*, 46 (5):794-809.
- Barker JL, Harrison NL, Mariani AP. 1986. Benzodiazepine pharmacology of cultured mammalian CNS neurons. *Life Sci*, 39 (21):1959-1968.
- Bhattacharya S, Linden J. 1996. Effects of long-term treatment with the allosteric enhancer, PD81,723, on Chinese hamster ovary cells expressing recombinant human A1 adenosine receptors. *Mol Pharmacol*, 50 (1):104-111.
- Bjorness TE, Kelly CL, Gao T, Poffenberger V, Greene RW. 2009. Control and function of the homeostatic sleep response by adenosine A1 receptors. *J Neurosci*, 29 (5):1267-1276.
- Borea PA, Gessi S, Merighi S, Vincenzi F, Varani K. 2018. Pharmacology of Adenosine Receptors: The State of the Art. *Physiol Rev*, 98 (3):1591-1625.
- Bridson SJ, Gandia J, Amaral OB, Ferre S, Lluís C, Franco R, Hill SJ, Ciruela F. 2008. Plasma membrane diffusion of G protein-coupled receptor oligomers. *Biochim Biophys Acta*, 1783 (12):2262-2268.
- Brown R, Ollerstam A, Johansson B, Skott O, Gebre-Medhin S, Fredholm B, Persson AE. 2001. Abolished tubuloglomerular feedback and increased plasma renin in adenosine A1 receptor-deficient mice. *Am J Physiol Regul Integr Comp Physiol*, 281 (5):R1362-1367.
- Brown RA, Clarke GW, Ledbetter CL, Hurle MJ, Denyer JC, Simcock DE, Cote JE, Savage TJ, Murdoch RD, Page CP, Spina D, O'Connor BJ. 2008. Elevated

- expression of adenosine A1 receptor in bronchial biopsy specimens from asthmatic subjects. *Eur Respir J*, 31 (2):311-319.
- Bruns RF, Fergus JH. 1990. Allosteric enhancement of adenosine A1 receptor binding and function by 2-amino-3-benzoylthiophenes. *Mol Pharmacol*, 38 (6):939-949.
- Bruns RF, Fergus JH, Coughenour LL, Courtland GG, Pugsley TA, Dodd JH, Tinney FJ. 1990. Structure-activity relationships for enhancement of adenosine A1 receptor binding by 2-amino-3-benzoylthiophenes. *Mol Pharmacol*, 38 (6):950-958.
- Burger WAC, Sexton PM, Christopoulos A, Thal DM. 2018. Toward an understanding of the structural basis of allosterism in muscarinic acetylcholine receptors. *J Gen Physiol*, 150 (10):1360-1372.
- Cheng RKY, Segala E, Robertson N, Deflorian F, Dore AS, Errey JC, Fiez-Vandal C, Marshall FH, Cooke RM. 2017. Structures of Human A1 and A2A Adenosine Receptors with Xanthines Reveal Determinants of Selectivity. *Structure*, 25 (8):1275-1285 e1274.
- Christopoulos A. 2002. Allosteric binding sites on cell-surface receptors: novel targets for drug discovery. *Nat Rev Drug Discov*, 1 (3):198-210.
- Christopoulos A, Kenakin T. 2002. G protein-coupled receptor allosterism and complexing. *Pharmacol Rev*, 54 (2):323-374.
- Ciruela F, Casado V, Mallol J, Canela EI, Lluís C, Franco R. 1995. Immunological identification of A1 adenosine receptors in brain cortex. *J Neurosci Res*, 42 (6):818-828.
- Ciruela F, Casado V, Rodrigues RJ, Lujan R, Burgueno J, Canals M, Borycz J, Rebola N, Goldberg SR, Mallol J, Cortes A, Canela EI, Lopez-Gimenez JF, Milligan G, Lluís C, Cunha RA, Ferre S, Franco R. 2006. Presynaptic control of striatal glutamatergic neurotransmission by adenosine A1-A2A receptor heteromers. *J Neurosci*, 26 (7):2080-2087.
- Cohen FR, Lazareno S, Birdsall NJ. 1996. The affinity of adenosine for the high- and low-affinity states of the human adenosine A1 receptor. *Eur J Pharmacol*, 309 (1):111-114.
- Cooper SL, Soave M, Jorg M, Scammells PJ, Woolard J, Hill SJ. 2019. Probe dependence of allosteric enhancers on the binding affinity of adenosine A1 -receptor agonists at rat and human A1 -receptors measured using NanoBRET. *Br J Pharmacol*, 176 (7):864-878.
- Copeland RA. 2011. Conformational adaptation in drug-target interactions and residence time. *Future Med Chem*, 3 (12):1491-1501.
- Copeland RA. 2016. The drug-target residence time model: a 10-year retrospective. *Nat Rev Drug Discov*, 15 (2):87-95.

- Copeland RA, Pompliano DL, Meek TD. 2006. Drug-target residence time and its implications for lead optimization. *Nat Rev Drug Discov*, 5 (9):730-739.
- Cordeaux Y, Ijzerman AP, Hill SJ. 2004. Coupling of the human A1 adenosine receptor to different heterotrimeric G proteins: evidence for agonist-specific G protein activation. *Br J Pharmacol*, 143 (6):705-714.
- Dana A, Baxter GF, Walker JM, Yellon DM. 1998. Prolonging the delayed phase of myocardial protection: repetitive adenosine A1 receptor activation maintains rabbit myocardium in a preconditioned state. *J Am Coll Cardiol*, 31 (5):1142-1149.
- de Witte WEA, Danhof M, van der Graaf PH, de Lange ECM. 2016. In vivo Target Residence Time and Kinetic Selectivity: The Association Rate Constant as Determinant. *Trends Pharmacol Sci*, 37 (10):831-842.
- Dhalla AK, Shryock JC, Shreeniwas R, Belardinelli L. 2003. Pharmacology and therapeutic applications of A1 adenosine receptor ligands. *Curr Top Med Chem*, 3 (4):369-385.
- Disse B, Speck GA, Rominger KL, Witek TJ, Jr., Hammer R. 1999. Tiotropium (Spiriva): mechanistical considerations and clinical profile in obstructive lung disease. *Life Sci*, 64 (6-7):457-464.
- Disse B, Reichl R, Speck G, Traunecker W, Ludwig Rominger KL, Hammer R. 1993. Ba 679 BR, a novel long-acting anticholinergic bronchodilator. *Life Sci*, 52 (5-6):537-544.
- Dowling MR, Charlton SJ. 2006. Quantifying the association and dissociation rates of unlabelled antagonists at the muscarinic M3 receptor. *Br J Pharmacol*, 148 (7):927-937.
- Draper-Joyce CJ, Khoshouei M, Thal DM, Liang YL, Nguyen ATN, Furness SGB, Venugopal H, Baltos JA, Plitzko JM, Danev R, Baumeister W, May LT, Wootten D, Sexton PM, Glukhova A, Christopoulos A. 2018. Structure of the adenosine-bound human adenosine A1 receptor-Gi complex. *Nature*, 558 (7711):559-563.
- Ehlert FJ. 1988. Estimation of the affinities of allosteric ligands using radioligand binding and pharmacological null methods. *Mol Pharmacol*, 33 (2):187-194.
- Fagerberg L, Hallstrom BM, Oksvold P, Kampf C, Djureinovic D, Odeberg J, Habuka M, Tahmasebpoor S, Danielsson A, Edlund K, Asplund A, Sjostedt E, Lundberg E, Szigyarto CA, Skogs M, Takanen JO, Berling H, Tegel H, Mulder J, Nilsson P, Schwenk JM, Lindskog C, Danielsson F, Mardinoglu A, Sivertsson A, von Feilitzen K, Forsberg M, Zwahlen M, Olsson I, Navani S, Huss M, Nielsen J, Ponten F, Uhlen M. 2014. Analysis of the human tissue-specific expression by genome-wide integration of transcriptomics and antibody-based proteomics. *Mol Cell Proteomics*, 13 (2):397-406.

- Ferguson DR, Kennedy I, Burton TJ. 1997. ATP is released from rabbit urinary bladder epithelial cells by hydrostatic pressure changes--a possible sensory mechanism? *J Physiol*, 505 (Pt 2):503-511.
- Fierens FL, Vanderheyden PM, Roggeman C, Vande Gucht P, De Backer JP, Vauquelin G. 2002. Distinct binding properties of the AT(1) receptor antagonist [(3)H]candesartan to intact cells and membrane preparations. *Biochem Pharmacol*, 63 (7):1273-1279.
- Förster T. 1948. Zwischenmolekulare Energiewanderung und Fluoreszenz. *Annalen der Physik*, 437 (1-2): 0055 - 0075.
- Fredholm BB, AP IJ, Jacobson KA, Klotz KN, Linden J. 2001. International Union of Pharmacology. XXV. Nomenclature and classification of adenosine receptors. *Pharmacol Rev*, 53 (4):527-552.
- Fredholm BB, Arslan G, Halldner L, Kull B, Schulte G, Wasserman W. 2000. Structure and function of adenosine receptors and their genes. *Naunyn Schmiedebergs Arch Pharmacol*, 362 (4-5):364-374.
- Fukushima Y, Oka Y, Saitoh T, Katagiri H, Asano T, Matsushashi N, Takata K, van Breda E, Yazaki Y, Sugano K. 1995. Structural and functional analysis of the canine histamine H2 receptor by site-directed mutagenesis: N-glycosylation is not vital for its action. *Biochem J*, 310 (Pt 2):553-558.
- Fung BK, Hurley JB, Stryer L. 1981. Flow of information in the light-triggered cyclic nucleotide cascade of vision. *Proc Natl Acad Sci U S A*, 78 (1):152-156.
- Gimenez-Llort L, Masino SA, Diao L, Fernandez-Teruel A, Tobena A, Halldner L, Fredholm BB. 2005. Mice lacking the adenosine A1 receptor have normal spatial learning and plasticity in the CA1 region of the hippocampus, but they habituate more slowly. *Synapse*, 57 (1):8-16.
- Gines S, Hillion J, Torvinen M, Le Crom S, Casado V, Canela EI, Rondin S, Lew JY, Watson S, Zoli M, Agnati LF, Verniera P, Lluís C, Ferré S, Fuxe K, Franco R. 2000. Dopamine D1 and adenosine A1 receptors form functionally interacting heteromeric complexes. *Proc Natl Acad Sci U S A*, 97 (15):8606-8611.
- Glukhova A, Thal DM, Nguyen AT, Vecchio EA, Jörg M, Scammells PJ, May LT, Sexton PM, Christopoulos A. 2017. Structure of the Adenosine A1 Receptor Reveals the Basis for Subtype Selectivity. *Cell*, 168 (5):867-877 e813.
- Grierson JP, Meldolesi J. 1995. Shear stress-induced [Ca²⁺]_i transients and oscillations in mouse fibroblasts are mediated by endogenously released ATP. *J Biol Chem*, 270 (9):4451-4456.
- Griffin BA, Adams SR, Tsien RY. 1998. Specific covalent labeling of recombinant protein molecules inside live cells. *Science*, 281 (5374):269-272.
- Guo D, Heitman LH, AP IJ. 2017. Kinetic Aspects of the Interaction between Ligand and G Protein-Coupled Receptor: The Case of the Adenosine Receptors. *Chem Rev*, 117 (1):38-66.

- Guo D, Venhorst SN, Massink A, van Veldhoven JP, Vauquelin G, AP IJ, Heitman LH. 2014. Molecular mechanism of allosteric modulation at GPCRs: insight from a binding kinetics study at the human A1 adenosine receptor. *Br J Pharmacol*, 171 (23):5295-5312.
- Hall DA. 2000. Modeling the functional effects of allosteric modulators at pharmacological receptors: an extension of the two-state model of receptor activation. *Mol Pharmacol*, 58 (6):1412-1423.
- Hanlon CD, Andrew DJ. 2015. Outside-in signaling--a brief review of GPCR signaling with a focus on the Drosophila GPCR family. *J Cell Sci*, 128 (19):3533-3542.
- Hara M, Tozawa F, Itazaki K, Mihara S, Fujimoto M. 1998. Endothelin ET(B) receptors show different binding profiles in intact cells and cell membrane preparations. *Eur J Pharmacol*, 345 (3):339-342.
- Hauser RA, Hubble JP, Truong DD, Istradefylline USSG. 2003. Randomized trial of the adenosine A(2A) receptor antagonist istradefylline in advanced PD. *Neurology*, 61 (3):297-303.
- Hoffmann C, Gaietta G, Bünemann M, Adams SR, Oberdorff-Maass S, Behr B, Vilardaga JP, Tsien RY, Ellisman MH, Lohse MJ. 2005. A FIAsh-based FRET approach to determine G protein-coupled receptor activation in living cells. *Nat Methods*, 2 (3):171-176.
- Jaakola VP, Griffith MT, Hanson MA, Cherezov V, Chien EY, Lane JR, Ijzerman AP, Stevens RC. 2008. The 2.6 angstrom crystal structure of a human A2A adenosine receptor bound to an antagonist. *Science*, 322 (5905):1211-1217.
- Jensen JB, Lyssand JS, Hague C, Hille B. 2009. Fluorescence changes reveal kinetic steps of muscarinic receptor-mediated modulation of phosphoinositides and Kv7.2/7.3 K⁺ channels. *J Gen Physiol*, 133 (4):347-359.
- Johansson B, Halldner L, Dunwiddie TV, Masino SA, Poelchen W, Gimenez-Llort L, Escorihuela RM, Fernandez-Teruel A, Wiesenfeld-Hallin Z, Xu XJ, Hardemark A, Betsholtz C, Herlenius E, Fredholm BB. 2001. Hyperalgesia, anxiety, and decreased hypoxic neuroprotection in mice lacking the adenosine A1 receptor. *Proc Natl Acad Sci U S A*, 98 (16):9407-9412.
- Joshi E, Chordia MD, Macdonald TL, Linden J, Olsson R. 2004. Regioselective oxidation of 2-amino-3-aryl-4,5-dialkylthiophenes by DMSO. *Bioorg Med Chem Lett*, 14 (4):929-933.
- Kazemi MH, Raoofi Mohseni S, Hojjat-Farsangi M, Anvari E, Ghalamfarsa G, Mohammadi H, Jadidi-Niaragh F. 2018. Adenosine and adenosine receptors in the immunopathogenesis and treatment of cancer. *J Cell Physiol*, 233 (3):2032-2057.
- Kenakin T. 2005. New concepts in drug discovery: collateral efficacy and permissive antagonism. *Nat Rev Drug Discov*, 4 (11):919-927.

- Kennedy DP, McRobb FM, Leonhardt SA, Purdy M, Figler H, Marshall MA, Chordia M, Figler R, Linden J, Abagyan R, Yeager M. 2014. The second extracellular loop of the adenosine A1 receptor mediates activity of allosteric enhancers. *Mol Pharmacol*, 85 (2):301-309.
- Kirsch GE, Codina J, Birnbaumer L, Brown AM. 1990. Coupling of ATP-sensitive K⁺ channels to A1 receptors by G proteins in rat ventricular myocytes. *Am J Physiol*, 259 (3 Pt 2):H820-826.
- Klotz KN. 2000. Adenosine receptors and their ligands. *Naunyn Schmiedebergs Arch Pharmacol*, 362 (4-5):382-391.
- Klotz KN, Lohse MJ. 1986. The glycoprotein nature of A1 adenosine receptors. *Biochem Biophys Res Commun*, 140 (1):406-413.
- Klotz KN, Lohse MJ, Schwabe U, Cristalli G, Vittori S, Grifantini M. 1989. 2-Chloro-N⁶-[³H]cyclopentyladenosine ([³H]CCPA)--a high affinity agonist radioligand for A1 adenosine receptors. *Naunyn Schmiedebergs Arch Pharmacol*, 340 (6):679-683.
- Klotz KN, Hessling J, Hegler J, Owman C, Kull B, Fredholm BB, Lohse MJ. 1998. Comparative pharmacology of human adenosine receptor subtypes - characterization of stably transfected receptors in CHO cells. *Naunyn Schmiedebergs Arch Pharmacol*, 357 (1):1-9.
- Koeppen M, Eckle T, Eltzschig HK. 2009. Selective deletion of the A1 adenosine receptor abolishes heart-rate slowing effects of intravascular adenosine in vivo. *PLoS One*, 4 (8):e6784.
- Kolakowski LF, Jr. 1994. GCRDb: a G-protein-coupled receptor database. *Receptors Channels*, 2 (1):1-7.
- Kollias-Baker C, Ruble J, Dennis D, Bruns RF, Linden J, Belardinelli L. 1994. Allosteric enhancer PD 81,723 acts by novel mechanism to potentiate cardiac actions of adenosine. *Circ Res*, 75 (6):961-971.
- Kruse AC, Ring AM, Manglik A, Hu J, Hu K, Eitel K, Hübner H, Pardon E, Valant C, Sexton PM, Christopoulos A, Felder CC, Gmeiner P, Steyaert J, Weis WI, Garcia KC, Wess J, Kobilka BK. 2013. Activation and allosteric modulation of a muscarinic acetylcholine receptor. *Nature*, 504 (7478):101-106.
- Kull B, Svenningsson P, Fredholm BB. 2000. Adenosine A(2A) receptors are colocalized with and activate g(olf) in rat striatum. *Mol Pharmacol*, 58 (4):771-777.
- Lakowicz JR. 2006. Principles of Fluorescence Spectroscopy. Third Aufl. New York: Springer Science+Business Media, LLC.
- Lee HT, Gallos G, Nasr SH, Emala CW. 2004. A1 adenosine receptor activation inhibits inflammation, necrosis, and apoptosis after renal ischemia-reperfusion injury in mice. *J Am Soc Nephrol*, 15 (1):102-111.

- Leff P. 1995. The two-state model of receptor activation. *Trends Pharmacol Sci*, 16 (3):89-97.
- Libert F, Van Sande J, Lefort A, Czernilofsky A, Dumont JE, Vassart G, Ensinger HA, Mendla KD. 1992. Cloning and functional characterization of a human A1 adenosine receptor. *Biochem Biophys Res Commun*, 187 (2):919-926.
- Linden J, Thai T, Figler H, Jin X, Robeva AS. 1999. Characterization of human A(2B) adenosine receptors: radioligand binding, western blotting, and coupling to G(q) in human embryonic kidney 293 cells and HMC-1 mast cells. *Mol Pharmacol*, 56 (4):705-713.
- Logothetis DE, Kurachi Y, Galper J, Neer EJ, Clapham DE. 1987. The beta gamma subunits of GTP-binding proteins activate the muscarinic K⁺ channel in heart. *Nature*, 325 (6102):321-326.
- Lohse MJ, Klotz KN, Lindenborn-Fotinos J, Reddington M, Schwabe U, Olsson RA. 1987. 8-Cyclopentyl-1,3-dipropylxanthine (DPCPX)--a selective high affinity antagonist radioligand for A1 adenosine receptors. *Naunyn Schmiedebergs Arch Pharmacol*, 336 (2):204-210.
- Louvel J, Guo D, Agliardi M, Mocking TA, Kars R, Pham TP, Xia L, de Vries H, Brussee J, Heitman LH, Ijzerman AP. 2014. Agonists for the adenosine A1 receptor with tunable residence time. A Case for nonribose 4-amino-6-aryl-5-cyano-2-thiopyrimidines. *J Med Chem*, 57 (8):3213-3222.
- Malaga-Dieguez L, Yang Q, Bauer J, Pankevych H, Freissmuth M, Nanoff C. 2010. Pharmacochaperoning of the A1 adenosine receptor is contingent on the endoplasmic reticulum. *Mol Pharmacol*, 77 (6):940-952.
- Mason PK, DiMarco JP. 2009. New pharmacological agents for arrhythmias. *Circ Arrhythm Electrophysiol*, 2 (5):588-597.
- Massink A, Amelia T, Karamychev A, AP IJ. 2020. Allosteric modulation of G protein-coupled receptors by amiloride and its derivatives. Perspectives for drug discovery? *Med Res Rev*, 40 (2):683-708.
- May LT, Briddon SJ, Hill SJ. 2010. Antagonist selective modulation of adenosine A1 and A3 receptor pharmacology by the food dye Brilliant Black BN: evidence for allosteric interactions. *Mol Pharmacol*, 77 (4):678-686.
- May LT, Leach K, Sexton PM, Christopoulos A. 2007. Allosteric modulation of G protein-coupled receptors. *Annu Rev Pharmacol Toxicol*, 47:1-51.
- McNamara N, Gallup M, Khong A, Sucher A, Maltseva I, Fahy J, Basbaum C. 2004. Adenosine up-regulation of the mucin gene, MUC2, in asthma. *FASEB J*, 18 (14):1770-1772.
- Meno JR, Higashi H, Cambray AJ, Zhou J, D'Ambrosio R, Winn HR. 2003. Hippocampal injury and neurobehavioral deficits are improved by PD 81,723 following hyperglycemic cerebral ischemia. *Exp Neurol*, 183 (1):188-196.

- Messerer R, Kauk M, Volpato D, Alonso Canizal MC, Klöckner J, Zabel U, Nuber S, Hoffmann C, Holzgrabe U. 2017. FRET Studies of Quinolone-Based Bitopic Ligands and Their Structural Analogues at the Muscarinic M1 Receptor. *ACS Chem Biol*, 12 (3):833-843.
- Miao Y, Bhattarai A, Nguyen ATN, Christopoulos A, May LT. 2018. Structural Basis for Binding of Allosteric Drug Leads in the Adenosine A1 Receptor. *Sci Rep*, 8 (1):16836.
- Mizumura T, Auchampach JA, Linden J, Bruns RF, Gross GJ. 1996. PD 81,723, an allosteric enhancer of the A1 adenosine receptor, lowers the threshold for ischemic preconditioning in dogs. *Circ Res*, 79 (3):415-423.
- Monod J, Jacob F. 1961. Teleonomic mechanisms in cellular metabolism, growth, and differentiation. *Cold Spring Harb Symp Quant Biol*, 26:389-401.
- Mukhopadhyay S, Ross EM. 1999. Rapid GTP binding and hydrolysis by G(q) promoted by receptor and GTPase-activating proteins. *Proc Natl Acad Sci U S A*, 96 (17):9539-9544.
- Müller CE, Jacobson KA. 2011. Recent developments in adenosine receptor ligands and their potential as novel drugs. *Biochim Biophys Acta*, 1808 (5):1290-1308.
- Nalli AD, Kumar DP, Al-Shboul O, Mahavadi S, Kuemmerle JF, Grider JR, Murthy KS. 2014. Regulation of Gbetagamma-dependent PLC-beta3 activity in smooth muscle: inhibitory phosphorylation of PLC-beta3 by PKA and PKG and stimulatory phosphorylation of Galphai-GTPase-activating protein RGS2 by PKG. *Cell Biochem Biophys*, 70 (2):867-880.
- Narlawar R, Lane JR, Doddareddy M, Lin J, Brussee J, Ijzerman AP. 2010. Hybrid ortho/allosteric ligands for the adenosine A(1) receptor. *J Med Chem*, 53 (8):3028-3037.
- Nguyen AT, Baltos JA, Thomas T, Nguyen TD, Munoz LL, Gregory KJ, White PJ, Sexton PM, Christopoulos A, May LT. 2016a. Extracellular Loop 2 of the Adenosine A1 Receptor Has a Key Role in Orthosteric Ligand Affinity and Agonist Efficacy. *Mol Pharmacol*, 90 (6):703-714.
- Nguyen AT, Vecchio EA, Thomas T, Nguyen TD, Aurelio L, Scammells PJ, White PJ, Sexton PM, Gregory KJ, May LT, Christopoulos A. 2016b. Role of the Second Extracellular Loop of the Adenosine A1 Receptor on Allosteric Modulator Binding, Signaling, and Cooperativity. *Mol Pharmacol*, 90 (6):715-725.
- Offermanns S, Simon MI. 1995. G alpha 15 and G alpha 16 couple a wide variety of receptors to phospholipase C. *J Biol Chem*, 270 (25):15175-15180.
- Oldham WM, Hamm HE. 2008. Heterotrimeric G protein activation by G-protein-coupled receptors. *Nat Rev Mol Cell Biol*, 9 (1):60-71.
- Ono Y, Fujibuchi W, Suwa M. 2005. Automatic gene collection system for genome-scale overview of G-protein coupled receptors in eukaryotes. *Gene*, 364:63-73.

- Park SW, Kim JY, Ham A, Brown KM, Kim M, D'Agati VD, Lee HT. 2012. A1 adenosine receptor allosteric enhancer PD-81723 protects against renal ischemia-reperfusion injury. *Am J Physiol Renal Physiol*, 303 (5):F721-732.
- Pavlos NJ, Friedman PA. 2017. GPCR Signaling and Trafficking: The Long and Short of It. *Trends Endocrinol Metab*, 28 (3):213-226.
- Peeters MC, Wisse LE, Dinaj A, Vroling B, Vriend G, Ijzerman AP. 2012. The role of the second and third extracellular loops of the adenosine A1 receptor in activation and allosteric modulation. *Biochem Pharmacol*, 84 (1):76-87.
- Rajagopal S, Shenoy SK. 2018. GPCR desensitization: Acute and prolonged phases. *Cell Signal*, 41:9-16.
- Romagnoli R, Baraldi PG, Moorman AR, Borea PA, Varani K. 2015. Current status of A1 adenosine receptor allosteric enhancers. *Future Med Chem*, 7 (10):1247-1259.
- Sato A, Terata K, Miura H, Toyama K, Loberiza FR, Jr., Hatoum OA, Saito T, Sakuma I, Gutterman DD. 2005. Mechanism of vasodilation to adenosine in coronary arterioles from patients with heart disease. *Am J Physiol Heart Circ Physiol*, 288 (4):H1633-1640.
- Schioth HB, Fredriksson R. 2005. The GRAFS classification system of G-protein coupled receptors in comparative perspective. *Gen Comp Endocrinol*, 142 (1-2):94-101.
- Schulte G, Fredholm BB. 2000. Human adenosine A(1), A(2A), A(2B), and A(3) receptors expressed in Chinese hamster ovary cells all mediate the phosphorylation of extracellular-regulated kinase 1/2. *Mol Pharmacol*, 58 (3):477-482.
- Seibt BF, Schiedel AC, Thimm D, Hinz S, Sherbiny FF, Müller CE. 2013. The second extracellular loop of GPCRs determines subtype-selectivity and controls efficacy as evidenced by loop exchange study at A2 adenosine receptors. *Biochem Pharmacol*, 85 (9):1317-1329.
- Shah SJ, Voors AA, McMurray JJV, Kitzman DW, Viethen T, Bomfim Wirtz A, Huang E, Pap AF, Solomon SD. 2019. Effect of Neladenoson Bialanate on Exercise Capacity Among Patients With Heart Failure With Preserved Ejection Fraction: A Randomized Clinical Trial. *JAMA*, 321 (21):2101-2112.
- Stumpf AD. 2015. Development of fluorescent FRET receptor sensors for investigation of conformational changes in adenosine A1 and A2A receptors [Dissertation]. Würzburg: Julius-Maximilians-Universität Würzburg.
- Stumpf AD, Hoffmann C. 2016. Optical probes based on G protein-coupled receptors - added work or added value? *Br J Pharmacol*, 173 (2):255-266.
- Sykes DA, Stoddart LA, Kilpatrick LE, Hill SJ. 2019. Binding kinetics of ligands acting at GPCRs. *Mol Cell Endocrinol*, 485:9-19.

- Tendera M, Gaszewska-Zurek E, Parma Z, Ponikowski P, Jankowska E, Kawecka-Jaszcz K, Czarnecka D, Krzeminska-Pakula M, Bednarkiewicz Z, Sosnowski M, Ochan Kilama M, Agrawal R. 2012. The new oral adenosine A1 receptor agonist capadenoson in male patients with stable angina. *Clin Res Cardiol*, 101 (7):585-591.
- UniProt C. 2019. UniProt: a worldwide hub of protein knowledge. *Nucleic Acids Res*, 47 (D1):D506-D515.
- Valant C, May LT, Aurelio L, Chuo CH, White PJ, Baltos JA, Sexton PM, Scammells PJ, Christopoulos A. 2014. Separation of on-target efficacy from adverse effects through rational design of a bitopic adenosine receptor agonist. *Proc Natl Acad Sci U S A*, 111 (12):4614-4619.
- van der Klein PA, Kourounakis AP, AP IJ. 1999. Allosteric modulation of the adenosine A(1) receptor. Synthesis and biological evaluation of novel 2-amino-3-benzoylthiophenes as allosteric enhancers of agonist binding. *J Med Chem*, 42 (18):3629-3635.
- van der Westhuizen ET, Valant C, Sexton PM, Christopoulos A. 2015. Endogenous allosteric modulators of G protein-coupled receptors. *J Pharmacol Exp Ther*, 353 (2):246-260.
- van Koppen CJ, Nathanson NM. 1990. Site-directed mutagenesis of the m2 muscarinic acetylcholine receptor. Analysis of the role of N-glycosylation in receptor expression and function. *J Biol Chem*, 265 (34):20887-20892.
- van Unen J, Stumpf AD, Schmid B, Reinhard NR, Hordijk PL, Hoffmann C, Gadella TW, Jr., Goedhart J. 2016. A New Generation of FRET Sensors for Robust Measurement of Galphai1, Galphai2 and Galphai3 Activation Kinetics in Single Cells. *PLoS One*, 11 (1):e0146789.
- Vilardaga JP, Bünemann M, Krasel C, Castro M, Lohse MJ. 2003. Measurement of the millisecond activation switch of G protein-coupled receptors in living cells. *Nat Biotechnol*, 21 (7):807-812.
- Waring MJ, Arrowsmith J, Leach AR, Leeson PD, Mandrell S, Owen RM, Pairaudeau G, Pennie WD, Pickett SD, Wang J, Wallace O, Weir A. 2015. An analysis of the attrition of drug candidates from four major pharmaceutical companies. *Nat Rev Drug Discov*, 14 (7):475-486.
- Wedegaertner PB, Wilson PT, Bourne HR. 1995. Lipid modifications of trimeric G proteins. *J Biol Chem*, 270 (2):503-506.
- Wei CJ, Li W, Chen JF. 2011. Normal and abnormal functions of adenosine receptors in the central nervous system revealed by genetic knockout studies. *Biochim Biophys Acta*, 1808 (5):1358-1379.
- Wilson CN, Vance CO, Lechner MG, Matuschak GM, Lechner AJ. 2014. Adenosine A1 receptor antagonist, L-97-1, improves survival and protects the kidney in a rat model of cecal ligation and puncture induced sepsis. *Eur J Pharmacol*, 740:346-352.

- Wright SC, Canizal MCA, Benkel T, Simon K, Le Gouill C, Matricon P, Namkung Y, Lukasheva V, König GM, Laporte SA, Carlsson J, Kostenis E, Bouvier M, Schulte G, Hoffmann C. 2018. FZD5 is a Galphaq-coupled receptor that exhibits the functional hallmarks of prototypical GPCRs. *Sci Signal*, 11 (559).
- Yan L, Burbiel JC, Maass A, Müller CE. 2003. Adenosine receptor agonists: from basic medicinal chemistry to clinical development. *Expert Opin Emerg Drugs*, 8 (2):537-576.
- Ye L, Neale C, Sljoka A, Lyda B, Pichugin D, Tsuchimura N, Larda ST, Pomes R, Garcia AE, Ernst OP, Sunahara RK, Prosser RS. 2018. Mechanistic insights into allosteric regulation of the A2A adenosine G protein-coupled receptor by physiological cations. *Nat Commun*, 9 (1):1372.

9 Acknowledgement

First of all I would like to thank my first supervisor, Prof. Dr. Carsten Hoffmann, for giving me the opportunity to join his group and to work with his outstanding FRET-technique, for providing scientific guidance and advice. He always promoted my participation in national and international conferences, which allowed me to present my work in Europe, Brazil and China. I would like to thank Prof. Dr. Klaus Benndorf for being my second supervisor and for his inspiring comments in the meetings of the Transregio 166 ReceptorLight. I would like to thank Prof. Dr. Stephen Hill for his brilliant and helpful input for this project and for his enthusiasm in our discussions.

I am thankful for being a member of the German Purine Club and the researcher consortium of the Transregio 166 ReceptorLight. The experiences I made at these conferences, retreats and symposia were very inspiring and motivating.

Furthermore I am very thankful for the support of all former and current members of the working group Hoffmann for sharing their knowledge and experiences with me. Special thanks to Dr. Amod Godbole for his valuable contributions in the writing process of this work.

Ich bedanke mich bei allen Kollegen aus Würzburg und Jena. In erster Linie bei Nicole Ziegler für ihre tatkräftige Unterstützung und die Einarbeitung am FRET-Mikroskop. Desweiteren bedanke ich mich bei Dr. Ulrike Zabel für ihre Klonierungsarbeiten und dass sie ihr fundiertes Fachwissen diesbezüglich mit mir geteilt hat. Danke an die gesamte Donnerstagsrunde für die tolle Atmosphäre bei meinen Würzburg-Aufenthalten. Desweiteren möchte ich mich bei Anne Kresinsky Dorith Schmid, Fabienne Haas und Karina Stinal für ihre Unterstützung unterschiedlichster Art bedanken.

Ich danke meiner Familie und meinen Freunden für ihre Geduld und ihr Verständnis, wenn ich aufgrund der Dienstreisen an Wochenenden und der anspruchsvollen Arbeit an vielen Ereignissen nicht teilnehmen konnte. Besonders bedanke ich mich bei Frederik für all seine Unterstützung, seine Geduld und dass er alle Höhen und Tiefen mit mir durchgestanden hat.

10 List of figures

Figure 1: GPCR signaling cycle.....	2
Figure 2: Structures of A1AR agonists.	8
Figure 3: Cooperativity of orthosteric ligand and allosteric modulator.	12
Figure 4: Receptor binding models.	14
Figure 5: Radioligand-based methods to measure orthosteric and allosteric kinetics at GPCR.	16
Figure 6: Structures of A1AR positive allosteric modulators.	18
Figure 7: Jablonski diagrams showing energy states of a fluorophore upon excitation and emission of light and energy transfer of two fluorophores.	20
Figure 8: Sensitized emission detection of FRET.	21
Figure 9: Protein sequence of rat adenosine A1 receptor.....	36
Figure 10: Orthosteric characterization of rat A1 FIAsh3 CFP receptor FRET sensor.....	38
Figure 11: Orthosteric kinetics of human and rat A1 FIAsh3 CFP receptor.	40
Figure 12: In the absence of orthosteric ligand PD 81,723 mediates no receptor response.	41
Figure 13: Measurement scheme for determining allosteric effects.....	42
Figure 14: Determination of allosteric modulator affinity.	44
Figure 15: Prolonged dissociation time in the presence of allosteric modulator.	45
Figure 16: Influence of allosteric modulator on orthosteric concentration-response curve.....	46
Figure 17: Probe dependency of PD 81,723.....	47
Figure 18: G protein-based FRET sensor and allosteric enhancement at G protein level.	48
Figure 19: Experimental procedure for determination of orthosteric and allosteric kinetics.....	50
Figure 20: Orthosteric and allosteric dissociation kinetics from OAR*.....	52
Figure 21: Modifications of the second extracellular loop and membrane localization of mutant receptor sensor.	55
Figure 22: Influence of mutations in the second extracellular loop on the kinetics of adenosine.	57
Figure 23: Affinity of PD 81,723 for human and rat mutants of second extra cellular loop.	58
Figure 24: Influence of allosteric modulator on orthosteric concentration-response curve of mutants in the second extracellular loop.....	60
Figure 25: Influence of mutations in the second extracellular loop on the kinetics of PD 81,723.....	62
Figure 26: Membrane localization of double mutant receptor FRET sensor.....	63
Figure 27: Kinetic rescue of human S161A by S161A M162V.....	64
Figure 28: Protein sequence alignment of hA1AR and ratA1AR.	83
Figure 29: Human mutant A1AR FRET sensor membrane localization before and after 24 h of 5 mM theophylline incubation.	84
Figure 30: Rat mutant A1AR FRET sensor membrane localization before and after 24 h of 5 mM theophylline incubation.	84
Figure 31: Superimposed active (grey) and inactive (black) backbones of human A1AR (PDB code: 6D9H, 5UEN).	85

Figure 32: Influence of mutants in the second extracellular loop on concentration-response curves of adenosine. 85

11 List of tables

Table 1: Binding affinities of adenosine receptor agonists.....	9
Table 2: Purchased chemicals and reagents	24
Table 3: Plasmids used in this work	26
Table 4: Cell lines used in this work	26
Table 5: Media used for cultivation of <i>E. coli</i>	27
Table 6: Buffer used for transformation of chemically competent <i>E. coli</i>	27
Table 7: Media used for cultivation of HEK293 cells	27
Table 8: Composition of physiological buffers used for HEK293 cells	28
Table 9: Equipment and software used in this work.....	28
Table 10: Composition of standard PCR reaction	29
Table 11: Ligation of DNA of interest and vector backbone with overlapping ends	31
Table 12: Digestion of DNA by restriction enzymes, general composition	31
Table 13: Transfection of HEK293 cells with Effectene transfection kit.....	33
Table 14: EC ₅₀ values of orthosteric agonists for rat and human A1 wt FRET sensor.	38
Table 15: Orthosteric and allosteric dissociation kinetics from OAR* of human and rat adenosine A1 receptors.....	51
Table 16: EC ₅₀ values of adenosine for human and rat ECL2 mutants compared to wt.....	56
Table 17: EC ₅₀ of PD 81,723 for human and rat ECL2 mutants compared to wt.	59
Table 18: Influence of mutants on the ability of PD 81,723 to shift the concentration-response curve of adenosine.	60
Table 19: Dissociation of 10 μM PD 81,723 from OAR*.	65
Table 20: EC ₅₀ values of adenosine for human and rat A1AR wt and mutants.	86
Table 21: EC ₅₀ values of PD 81,723 for human and rat A1AR wt and mutants.	86
Table 22: Influence of mutants on the ability of PD 81,723 to shift the concentration-response curve of adenosine.	87
Table 23: Association and dissociation kinetics of 100 μM adenosine to and from human A1AR.	87
Table 24: Association and dissociation kinetics of 100 μM adenosine to and from rat A1AR	87
Table 25: Calculation of kinetic K _{D FRET} of 100 μM adenosine.	88
Table 26: Association of EC ₃₀ of Ado to OR*.....	88
Table 27: Association of 10 μM PD 81,723 to the human receptor occupied by adenosine (EC ₃₀).	88
Table 28: Dissociation kinetics from OAR* of human A1AR.	89
Table 29: Dissociation kinetics from OAR* of rat A1AR.	89
Table 30: Calculation of kinetic K _{D FRET} of 10 μM PD 81,723.	89

12 Publications and conferences

12.1 Publications

Co-authorship:

Grundmann M, Merten N, Malfacini D, Inoue A, Preis P, Simon K, Rüttiger N, Ziegler N, Benkel T, Schmitt NK, Ishida S, Müller I, Reher R, Kawakami K, Inoue A, Rick U, Kühl T, Imhof D, Aoki J, König GM, Hoffmann C, Gomeza J, Wess J, Kostenis E

Lack of beta-arrestin signaling in the absence of active G proteins.

Nature Communications 9, Article number: 341 (2018)

<https://doi.org/10.1038/s41467-017-02661-3>

Manuscript in preparation:

Mechanistic insight in allosteric modulation of adenosine A1 receptor with endogenous ligand adenosine. (Rüttiger et al.)

12.2 Attended conferences

- 2nd German Pharm-Tox Summit. March 2016 in Heidelberg. Germany
- 7th Joint Italian-German Purine club meeting “Advances in Basic and Translational Purinergic Research” July 2017. Rom. Italy
Award for best poster communication
- International Symposium on GPCRs and G proteins- “turning scientific discoveries with cutting edge methods to cutting edge science” September 2017 in Bonn. Germany
- 1st International ReceptorLight Symposium - high-end light microscopy elucidates membrane receptor function. June 2017 in Würzburg. Germany

- 7th Focused Meeting on Cell Signalling. April 2018 in Nottingham. United Kingdom
- Purines 2018 International - Basic and translational science on purinergic signaling and its components for a healthy and better world. June 2018. Foz do Iguaçu. Brazil
Poster price "Pedro Muanis Persechini Mention of Honor"
- 4th German Pharm-Tox Summit 2019 in Stuttgart. Germany
- 2nd International ReceptorLight Symposium - high-end light microscopy elucidates membrane receptor function. June 2019 in Jena. Germany

13 Curriculum vitae

14 Ehrenwörtliche Erklärung

Hiermit erkläre ich, dass mir die Promotionsordnung der Medizinischen Fakultät der Friedrich-Schiller-Universität bekannt ist,

ich die Dissertation selbst angefertigt habe und alle von mir benutzten Hilfsmittel, persönlichen Mitteilungen und Quellen in meiner Arbeit angegeben sind,

mich folgende Personen bei der Auswahl und Auswertung des Materials sowie bei der Herstellung des Manuskripts unterstützt haben: Prof. Dr. Carsten Hoffmann,

die Hilfe eines Promotionsberaters nicht in Anspruch genommen wurde und dass Dritte weder unmittelbar noch mittelbar geldwerte Leistungen von mir für Arbeiten erhalten haben, die im Zusammenhang mit dem Inhalt der vorgelegten Dissertation stehen,

dass ich die Dissertation noch nicht als Prüfungsarbeit für eine staatliche oder andere wissenschaftliche Prüfung eingereicht habe und

dass ich die gleiche, eine in wesentlichen Teilen ähnliche oder eine andere Abhandlung nicht bei einer anderen Hochschule als Dissertation eingereicht habe.

Ort, Datum

Unterschrift des Verfassers